

NATIONAL ADVISORY COMMITTEE FOR AERONAUTICS

L-109

WARTIME REPORT

ORIGINALLY ISSUED

November 1945 as
Advance Restricted Report L5H09

LANGLEY FULL-SCALE TUNNEL INVESTIGATION OF THE FACTORS
AFFECTING THE DIRECTIONAL STABILITY AND TRIM
CHARACTERISTICS OF A FIGHTER-TYPE AIRPLANE

By Harold H. Sweberg, Eugene R. Guryansky,
and Roy H. Lange

Langley Memorial Aeronautical Laboratory
Langley Field, Va.

PROPERTY OF JET PROPULSION LABORATORY LIBRARY
CALIFORNIA INSTITUTE OF TECHNOLOGY



WASHINGTON

NACA WARTIME REPORTS are reprints of papers originally issued to provide rapid distribution of advance research results to an authorized group requiring them for the war effort. They were previously held under a security status but are now unclassified. Some of these reports were not technically edited. All have been reproduced without change in order to expedite general distribution.

NATIONAL ADVISORY COMMITTEE FOR AERONAUTICS

ADVANCE RESTRICTED REPORT

LANGLEY FULL-SCALE TUNNEL INVESTIGATION OF THE FACTORS
AFFECTING THE DIRECTIONAL STABILITY AND TRIM
CHARACTERISTICS OF A FIGHTER-TYPE AIRPLANE

By Harold H. Sweberg, Eugene R. Guryansky
and Roy H. Lange

S U M M A R Y

Tests were made in the Langley full-scale tunnel of the Grumman XF6F-4 airplane in order to investigate the factors that affect the directional stability and trim characteristics of a typical fighter-type airplane. Eight representative flight conditions were investigated in detail. The separate contributions of the wing-fuselage combination, the vertical tail, and the propeller to the directional stability of the airplane in each condition were determined. Extensive air-flow surveys of sidewash angle and dynamic-pressure ratio along a line coincident with the rudder hinge line were made for each condition investigated to aid in evaluating the slipstream effects. The data obtained from the air-flow surveys were also used to investigate methods for calculating the contribution of the vertical tail to the airplane directional stability.

The results of the tests showed that, for the conditions investigated, the directional stability of the airplane was smallest for the gliding condition with flaps retracted and was greatest for the wave-off condition with flaps deflected 50° . The variation of sidewash angle at the vertical tail with angle of yaw was destabilizing for all conditions investigated. Propeller operation increased the magnitude of the destabilizing sidewash but, at small angles of yaw, also increased the dynamic pressure at the vertical tail sufficiently to make the combined effect stabilizing. The lateral displacement of the slipstream with respect to the vertical tail at angles of yaw larger than approximately $\pm 10^\circ$ caused a reduction in the contribution of the vertical tail to the airplane directional stability at positive angles of yaw and an increase

at negative angles of yaw. Flap deflection tended to increase the directional stability of the airplane regardless of the condition of propeller operation.

The rudder deflection required for directional trim was greatest for the wave-off condition with the flaps deflected 50° . The large changes in the directional trim of the airplane resulting from propeller operation are primarily due to the effects of the slipstream on the wing-fuselage combination and on the vertical tail and are only secondarily due to the direct effects of the propeller forces.

I N T R O D U C T I O N

The importance of the effects of propeller operation on the directional stability and trim characteristics of an airplane is well known. Past experience has shown that the directional trim is usually critical for a take-off or low-speed climb condition in which high propeller-thrust and torque coefficients produce large increments of yawing-moment coefficient. For such conditions, a pilot may often find that, because of the large trim changes involved, he has insufficient rudder control and is unable to maintain the desired heading. The directional stability is usually lowest for a condition of high angle of attack and low power, during which the contribution of the vertical tail to directional stability is lowest because of the low slipstream velocity and the relatively large loss in dynamic pressure due to the fuselage and canopy wakes.

Analyses have been made in the past of wind-tunnel data on directional stability and control (references 1 and 2) but these analyses were based mainly on the results of scattered tests of a large number of airplanes and airplane models and did not include any systematic test results showing the effects of propeller operation on the directional stability and control characteristics of a single design. In particular, only meager data were available to show the effects of propeller operation on the air flow in the region of the vertical tail. In order to obtain some systematic wind-tunnel-test data relative to these effects, an investigation was conducted in the Langley full-scale tunnel on the Grumman XF6F-4 airplane. The investigation included measurements of the

directional stability and control characteristics of the airplane for a wide range of flight conditions. For each flight condition investigated, tests were made of the complete airplane, of the airplane without propeller, of the airplane without vertical tail, and of the airplane without both propeller and vertical tail. The separate contributions of the propeller, the vertical tail, and the wing-fuselage combination to the airplane directional stability and trim could thus be evaluated. In addition to these force tests, measurements were made of the dynamic pressure and the angularity of the air flow at the vertical tail. Particular attention was given to these air-flow measurements inasmuch as the available data on this subject are very limited.

S Y M B O L S

C_L	lift coefficient (L/q_0S)
C_Y	lateral-force coefficient (Y/q_0S)
C_n	yawing-moment coefficient (N/q_0Sb)
T_c	thrust coefficient ($T_e/2q_0D^2$)
Q_c	torque coefficient ($Q/2q_0D^3$)
L	force along Z-axis; positive when acting upward
Y	force along Y-axis; positive when acting to the right
N	moment about Z-axis; positive when it tends to turn nose to right
T_e	effective propeller thrust ($X_R - X'$)
X_R	resultant force along X-axis with propeller operating
X'	force along X-axis, propeller removed
Q	propeller torque
D	propeller diameter (13.08 ft)

- S wing area (334 sq ft)
- S_t vertical-tail area (19.0 sq ft as defined in text)
- l distance from airplane center of gravity to quarter-chord point of mean vertical-tail chord, measured parallel to fuselage reference line (19.5 ft)
- b wing span (42.83 ft)
- b_t span of vertical tail surface (4.25 ft as defined in text)
- c_t section chord of vertical tail
- ψ angle of yaw, degrees; positive with left wing forward
- α angle of attack of fuselage reference line relative to free-stream direction, degrees
- δ_f angle of flap deflection, degrees
- δ_r angle of rudder deflection, degrees; positive when trailing edge of rudder is moved to left
- β propeller blade angle at 0.75 radius or angle of sideslip, degrees
- σ sidewash angle, degrees; positive when flow is from right to left when airplane is viewed from rear
- σ_{av} average sidewash angle along rudder hinge line weighted for chord and dynamic pressure, degrees
- $$\left(\sigma_{av} = \frac{1}{(q/q_0)_{av} S_t} \int_0^{b_t} c_t \frac{q}{q_0} \sigma db_t \right)$$
- $\frac{d\sigma_{av}}{d\psi}$ rate of change of average sidewash angle with angle of yaw
- q local dynamic pressure
- q_0 free-stream dynamic pressure

q/q_0 ratio of local dynamic pressure to free-stream dynamic pressure

$(q/q_0)_{av}$ average dynamic-pressure ratio along rudder hinge line weighted for chord

$$\left((q/q_0)_{av} = \frac{1}{S_t} \int_0^{b_t} c_t \frac{q}{q_0} db_t \right)$$

V_i indicated airspeed

$C_{n\psi}$ rate of change of C_n with respect to ψ , per degree

$C_{Y\psi}$ rate of change of C_Y with respect to ψ , per degree

$\left(\frac{dC_N}{da} \right)_t$ rate of change of vertical-tail normal-force coefficient with angle of attack, per degree

$\frac{dC_n}{d\delta_r}$ rate of change of C_n with respect to δ_r , per degree

$(\delta_r)_{C_n=0}$ rudder deflection at zero yawing-moment coefficient, degrees

$(C_Y)_{C_n=0}$ lateral-force coefficient at zero yawing-moment coefficient

Subscripts:

t vertical tail

p propeller

s slipstream

av average

A I R P L A N E A N D A P P A R A T U S

Tests were made of the Grumman XF6F-4, which is a low midwing single-place fighter airplane weighing about 11,400 pounds and equipped with a Pratt & Whitney R-2800-27 engine rated at 1600 horsepower at 2400 rpm at an altitude of 5700 feet. The rear portion of the fuselage is wedge shaped, and the gap between the rudder and fin is sealed. The maximum rudder travel is $\pm 33^\circ$. A three-view drawing showing the principal dimensions and areas of the airplane is given in figure 1 and photographs of the airplane mounted in the Langley full-scale tunnel are given in figure 2.

For some of the tests, the vertical tail was removed and the gap left by its removal was faired to the contour of the fuselage by a sheet of aluminum. A sketch showing the tail fairing superimposed on the vertical tail surface is given in figure 3, which shows also the principal dimensions of the vertical tail surface.

The air-flow measurements were obtained by means of the combined yaw, pitch, and pitot-static tube shown in detail in figure 4. Photographs of this instrument mounted in position for the air-flow measurements are given in figure 5.

M E T H O D S A N D T E S T S

All the tests were made with the airplane landing gear retracted and the cowlings flaps closed at a tunnel airspeed of approximately 60 miles per hour, which corresponds to a Reynolds number of approximately 4,380,000 based on a mean wing chord of 7.80 feet. The ailerons and elevators were locked at 0° deflection for all the tests and the landing flaps were locked at 50° when deflected. No attempt was made to duplicate the "blow-up" characteristics of the landing flaps. The directional stability and trim characteristics of the airplane were obtained for the eight representative flight conditions outlined in table I.

Directional-stability measurements.- The directional stability characteristics of the airplane, for each flight condition, were investigated by measuring the forces and moments on the airplane at approximately 5° increments

of angle of yaw between $\pm 15^\circ$, which was the maximum yaw-angle range possible with the present airplane-support setup in the Langley full-scale tunnel. For each of the eight conditions, tests were made of the airplane with the propeller both removed and operating and with the vertical tail surface both removed and in place.

Directional-trim measurements.- The directional trim characteristics of the airplane were determined from rudder-effectiveness tests. Only four of the conditions listed in table I were investigated; namely, the landing, the wave-off, the gliding, and the low-speed climb ($V_1 = 98$ mph) conditions. Rudder-effectiveness tests also were made for similar conditions with the propeller removed.

Air-flow measurements.- Surveys of the velocity and angularity of the air flow in the region of the vertical tail were made for all the conditions listed in table I. At each angle of attack, surveys were made for propeller-removed and propeller-operating conditions at angles of yaw of approximately 0° , $\pm 5^\circ$, $\pm 10^\circ$, and $\pm 15^\circ$. The surveys were made with the vertical tail surface replaced by the tail fairing and consisted of measurements taken every 6 inches along a line coincident with the rudder hinge line and extending from approximately 4 inches above the tail fairing to approximately 12 inches above the top of the vertical tail surface. (See fig. 3.)

Power-on tests.- For the power-on tests, it was desired to simulate the variations shown in figure 6 of thrust and torque coefficient with lift coefficient for constant-power operation at sea level. It was found that these relationships could very nearly be produced with a constant propeller-blade-angle setting of 24.8° measured at the 0.75 radius; hence this blade-angle setting was used for all the tests with the propeller operating. A comparison of the variation of thrust coefficient with torque coefficient for constant-power operation and for the propeller with a blade-angle setting of 24.8° measured at the 0.75 radius is shown in figure 7. For the idling-power conditions, the engine was run at the lowest speed considered possible (700 rpm) without fouling the engine spark plugs. The thrust and torque coefficients thus obtained for the idling-power conditions were 0.01 and 0.005, respectively.

Accuracy of test results.- The accuracy of the results of the force tests is shown by the scatter of the test points. The accuracy of the combined yaw, pitch, and pitot-static tube is estimated to be about $\pm 0.25^\circ$ for the yaw- and pitch-angle measurements and about $\pm 0.01q_0$ for the dynamic-pressure measurements. Deviations of the test results from zero for apparently symmetrical conditions are probably due to differences in the airplane on the two sides of the plane of symmetry and to asymmetries in the tunnel flow.

RESULTS AND DISCUSSION

The data are given in standard nondimensional-coefficient form with respect to the stability axes and the center-of-gravity location shown in figure 1. The stability axes are a system of axes having their origin at the center of gravity and in which the Z-axis is in the plane of symmetry and perpendicular to the relative wind, the X-axis is in the plane of symmetry and perpendicular to the Z-axis, and the Y-axis is perpendicular to the plane of symmetry.

The presentation of the test results and the analysis of the data have been grouped into two main sections. The first section gives results showing the directional stability characteristics of the complete airplane for the various flight conditions investigated and an analysis of the effects of the wing-fuselage combination, the vertical tail, and the propeller on the airplane directional stability. The results of the air-flow measurements in the region of the vertical tail also are included in this section. The second section presents rudder-effectiveness data from which the directional trim characteristics of the airplane have been determined.

DIRECTIONAL STABILITY

The results of the force tests made to determine the directional stability characteristics of the airplane for each of the eight test conditions listed in table I are given in figure 8. Each part of figure 8 shows curves of C_n and C_y against ψ for one specific flight

attitude for the complete airplane, for the airplane with the propeller removed, for the airplane with the vertical tail removed, and for the airplane with both the propeller and the vertical tail removed. No test points are shown in figure 8 for the propeller-removed data, inasmuch as these data were obtained from faired curves. Values of $C_{n\psi}$ and $C_{Y\psi}$ for the complete airplane in each flight attitude investigated are given in table I.

Before a detailed discussion is presented of the various factors that affect the directional stability characteristics of the airplane, a few of the outstanding trends indicated by the test results of figure 8 are listed as follows:

(1) The directional-stability parameter $C_{n\psi}$ at small angles of yaw (between $\pm 5^\circ$) is smallest for the gliding condition with flaps retracted. For this condition, $C_{n\psi} = -0.00015$.

(2) The directional-stability parameter, at small angles of yaw, is largest for the high-power condition with flaps deflected (wave-off condition). For this condition, $C_{n\psi} = -0.00147$.

(3) For the conditions with high thrust coefficients, the directional stability decreases at angles of yaw greater than approximately 10° and increases at negative angles of yaw greater than approximately -10° .

(4) Flap deflection tends to increase the airplane directional stability.

Effects of Wing-Fuselage Combination and Vertical

Tail with Propeller Removed

Wing-fuselage combination. - Values of $C_{n\psi}$ and $C_{Y\psi}$ for the wing-fuselage combination are shown plotted in figure 9 as a function of angle of attack for flaps retracted and flaps deflected 50° . These values of $C_{n\psi}$ and $C_{Y\psi}$ were obtained from the results shown in figure 8 for the airplane with the propeller and the vertical tail removed. The variation of yawing-moment coefficient

with angle of yaw of the wing-fuselage combination with flaps retracted is unstable for the angle-of-attack range investigated. Increasing the angle of attack, however, decreases the unstable yawing-moment variation of the wing-fuselage combination. A further decrease in the unstable yawing-moment variation occurs with flap deflection and causes the wing-fuselage combination to become stable at angles of attack greater than about 8° . This increase in stability with increasing angle of attack and flap deflection is probably due partly to an increase in directional stability of the wing alone with increasing angle of attack (fig. 8 of reference 3) and partly to an increase in the directional stability caused by a favorable effect of the wing-fuselage interference (figs. 4 and 5 of reference 4).

The variation of lateral-force coefficient with angle of yaw for the wing-fuselage combination is positive for the range of angle of attack and flap deflection investigated. Increasing the angle of attack and deflecting the flaps decreases the rate of change of lateral-force coefficient with angle of yaw.

Air-flow surveys.- The results of the air-flow measurements for the propeller-removed conditions are given in figure 10, which shows the variation with height above the fuselage along the rudder hinge line of the sidewash angle σ and the dynamic-pressure ratio q/q_0 for angles of yaw of approximately 0° , $\pm 5^\circ$, $\pm 10^\circ$, and $\pm 15^\circ$. Weighted average values of the sidewash angle and dynamic-pressure ratio along the rudder hinge line are given in table II.

The surveys (fig. 10) show that, for this airplane, the variation of average sidewash angle at the vertical tail with angle of yaw $d\sigma/d\psi$ was, in general, positive (destabilizing). The data show that the direction of flow from the fuselage wake and air beside it (region in which sharp loss in dynamic pressure occurs) is strongly destabilizing. Inasmuch as the vertical-tail chord is largest near the fuselage, the effect of the flow in this region on the contribution of the vertical tail to the airplane directional stability should predominate. The flow above the fuselage wake appears, in most cases, to be slightly destabilizing for negative angles of yaw and to have little effect on the stability at positive angles of yaw. Increasing the angle of attack or deflecting the flaps tends to increase the destabilizing effect of the

sidewash. These results are, in general, contrary to the results published in reference 5, which indicate that the sidewash is usually stabilizing for low-wing airplanes. The discrepancy may be due to the fact that, for the present series of tests, the horizontal tail and canopy were in place and the rear portion of the fuselage was wedge shaped; whereas the tests of reference 5 were made on a smooth circular fuselage with no horizontal tail.

The data given in table III show that the dynamic-pressure ratio at the vertical tail has its minimum value at small angles of yaw and increases as the angle of yaw is increased in either direction. For any given angle of yaw, the contribution of the vertical tail to the airplane directional stability is directly proportional to the dynamic-pressure ratio at that angle of yaw. At small angles of yaw (between $\pm 5^\circ$) the vertical tail lies directly in the path of the fuselage and canopy wakes and hence q/q_0 for these conditions reaches its minimum value. As the angle of yaw is increased in either direction, the vertical tail moves away from the fuselage and canopy wakes and q/q_0 increases. Inasmuch as the fuselage boundary-layer and canopy wakes increase with increasing angle of attack, the loss in q/q_0 at the tail increases with increasing angle of attack.

Vertical tail.- Experimental increments of yawing-moment and lateral-force coefficients due to the vertical tail were obtained from the data of figure 8 for the propeller-removed conditions and are shown plotted in figures 11 and 12 for all the airplane attitudes investigated. Figures 11 and 12 show also increments of yawing-moment and lateral-force coefficients due to the vertical tail that were computed on the basis of the results of the air-flow surveys.

The force-test data show that the contribution of the vertical tail to the airplane directional stability is lower in the yaw-angle range between -5° and 5° than at the higher angles of yaw and, in addition, the contribution of the vertical tail decreases with increasing angle of attack and flap deflection. Numerical values for the slopes $C_{n\psi_t}$ and $C_{Y\psi_t}$ are given in table III.

The trends shown by these results are in agreement with the conclusions drawn from the results of the air-flow surveys.

An analysis has been made of the results of the air-flow surveys and the force tests in order to investigate methods for computing the contribution of the vertical tail to the airplane directional stability. The increments of yawing-moment and lateral-force coefficients due to the vertical tail are given by the following expressions:

$$\Delta C_{n_t} = - \left(\frac{dC_N}{da} \right)_t (\psi - \sigma_{av}) (q/q_0)_{av} \frac{S_t}{S} \frac{l}{b} \quad (1)$$

$$\Delta C_{y_t} = -\Delta C_{n_t} \frac{b}{l} \quad (2)$$

The values of σ_{av} and $(q/q_0)_{av}$ in equation (1), which were determined from the air-flow surveys, are assumed to apply to the small area below the lower limit of the air-flow measurements.

The results of the air-flow surveys - when used in conjunction with the recommendations given in reference 1 with regard to the determination of the tail area, tail span, and tail lift-curve slope - were found to give values of C_{n_t} and C_{y_t} that averaged about 20 percent larger than the values obtained by the force tests. The values of the vertical-tail area and vertical-tail span determined by the methods of reference 1, however, include areas in excess of that part of the vertical tail above the fuselage. The surveys indicated that the contribution of these areas to the airplane directional stability would be small because of the large destabilizing side-wash and low dynamic pressure in that region. Consequently, for further calculations, the area of the vertical tail was considered equal to the actual vertical-tail area removed from the airplane during the tests ($S_t = 19$ sq ft) and the span of the vertical tail was considered equal to the height of the vertical tail above the top of the tail fairing ($b_t = 4.25$ ft). (See fig. 3.) All the terms of equation (1) except $(dC_N/da)_t$ are known from either the surveys or the force tests. The term $(dC_N/da)_t$ includes the end-plate effect of the horizontal tail and fuselage on the vertical tail (references 1 and 6)

modified by the interference effect of the vertical tail on the fuselage. The lift-curve slope for an isolated tail may be determined from figure 3 of reference 1 as a function of tail aspect ratio. The analysis of the results of the force tests and the air-flow surveys revealed that the geometric aspect ratio of the vertical tail b_t^2/S_t should be multiplied by 1.55 to account for the end-plate and interference effects. Although this value is numerically the same as that recommended in reference 1, the agreement is coincidental in view of the difference in definitions of tail area and tail span. The comparison given in figures 11 and 12 of the increments of C_n and C_y due to the vertical tail, as determined from the force tests and as calculated from equations (1) and (2) by use of the air-flow-survey data and the correction factor of 1.55 for the geometric aspect ratio of the vertical tail, is given to show the range of application of the present method for the XF6F-4 airplane. Good agreement is obtained for the complete range of angle of attack and yaw for all conditions investigated.

In order to calculate the contribution of the vertical tail to the airplane directional stability, the variation of sidewash angle and dynamic-pressure ratio with angle of yaw must be known because

$$C_{n\psi_t} = - \left(\frac{dC_N}{d\alpha} \right)_t \frac{d(\psi - \sigma_{av})(q/q_0)_{av}}{d\psi} \frac{S_t}{S} \frac{l}{b} \quad (3)$$

and

$$C_{Y\psi_t} = -C_{n\psi_t} \frac{b}{l} \quad (4)$$

Equation (3) shows that the contribution of the vertical tail to the airplane directional stability is directly proportional to the derivative of $(\psi - \sigma_{av})(q/q_0)_{av}$ with respect to the angle of yaw. The term $(\psi - \sigma_{av})(q/q_0)_{av}$, which is designated the air-flow factor, is shown plotted in figure 13, and average values of the slopes $\frac{d(\psi - \sigma_{av})(q/q_0)_{av}}{d\psi}$ between $\psi = -5^\circ$ and $\psi = 5^\circ$ are given in table III. This table indicates also the effect

on the contribution of the vertical tail to the airplane directional stability of the decrease in the derivative of the air-flow factor with angle of attack and flap deflection. For test conditions with flaps deflected 50° , the destabilizing effect of the sidewash and the loss in q/q_0 is sufficient to reduce the contribution of the vertical tail to the airplane directional stability by about 50 percent of the value that would be obtained if $\frac{d(\psi - \sigma_{av})(q/q_0)_{av}}{d\psi}$ were equal to 1.0. The comparison given in table III of the values of $C_{n_{\psi_t}}$ and $C_{Y_{\psi_t}}$ obtained from the force tests and calculated from equations (3) and (4) by use of the air-flow-survey data and the correction factor of 1.55 for the geometric tail aspect ratio shows fairly good agreement between these slopes.

Effects of Propeller Operation

The total increments of yawing-moment and lateral-force coefficients due to propeller operation are given in figure 14 for each of the conditions investigated. These increments were obtained from the experimental data plotted in figure 8 and are the differences in C_n and C_Y for the complete airplane with the propeller operating and the propeller removed.

For the airplane with flaps retracted (fig. 14(a)), propeller operation was destabilizing at angles of yaw from about -10° to 15° ; the instability was greatest at large positive angles of yaw. At angles of yaw between -10° and -15° , propeller operation gave a stable variation of ΔC_{n_p} against ψ . None of the effects of propeller operation was proportional to the power applied or to the thrust coefficient; in fact, at small angles of yaw (between $\pm 5^\circ$), the instability caused by propeller operation was about the same for all conditions, regardless of the thrust coefficient and angle of attack. The effect of propeller operation on the directional stability of the airplane with flaps deflected 50° at small angles of yaw (fig. 14(b)) was, in general, to increase the stability for the wave-off condition, to decrease the stability for the landing

condition slightly, and to cause no appreciable change in the stability for the landing-approach condition. The average increase in directional stability due to propeller operation for the wave-off condition (rated power, $T_c = 0.51$), at angles of yaw between $\pm 5^\circ$, was very large ($\Delta C_{n\psi_p} = -0.00105$).

The effects of propeller operation on the directional stability characteristics of the airplane can be conveniently considered under the following groups:

- (1) Direct effect of the propeller forces on the airplane directional stability
- (2) Effects of the propeller slipstream on the contribution of the wing-fuselage combination to the airplane directional stability
- (3) Effects of the propeller slipstream on the contribution of the vertical tail to the airplane directional stability

Direct effect of propeller forces.- Methods for computing the direct effect of the propeller forces on the variation of lateral-force and yawing-moment coefficient with angle of yaw are given in reference 7. The dashed lines shown in figures 15 and 16 are increments of C_n and C_y due to the propeller forces that were calculated by equation (7) of reference 7. (The propeller side-force factor was 99.2.) The calculations show that the direct effect of the propeller forces is to decrease the airplane directional stability for all conditions investigated. This effect is greatest for the low-speed climb condition ($C_L = 1.39$, $T_c = 0.51$), for which the decrease in directional stability due to the isolated propeller is 0.00038.

Effect of slipstream on wing-fuselage combination.- The effects of the propeller slipstream on the lateral-force and yawing-moment variations with angle of yaw of the wing-fuselage combination may be indirectly obtained from the experimental results. The increments of C_n and C_y due to propeller operation for the airplane with vertical tail removed, increments which were obtained from the force tests, are shown by the solid lines in

figures 15 and 16 for each condition investigated. These increments include the direct effect of the propeller forces and the effects of the passage of the slipstream over the wing-fuselage combination. The difference between the solid and the dashed lines in figures 15 and 16 are therefore presumed to be due only to the effects of the slipstream on the wing-fuselage combination.

The data show that for all conditions with the flaps retracted, at angles of yaw between $\pm 5^\circ$, the slipstream effects on the wing-fuselage combination caused destabilizing variations of yawing-moment coefficient with angle of yaw. At the low thrust coefficients this effect was small; at $T_c = 0.51$, however, the slipstream caused a destabilizing increment of $C_{n\psi_p}$ of about 0.00047. For

the flaps-deflected conditions, the directional stability of the airplane was not changed appreciably by the slipstream effects on the wing-fuselage combination for angles of yaw between 5° and -15° but was considerably decreased for angles of yaw between 5° and 15° .

Effect of slipstream on air flow in region of vertical tail.- The results of the surveys with the propeller operating are given in figures 17(a) to 17(e) for the flaps-retracted conditions and in figures 17(f) to 17(h) for the conditions with flaps deflected 50° . Weighted average values of the sidewash angles and the dynamic-pressure ratios at the vertical tail determined from these surveys are given in table IV.

For all conditions investigated, the variation of the average sidewash angle at the vertical tail with angle of yaw was generally destabilizing (positive $d\sigma_{av}/d\psi$). The destabilizing effect of the sidewash appeared to increase with thrust coefficient and angle of attack and to decrease with flap deflection. (See table IV.) The most important factor contributing to the destabilizing effect of the sidewash is the flow from the fuselage boundary layer, which exists in the region in which, for the present airplane, the vertical-tail chord is largest. The destabilizing sidewash in the region of the fuselage boundary layer was smaller in magnitude for the flaps-deflected conditions (figs. 17(f) to 17(h)) than for the flaps-retracted conditions (figs. 17(a) to 17(e)). The data show that the air flow at the vertical tail in the region above the fuselage boundary layer is

dependent on the conditions of propeller operation. As the thrust coefficient increased from one condition to another, the sidewash in this region became increasingly negative (flow from left to right when airplane is viewed from the rear). This effect may be accounted for by the slipstream rotation. The vertical tail was in the region of the rotating flow from the upper half of the propeller, which for right-hand propeller operation caused the air to flow from left to right. A further effect of the propeller rotation was a lateral displacement (toward the right) of the slipstream in the region of the vertical tail due to the tangential-velocity components of the rotating flow. The result was that, as the airplane was yawed nose left (negative yaw), the vertical tail tended to move into the center of the slipstream and the sidewash became increasingly negative; as the airplane was yawed nose right, however, the vertical tail tended to move away from the center of the slipstream and the sidewash became decreasingly negative. These tendencies indicate that increasing the slipstream rotation tends to increase the destabilizing effect of the sidewash.

The effect of the increased dynamic pressure at the vertical tail due to the propeller slipstream was to increase the contribution of the vertical tail to the airplane directional stability, inasmuch as the average sidewash was never large enough to cause the contribution of the vertical tail to be destabilizing. Surveys (fig. 17) showed that the disposition of the slipstream at the vertical tail was such that the maximum dynamic pressure occurred at the sections near the middle of the tail for zero angle of yaw and at the sections about one-third of the tail height above the top of the fuselage for other angles of yaw. The dynamic pressure was a minimum at the bottom of the vertical tail as a result of the large dynamic-pressure losses due to the fuselage and canopy wakes. The displacement of the slipstream with respect to the vertical tail, as the angle of yaw is changed in either direction, can be observed from the dynamic-pressure measurements. The results (fig. 17 and table IV) show that the dynamic pressure at the vertical tail is highest for negative angles of yaw and is lowest for positive angles of yaw. These results indicate that the contribution of the vertical tail to the directional stability of the airplane with the propeller operating will be greatest at negative angles of yaw.

Effect of slipstream on vertical tail.- Experimental increments of lateral-force and yawing-moment coefficients

due only to the effects of the propeller slipstream on the vertical tail surface were obtained from the data of figure 8. The increments, which are the difference between the increments of C_Y and C_n due to the vertical tail with the propeller operating and with the propeller removed, are shown in figure 18. In general, these results substantiate the conclusions drawn from the air-flow surveys in regard to the effects of the propeller slipstream on the vertical-tail contribution to the airplane directional stability. The variation of ΔC_{nt_s}

with angle of yaw is such as to decrease the airplane directional stability at high positive angles of yaw and to increase the directional stability at high negative angles of yaw. Except at $T_c = 0.01$, at which the effects of the slipstream are small, the directional stability is increased for all conditions in the low-yaw-angle range (between $\pm 5^\circ$) as a result of the slipstream. This stabilizing effect of the slipstream at small angles of yaw increases as the thrust coefficient increases.

The total increments of C_n and C_Y due to the vertical tail are given in figures 19 and 20 for the conditions with the propeller operating. These increments were obtained from the data of figure 8 as the differences between the propeller-operating results with the vertical tail installed on the airplane and with the vertical tail removed. Also shown in figures 19 and 20 are increments of C_{nt} and C_{Y_t} that were calculated from equations (1) and (2) by use of the air-flow-survey data with the propeller operating and the effective lift-curve slope of the vertical tail determined from the data for the propeller-removed conditions. Curves showing the variations of the air-flow factor with angle of yaw for the propeller-operating conditions are given in figure 21. The agreement between the calculated and the experimental results shown in figures 19 and 20 is good.

Experimental values of the slope $\frac{d(\psi - \sigma_{av})(q/q_0)_{av}}{d\psi}$,

which is used in equations (3) and (4) for calculating the contribution of the vertical tail to the airplane directional stability, are given in table V. These values show that the effect of the vertical tail in increasing the airplane directional stability is greatest for the conditions with the highest thrust coefficients and decreases as the thrust coefficient decreases.

Numerical values of $C_{n\psi_t}$ and $C_{y\psi_t}$ obtained from the force tests and calculated from equations (3) and (4) by use of the air-flow-survey data and the tail lift-curve slope previously determined are also given in table V. The satisfactory agreement between the results indicates that little change in the effective slope of the lift curve of the tail occurs as a result of the propeller slipstream.

DIRECTIONAL TRIM

The results of the rudder-effectiveness tests are given in figures 22(a) to 22(c) for the airplane with the flaps retracted and the propeller operating to simulate a gliding condition and two low-speed climb conditions and in figures 22(d) and 22(e) for the airplane with the flaps deflected 50° and the propeller operating to simulate a landing and a wave-off condition. The results of the tests with the propeller removed are given in figure 23 for the airplane with flaps retracted and with flaps deflected 50° . The more important results of the rudder-effectiveness tests are summarized in figure 24, which shows curves of $dC_n/d\delta_r$, $(\delta_r)_{C_n=0}$, and $(C_y)_{C_n=0}$ plotted against angle of yaw for each condition investigated. All the values of the slope $dC_n/d\delta_r$ were measured at zero rudder deflection as a basis for comparison.

For the propeller-removed conditions, $dC_n/d\delta_r$ reaches its minimum value near zero angle of yaw and increases as the angle of yaw is increased in either direction (fig. 24). The dynamic-pressure losses at the vertical tail are greatest at zero yaw, and the losses decrease as the angle of yaw is increased in either direction. For the propeller-operating conditions, the rudder effectiveness increases as the thrust coefficient increases from one particular condition to another because of an increase in the dynamic-pressure ratio at the vertical tail (fig. 24). For all the conditions investigated with the propeller operating, except the gliding condition with flaps retracted, $dC_n/d\delta_r$ attains its maximum value at high negative angles of yaw and its minimum value at high positive

angles of yaw (fig. 24); the dynamic pressure at the vertical tail reaches its maximum value for high negative angles of yaw and reaches its minimum value for high positive angles of yaw. An analysis of the test results showed that the values of $dC_n/d\delta_r$ are very nearly directly proportional to the dynamic-pressure ratio at the vertical tail.

The rudder deflections and angles of sideslip required to trim simultaneously the airplane yawing moments and lateral forces for each condition investigated were determined from the data of figure 24 and are given in table VI. For the conditions with the propeller removed, the data show that the values of δ_r and β for zero yawing-moment coefficient are small. For the conditions with the propeller operating, the data show that the rudder deflections required for directional trim are greatest for the two low-speed high-power conditions. (See table VI.) These deflections, however, are considerably lower than the maximum available rudder travel on the Grumman XF6F-4 airplane.

The data show that the amount of rudder deflection required for directional trim in any condition is primarily dependent on the effects of the propeller slipstream on the vertical tail and on the wing-fuselage combination and, to a lesser degree, on the direct effect of the propeller forces. The increments of C_n and C_Y at zero yaw due to the effects of the slipstream on the vertical tail, the effects of the slipstream on the wing-fuselage combination, and the direct effect of the propeller forces are given in table VII for the wave-off and low-speed climb conditions. Of the total increment of C_n at zero yaw due to propeller operation for the low-speed-climb condition, 77 percent was due to slipstream effects and 23 percent was due to the effects of the propeller forces. For the wave-off condition, 98 percent of the total increment of C_n at zero yaw due to propeller operation was caused by slipstream effects.

The curves in figure 24 of $(\delta_r)_{C_n=0}$ against ψ , besides indicating the rudder deflections required to trim the airplane yawing moments, are a measure of the airplane directional stability. The conclusions regarding the airplane directional stability characteristics, which are derived from these results, are substantially the same as those derived from the curves of

figure 8 showing the variations of C_n against ψ for $\delta_r = 0$.

S U M M A R Y O F R E S U L T S

Data are presented of measurements made in the Langley full-scale tunnel on the Grumman XF6F-4 airplane to investigate the factors affecting the directional stability and trim characteristics of a typical fighter-type airplane. Although these data are quantitative for this particular airplane, the trends are believed to be generally applicable to reasonably similar airplanes. The results are summarized as follows:

1. For the conditions investigated, the value of the directional-stability parameter $C_{n\psi}$ at angles of yaw between $\pm 5^\circ$ was smallest for the gliding condition with flaps retracted ($C_{n\psi} = -0.00015$) and was largest for the wave-off condition with flaps deflected 50° ($C_{n\psi} = -0.00147$). With the values measured in the low-yaw-angle range used as a reference, the airplane directional stability for the conditions with high thrust coefficients was decreased at large positive angles of yaw and was increased at large negative angles of yaw.
2. For the XF6F-4 airplane, the variation of average sidewash angle at the vertical tail with angle of yaw was generally such as to decrease the contribution of the vertical tail to the airplane directional stability. Propeller operation increased the magnitude of the destabilizing effect of the sidewash but, at small angles of yaw, also increased the dynamic pressure at the tail sufficiently to make the combined effect stabilizing.
3. The wing-fuselage combination with flaps retracted was directionally unstable for the angle-of-attack range investigated. Increasing the angle of attack and deflecting the flaps decreased the unstable variation of yawing-moment coefficient with angle of yaw of the wing-fuselage combination.
4. For all the conditions investigated with the flaps retracted, the contribution of the propeller decreased the directional stability of the airplane at small angles of yaw. With the flaps deflected 50° , at

small angles of yaw, the contribution of the propeller increased the airplane directional stability appreciably for the wave-off condition, decreased the airplane directional stability slightly for the landing condition, and caused no appreciable change in the stability for the landing-approach condition.

5. The propeller slipstream increased the contribution of the vertical tail to the airplane directional stability at small angles of yaw. As a result of the lateral displacement of the slipstream with respect to the vertical tail, the contribution of the vertical tail to the airplane directional stability was greatest at negative angles of yaw and was smallest at positive angles of yaw.

6. The destabilizing contribution of the wing-fuselage combination to the directional stability of the airplane for the conditions with the flaps retracted, at angles of yaw between $\pm 5^\circ$, was increased by the effects of the propeller slipstream. The directional stability of the airplane for the conditions with the flaps deflected 50° was not changed appreciably by the slipstream effects on the wing-fuselage combination at angles of yaw between 5° and -15° but was considerably decreased at angles of yaw between 5° and 15° .

7. The amount of rudder deflection required for directional trim is primarily dependent on the slipstream effects and only secondarily dependent on the direct effect of the propeller forces. Of the total increment of yawing-moment coefficient at zero yaw due to propeller operation for the low-speed climb condition, 77 percent was due to slipstream effects and 23 percent was due to the effects of the propeller forces. For the wave-off condition, 98 percent of the total increment of yawing-moment coefficient at zero yaw due to propeller operation was caused by slipstream effects. The wave-off condition, at a lift coefficient of 1.39, required the largest amount of rudder deflection for trim ($\delta_r = -18.5^\circ$).

8. A comparison of the results of the extensive airflow surveys with the results of the force tests made possible the determination of a value for the effective-lift-curve slope of the vertical tail; this value permitted

calculation of the contribution of the vertical tail to the directional stability of the airplane within acceptable limits.

Langley Memorial Aeronautical Laboratory
National Advisory Committee for Aeronautics
Langley Field, Va.

R E F E R E N C E S

1. Pass, H. R.: Analysis of Wind-Tunnel Data on Directional Stability and Control. NACA TN No. 775, 1940.
2. Imlay, Frederick H.: The Estimation of the Rate of Change of Yawing Moment with Sideslip. NACA TN No. 636, 1938.
3. Shortal, Joseph A.: Effect of Tip Shape and Dihedral on Lateral-Stability Characteristics. NACA Rep. No. 548, 1935.
4. Recant, I. G., and Wallace, Arthur R.: Wind-Tunnel Investigation of Effect of Yaw on Lateral-Stability Characteristics. IV - Symmetrically Tapered Wing with a Circular Fuselage Having a Wedge-Shaped Rear and a Vertical Tail. NACA ARR, March 1942.
5. Recant, Isidore G., and Wallace, Arthur R.: Wind-Tunnel Investigation of the Effect of Vertical Position of the Wing on the Side Flow in the Region of the Vertical Tail. NACA TN No. 804, 1941.
6. Katzoff, S., and Mutterperl, William: The End-Plate Effect of a Horizontal-Tail Surface on a Vertical-Tail Surface. NACA TN No. 797, 1941.
7. Ribner, Herbert S.: Notes on the Propeller and Slipstream in Relation to Stability. NACA ARR No. L4I12a, 1944.

TABLE I.- VALUES OF $C_{n\psi}$ AND $C_{Y\psi}$ FOR COMPLETE AIRPLANE WITH PROPELLER OPERATING

Condition	Power	δ_f (deg)	α (deg)	C_L	V_i (mph)	$C_{n\psi}$ (a)	$C_{Y\psi}$ (a)
Climb	Rated ($T_c = 0.05$)	0	1.0	0.24	235	-0.00050	0.0075
Climb	Rated ($T_c = 0.11$)	0	3.4	.43	176	-.00043	.0075
Climb	Rated ($T_c = 0.30$)	0	8.9	.96	118	-.00046	.0076
Climb	Rated ($T_c = 0.51$)	0	12.3	1.39	98	-.00033	.0070
Glide	Idling ($T_c = 0.01$)	0	9.2	.83	127	-.00015	.0043
Landing approach	0.65 rated ($T_c = 0.33$)	50	5.8	1.37	99	-.00066	.0099
Wave-off	Rated ($T_c = 0.51$)	50	4.9	1.39	98	-.00147	.0197
Landing	Idling ($T_c = 0.01$)	50	11.8	1.58	92	-.00046	.0038

^aValues given for slopes are average values between $\psi = 5^\circ$ and $\psi = -5^\circ$.

NATIONAL ADVISORY
COMMITTEE FOR AERONAUTICS

TABLE II.- WEIGHTED AVERAGE VALUES OF SIDEWASH ANGLE AND DYNAMIC-PRESSURE RATIO AT VERTICAL TAIL; PROPELLER REMOVED

NACA ARR No. 15H09

FLAPS RETRACTED								
ψ (deg)	σ_{av} (deg)	$\left(\frac{q}{q_0}\right)_{av}$	σ_{av} (deg)	$\left(\frac{q}{q_0}\right)_{av}$	σ_{av} (deg)	$\left(\frac{q}{q_0}\right)_{av}$	σ_{av} (deg)	$\left(\frac{q}{q_0}\right)_{av}$
	$\alpha = 1.00^\circ$ $C_L = 0.23$		$\alpha = 3.4^\circ$ $C_L = 0.40$		$\alpha = 9.2^\circ$ $C_L = 0.83$		$\alpha = 13.0^\circ$ $C_L = 1.08$	
-14.6	-0.1	1.00	-1.7	0.94	-2.2	0.88	-2.0	0.82
-9.9	.4	.98	0	.96	-1.7	.88	-2.4	.78
-5.1	.8	.97	.1	.94	-1.3	.91	-1.2	.85
0	1.2	.92	.6	.91	-1.0	.87	0	.71
5.0	.8	.94	.7	.93	.8	.90	1.7	.88
10.0	1.1	1.00	1.0	1.00	2.1	.90	2.1	.77
14.7	1.4	.97	1.9	.96	2.2	.86	1.5	.77
FLAPS DEFLECTED 50°								
ψ (deg)	σ_{av} (deg)	$\left(\frac{q}{q_0}\right)_{av}$	σ_{av} (deg)	$\left(\frac{q}{q_0}\right)_{av}$	σ_{av} (deg)	$\left(\frac{q}{q_0}\right)_{av}$		
	$\alpha = 5.6^\circ$ $C_L = 1.09$		$\alpha = 6.3^\circ$ $C_L = 1.11$		$\alpha = 11.8^\circ$ $C_L = 1.56$			
-14.6	-2.8	0.94	-2.9	0.95	-2.8	0.88		
-9.9	-3.2	.96	-3.9	.93	-2.9	.88		
-5.1	-4.3	.94	-4.2	.90	-1.9	.88		
0	-2.1	.92	-2.0	.90	-1.7	.86		
5.0	.4	.92	.6	.93	.7	.90		
10.0	1.5	.98	1.8	.96	1.2	.91		
14.7	1.4	.97	1.7	.96	1.7	.92		

NATIONAL ADVISORY
COMMITTEE FOR AERONAUTICS

TABLE III.- CONTRIBUTION OF VERTICAL TAIL TO $C_{Y\psi}$ AND $C_{n\psi}$; PROPELLER REMOVED

a (deg)	C_L	δ_f (deg)	$\frac{d(\psi - \sigma_{av}) \left(\frac{q}{q_0} \right)_{av}}{d\psi}$ (a)	$C_{Y\psi t}$ (a)		$C_{n\psi t}$ (a)	
				From force tests	Calculated from surveys	From force tests	Calculated from surveys
1.0	0.23	0	0.94	0.0021	0.0019	-0.00086	-0.00087
3.4	.43	0	.91	.0019	.0019	-.00089	-.00084
8.9	.80	0	.74	.0012	.0015	-.00070	-.00069
9.2	.83	0	.71	.0012	.0014	-.00058	-.00066
12.3	1.04	0	.58	.0010	.0012	-.00050	-.00054
4.9	1.04	50	.55	.0011	.0011	-.00060	-.00051
5.8	1.11	50	.48	.0010	.0010	-.00066	-.00045
11.8	1.56	50	.64	.0012	.0013	-.00043	-.00059

^aValues given for slopes are average values between $\psi = 5^\circ$ and $\psi = -5^\circ$.

NATIONAL ADVISORY
COMMITTEE FOR AERONAUTICS

TABLE IV.- WEIGHTED AVERAGE VALUES OF SIDEWASH ANGLE AND DYNAMIC-PRESSURE RATIO AT THE VERTICAL TAIL; PROPELLER OPERATING

FLAPS RETRACTED										
Angle of yaw, ψ (deg)	σ_{av} (deg)	$\left(\frac{q}{q_0}\right)_{av}$	σ_{av} (deg)	$\left(\frac{q}{q_0}\right)_{av}$	σ_{av} (deg)	$\left(\frac{q}{q_0}\right)_{av}$	σ_{av} (deg)	$\left(\frac{q}{q_0}\right)_{av}$	σ_{av} (deg)	$\left(\frac{q}{q_0}\right)_{av}$
	$\alpha = 1.0^\circ$ $C_L = 0.24$ Rated power ($T_c = 0.05$)		$\alpha = 3.4^\circ$ $C_L = 0.43$ Rated power ($T_c = 0.11$)		$\alpha = 8.9^\circ$ $C_L = 0.96$ Rated power ($T_c = 0.30$)		$\alpha = 9.2^\circ$ $C_L = 0.83$ $T_c = 0.01$		$\alpha = 12.3^\circ$ $C_L = 1.39$ Rated power ($T_c = 0.51$)	
-14.6	-2.2	1.16	-3.6	1.30	-7.3	2.18	-3.6	1.11	-12.4	2.54
-9.9	-1.5	1.21	-3.5	1.46	-5.2	1.98	-4.0	1.10	-12.0	2.34
-5.1	-.6	1.16	-2.6	1.17	-5.7	1.85	-2.1	1.00	-7.9	2.29
0	-.8	1.12	-1.7	1.20	-3.7	1.66	-1.1	.97	-6.8	2.55
5.0	-.7	1.09	-1.1	1.23	-2.6	1.76	1.0	.90	-4.3	2.38
10.0	-.1	1.16	-.8	1.31	-2.1	1.71	1.0	1.01	-3.5	1.61
14.7	1.7	1.05	.8	1.14	.9	1.26	1.9	.97	-.8	1.38
FLAPS DEFLECTED 50°										
Angle of yaw, ψ (deg)	σ_{av} (deg)	$\left(\frac{q}{q_0}\right)_{av}$	σ_{av} (deg)	$\left(\frac{q}{q_0}\right)_{av}$	σ_{av} (deg)	$\left(\frac{q}{q_0}\right)_{av}$	σ_{av} (deg)	$\left(\frac{q}{q_0}\right)_{av}$	σ_{av} (deg)	$\left(\frac{q}{q_0}\right)_{av}$
	$\alpha = 4.9^\circ$ $C_L = 1.39$ Rated power ($T_c = 0.51$)		$\alpha = 5.8^\circ$ $C_L = 1.37$ 0.65 rated power ($T_c = 0.33$)			$\alpha = 11.8^\circ$ $C_L = 1.58$ $T_c = 0.01$				
-14.6	-7.9	2.74	-6.3	1.87	-4.2				1.29	
-9.9	-7.0	2.35	-6.7	1.73	-4.8				1.11	
-5.1	-7.2	2.30	-6.5	1.70	-4.4				.98	
0	-5.2	2.57	-4.1	1.72	-2.0				.95	
5.0	-3.9	2.53	-3.9	1.79	.1				.90	
10.0	-3.7	1.73	-3.2	1.55	1.4				1.02	
14.7	-2.6	1.23	-1.5	1.19	.6				1.00	

TABLE V.- CONTRIBUTION OF VERTICAL TAIL TO $C_{n\psi_t}$ AND $C_{Y\psi_t}$; PROPELLER OPERATING

α (deg)	C_L	Power	δ_f (deg)	$d(\psi - \sigma_{av}) \left(\frac{q}{q_0} \right)_{av}$	$C_{Y\psi_t}$ (a)		$C_{n\psi_t}$ (a)	
				$d\psi$ (a)	From force tests	Calculated from surveys	From force tests	Calculated from surveys
1.0	0.24	Rated ($T_c = 0.05$)	0	1.15	0.0025	0.0023	-0.00114	-0.00106
3.4	.43	Rated ($T_c = 0.11$)	0	1.09	.0022	.0022	-.00099	-.00101
8.9	.96	Rated ($T_c = 0.30$)	0	1.38	.0030	.0028	-.00124	-.00128
9.2	.83	$T_c = 0.01$	0	.70	.0014	.0014	-.00062	-.00065
12.3	1.39	Rated ($T_c = 0.51$)	0	1.42	.0025	.0029	-.00126	-.00131
4.9	1.39	Rated ($T_c = 0.51$)	50	1.77	.0039	.0036	-.00183	-.00164
5.8	1.37	0.65 rated ($T_c = 0.33$)	50	1.31	.0032	.0027	-.00105	-.00121
11.8	1.58	$T_c = 0.01$	50	.51	.0012	.0010	-.00050	-.00047

^aValues given for slopes are average values between $\psi = 5^\circ$ and $\psi = -5^\circ$.

NATIONAL ADVISORY
COMMITTEE FOR AERONAUTICS

TABLE VI.- DIRECTIONAL TRIM CHARACTERISTICS OF THE XF6F-4 AIRPLANE

Condition	Power	δ_f (deg)	α (deg)	C_L	δ_r ($C_n = 0;$ $C_Y = 0$) (deg)	β ($C_n = 0;$ $C_Y = 0$) (deg)
-----	Propeller removed	$\left\{ \begin{array}{l} 0 \\ 0 \\ 50 \\ 50 \end{array} \right.$	9.2	0.83	-0.3	0.6
-----			13.0	1.08	.6	1.2
-----			5.6	1.09	-.4	3.2
-----			11.8	1.56	6.0	6.0
Climb	Rated ($T_c = 0.30$)	0	8.9	.96	-11.5	-7.6
Climb	Rated ($T_c = 0.51$)	0	12.3	1.39	-15.0	-11.0
Glide	$T_c = 0.01$	0	9.2	.83	-3.0	-.4
Wave-off	Rated ($T_c = 0.51$)	50	4.9	1.39	-18.5	-4.8
Landing	$T_c = 0.01$	50	11.8	1.58	-3.7	-.4

NATIONAL ADVISORY
COMMITTEE FOR AERONAUTICS

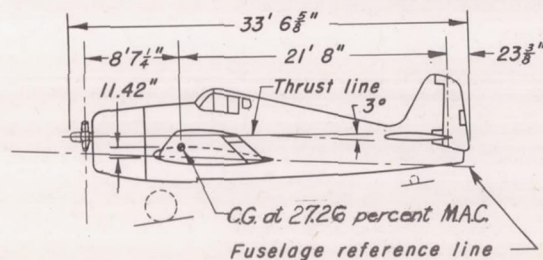
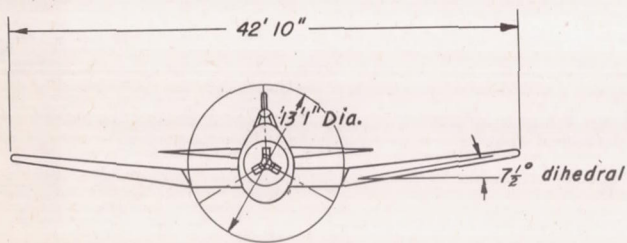
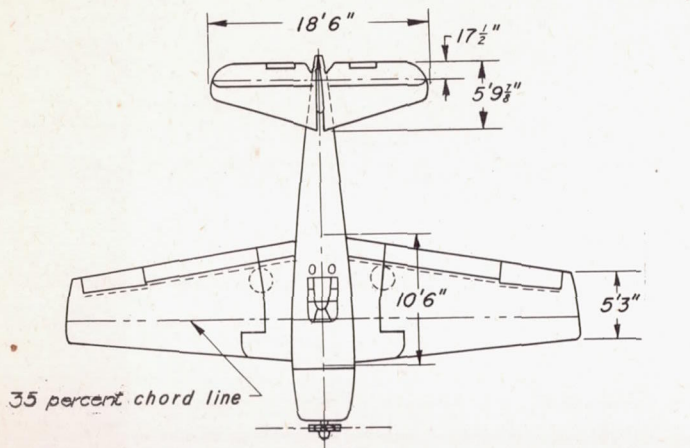
TABLE VII.- INCREMENTS OF C_n AND C_Y AT ZERO YAW DUE TO
PROPELLER OPERATION

Condition	Power	Increment due to effect of slipstream on wing-fuselage combination		Increment due to effect of slipstream on vertical tail		Increment due to direct effect of propeller forces	
		ΔC_n	ΔC_Y	ΔC_n	ΔC_Y	ΔC_n	ΔC_Y
Low-speed climb ($\delta_f = 0^\circ$; $\alpha = 12.3^\circ$; $C_L = 1.39$)	Rated ($T_c = 0.51$)	-0.0022	-0.064	-0.0144	0.016	0.0049	-----
Wave-off ($\delta_f = 50^\circ$; $\alpha = 4.9^\circ$; $C_L = 1.39$)	Rated ($T_c = 0.51$)	-0.0146	-0.028	-0.0100	0.018	-0.0010	-----

NATIONAL ADVISORY
COMMITTEE FOR AERONAUTICS

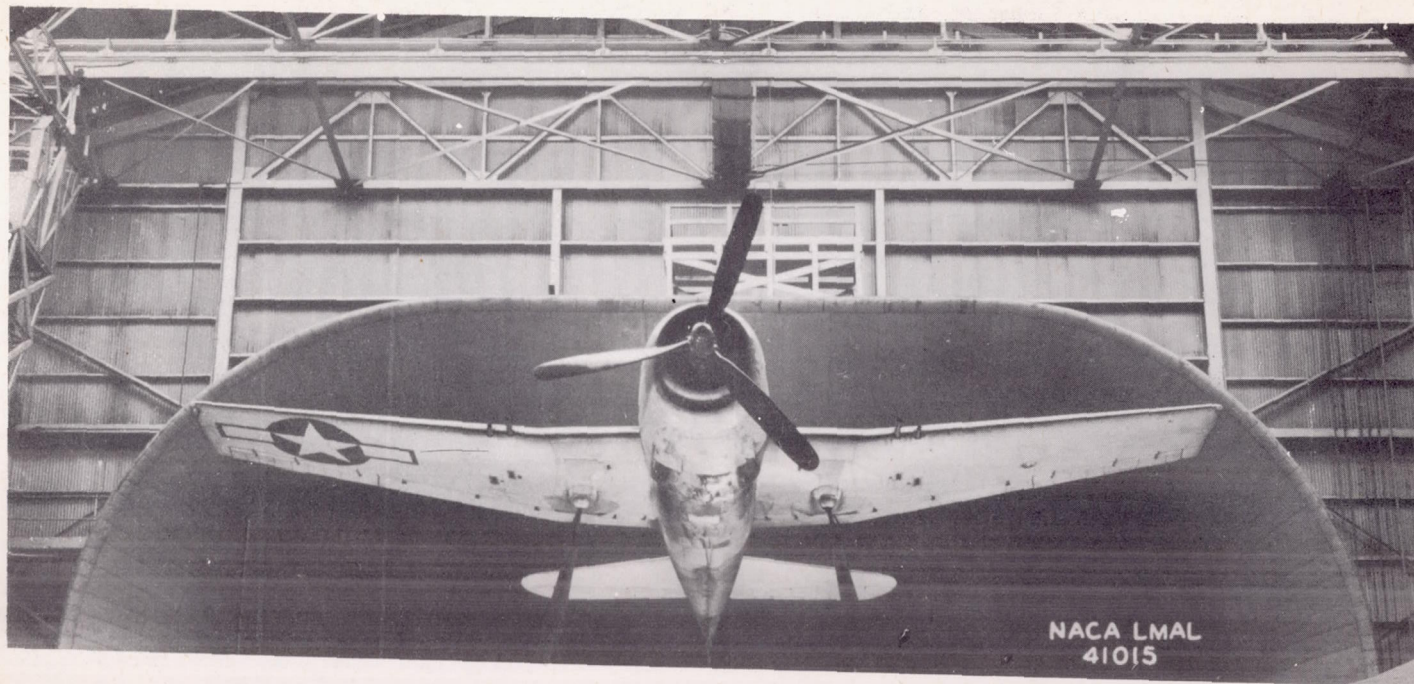
Wing area (including ailerons, flaps, and 48.5 sq ft of body area) 334 sq ft
 Control surface areas:
 Full flap area (NACA slotted) 39.8 sq ft
 Total horizontal tail surface area... 77.84 sq ft
 Fin area (incl. 1.9 sq ft of contained rudder balance)..... 14.4 sq ft
 Rudder area aft of hinge (incl. 0.62 sq ft of tab)..... 9.0 sq ft

Engine..... Pratt and Whitney R-2800-27
 BHP normal rating, 1600 at 2400 rpm at 5700 ft
 Hamilton Standard Hydromatic Propeller,
 Blade Design 6501A-0
 Propeller gear ratio, 2:1
 Gross weight, 11,400 lb



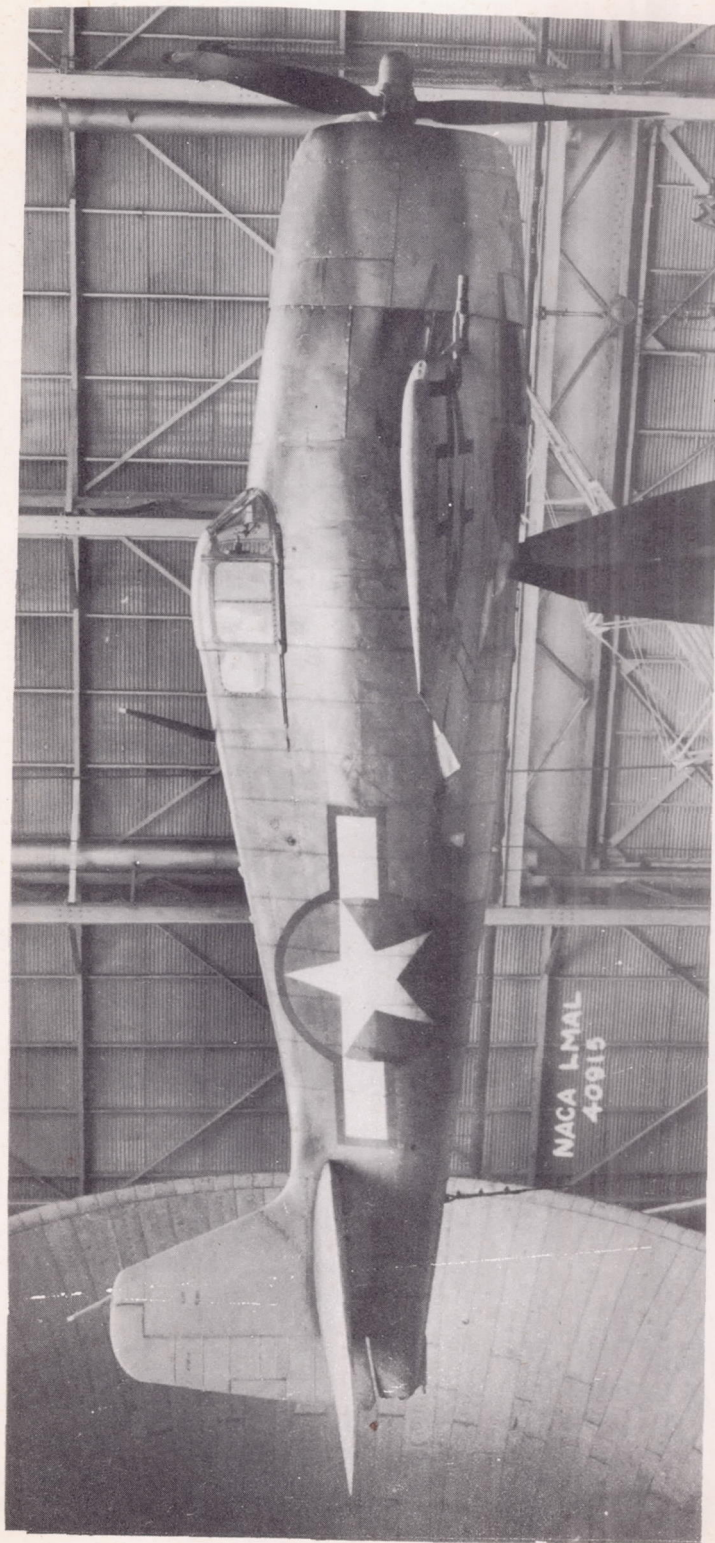
NATIONAL ADVISORY
 COMMITTEE FOR AERONAUTICS

Figure 1.- Three-view drawing of the XF6F-4 airplane.



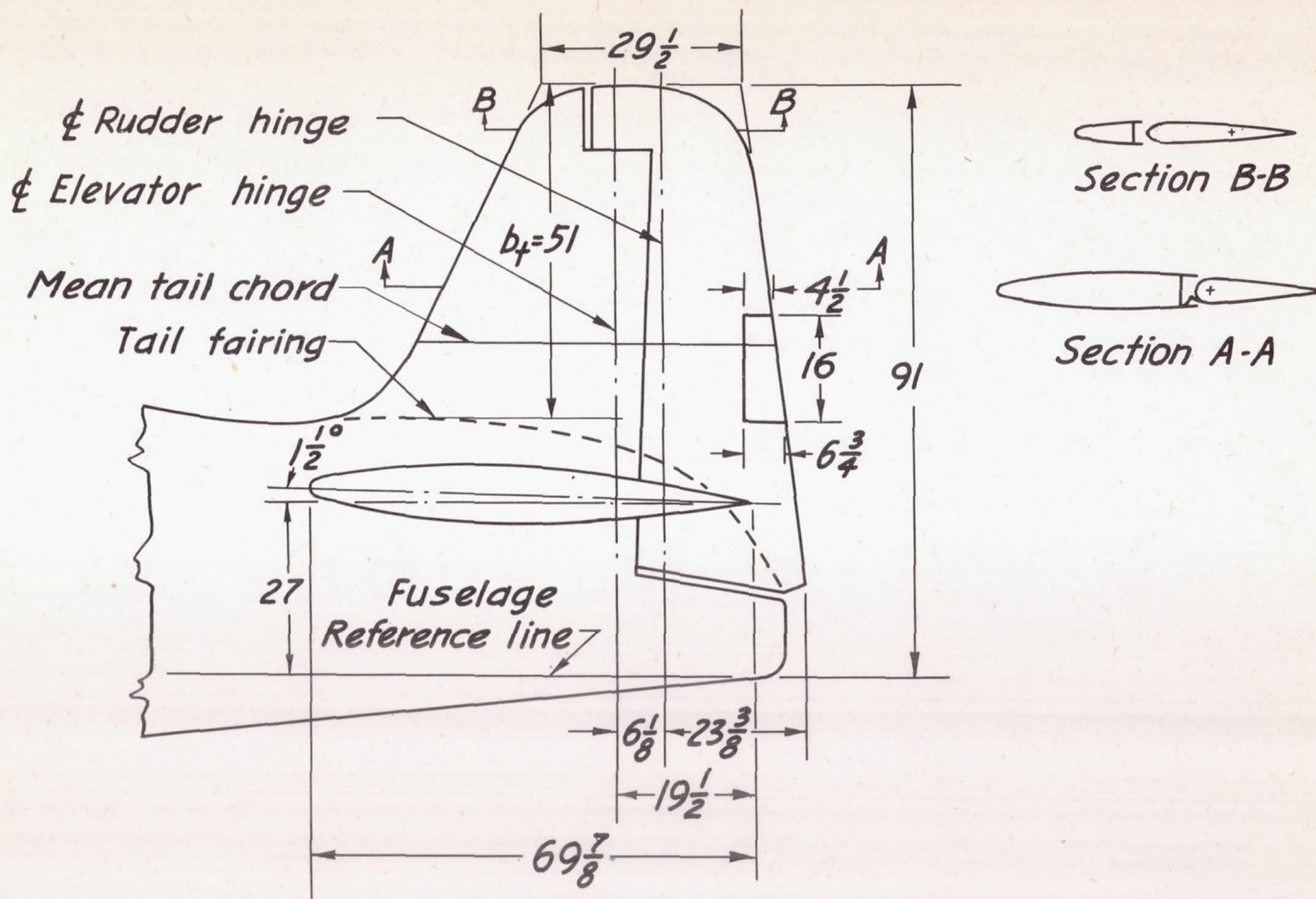
(a) Front view.

Figure 2.- Grumman XF6F-4 airplane mounted in Langley full-scale tunnel.



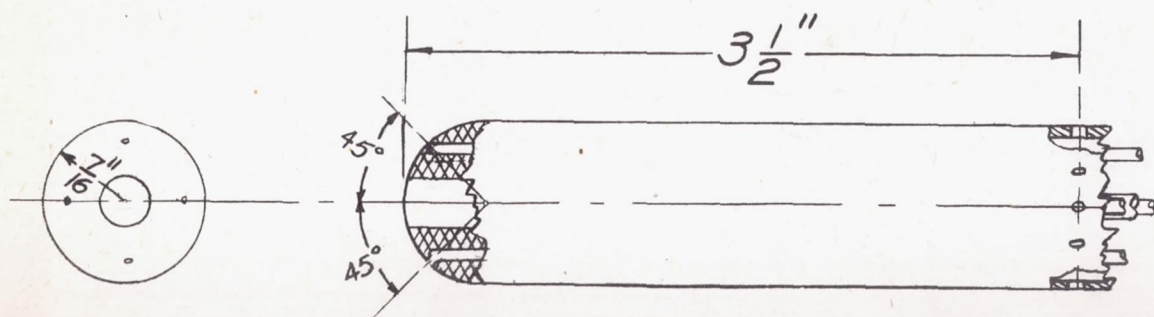
(b) Side view.

Figure 2.- Concluded.



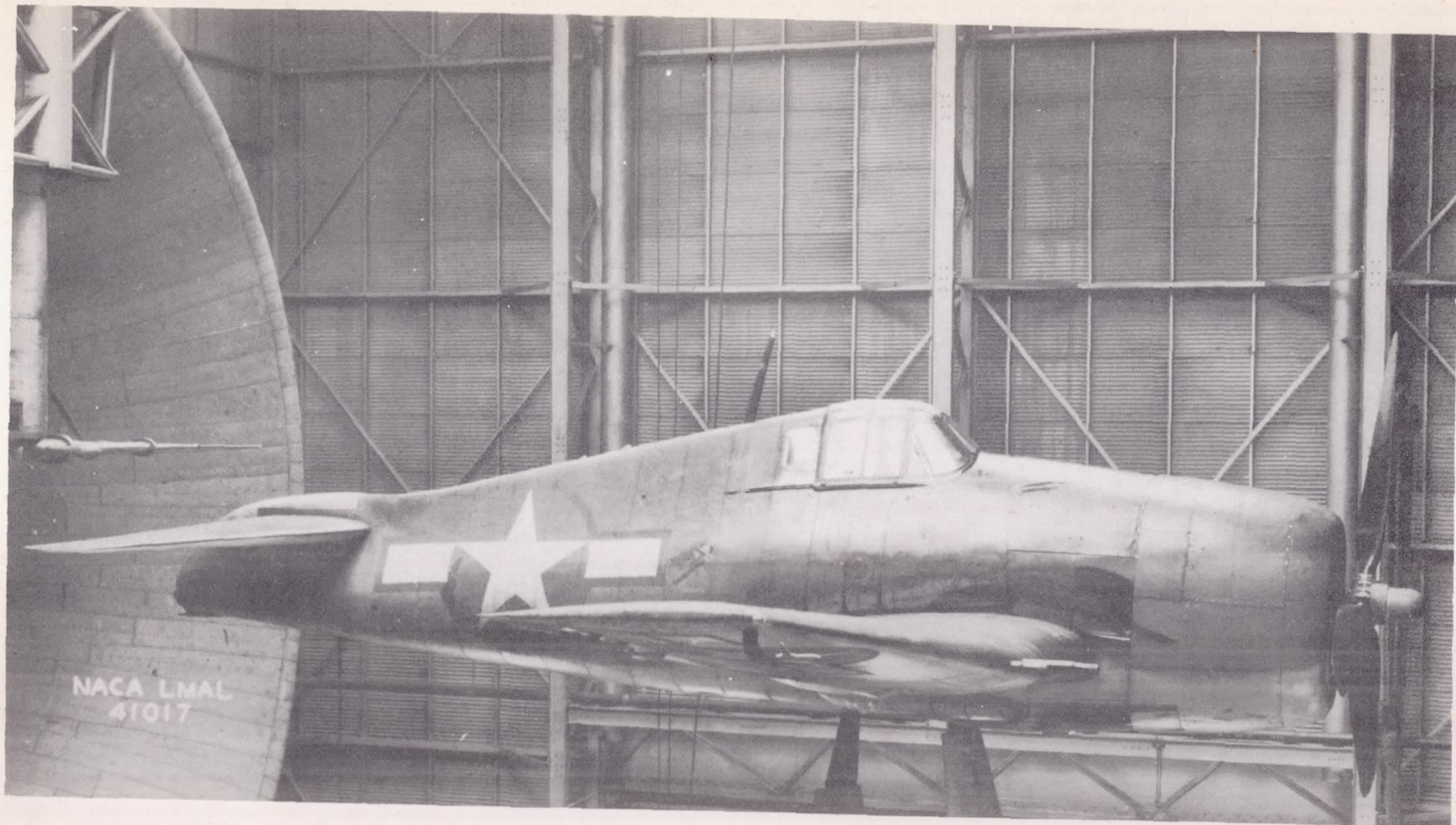
NATIONAL ADVISORY
 COMMITTEE FOR AERONAUTICS

Figure 3. - Sketch of empennage showing relation of tail fairing to vertical tail surface. (All dimensions are given in inches.)



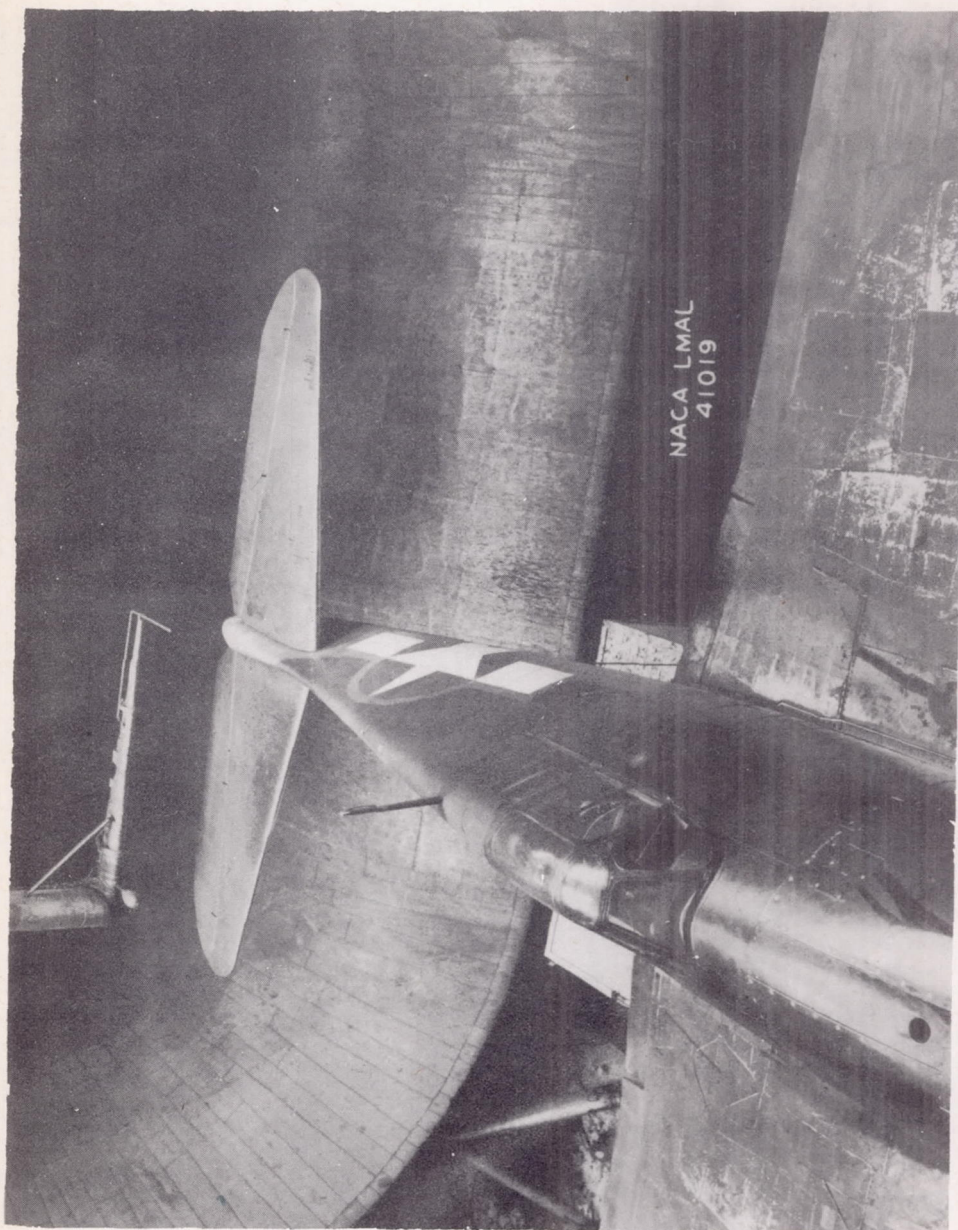
NATIONAL ADVISORY
COMMITTEE FOR AERONAUTICS

Figure 4.- Line drawing showing combined pitch, yaw, and pitot-static tube used for the surveys.



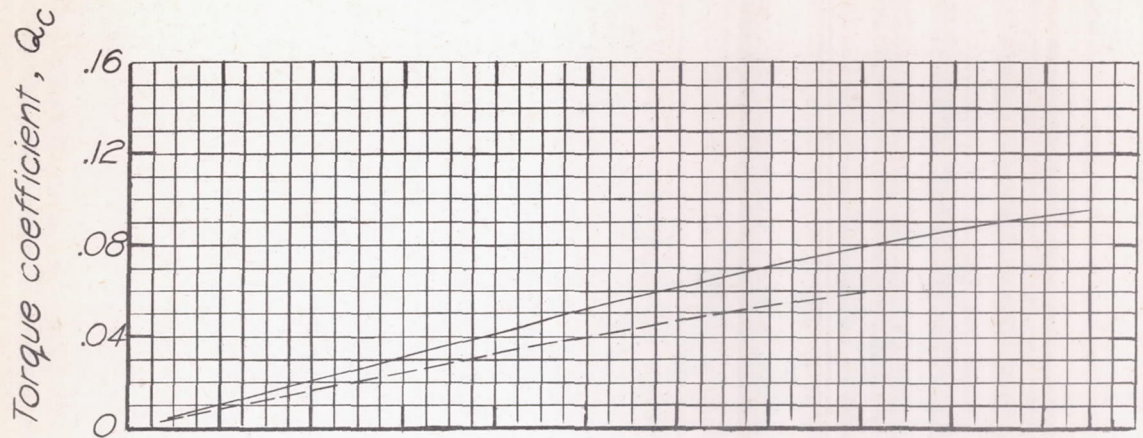
(a) Three-quarter side view.

Figure 5.- Survey tube mounted in position for air-flow measurements.

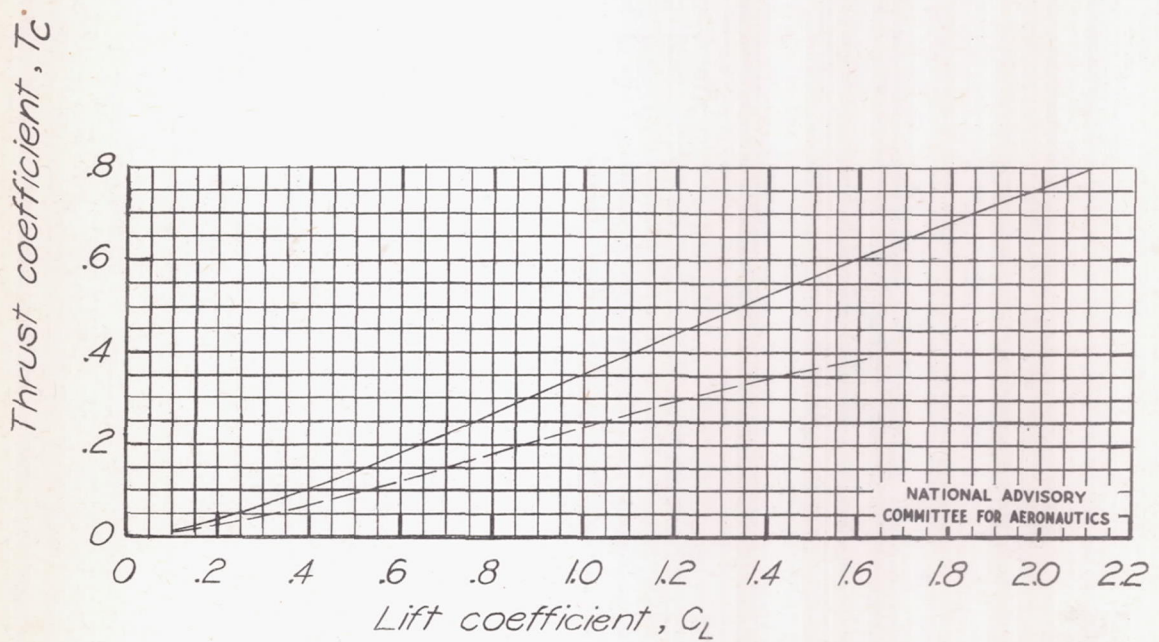


(b) Top view.

Figure 5.- Concluded.



	Horsepower	Engine rpm
— Rated power	1600	2400
- - - 0.65 rated power	1040	1960



NATIONAL ADVISORY
COMMITTEE FOR AERONAUTICS

Figure 6 .- Calculated variations of T_c and Q_c with C_L for constant-power operation at sea level.

	Horsepower	Engine rpm
——— Rated power	1600	2400
--- 0.65 rated power	1040	1960
----- $\beta, 24.8^\circ$ measured at 0.75 R		

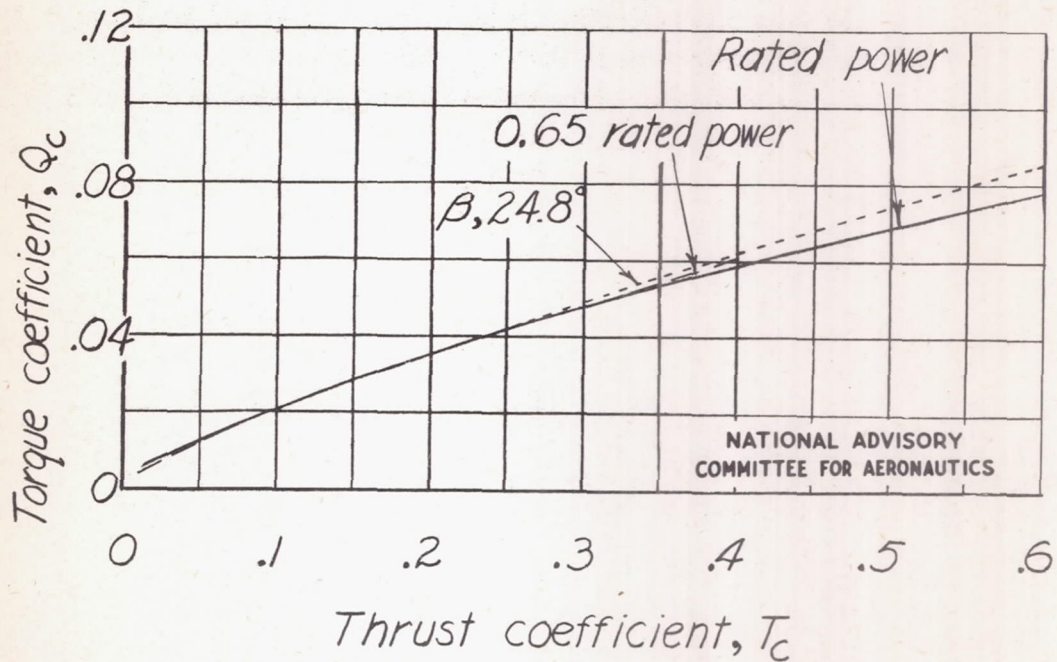
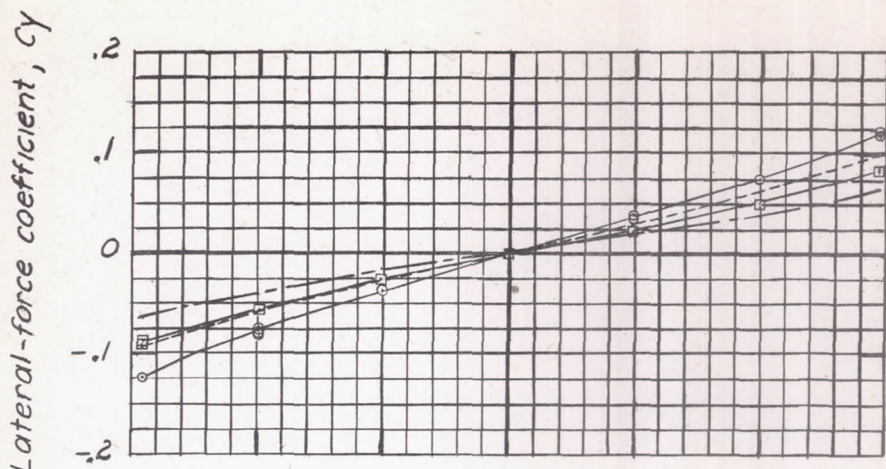
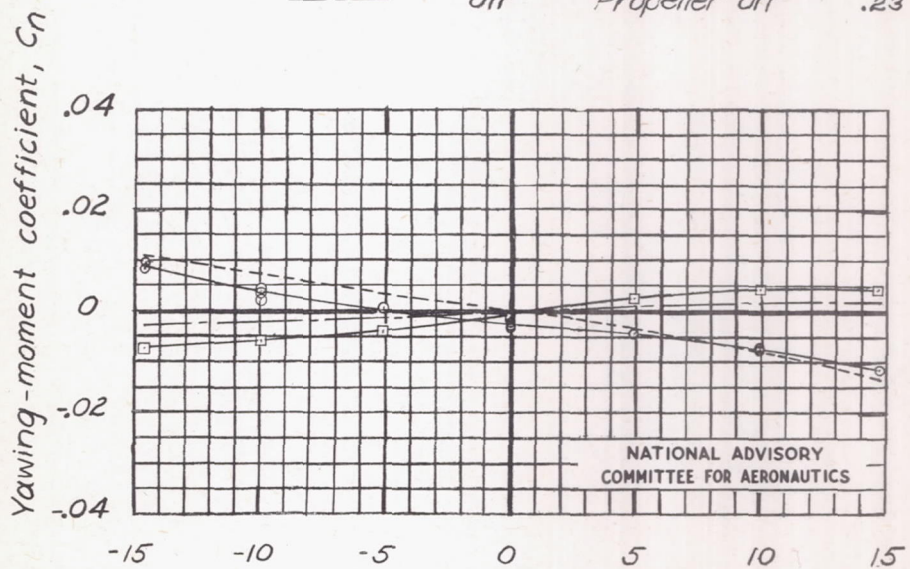


Figure 7. - Comparison of variation of T_c with Q_c for constant-power operation and for the propeller with blade angle fixed at 24.8° at 0.75 radius.



Vertical tail	Power	Lift coefficient, C_L
○	On	Rated ($T_c=0.05$) 0.24
□	Off	Rated ($T_c=0.05$) .24
○	On	Propeller off .23
□	Off	Propeller off .23

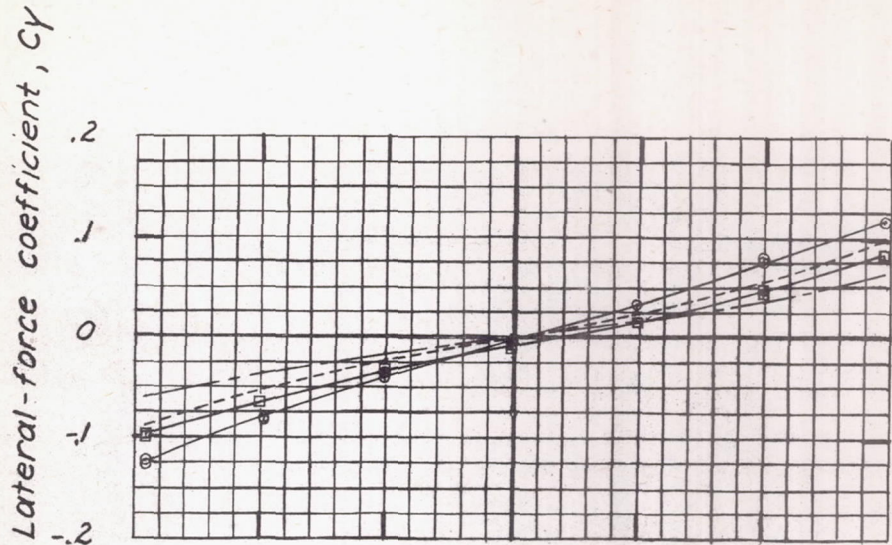


NATIONAL ADVISORY
COMMITTEE FOR AERONAUTICS

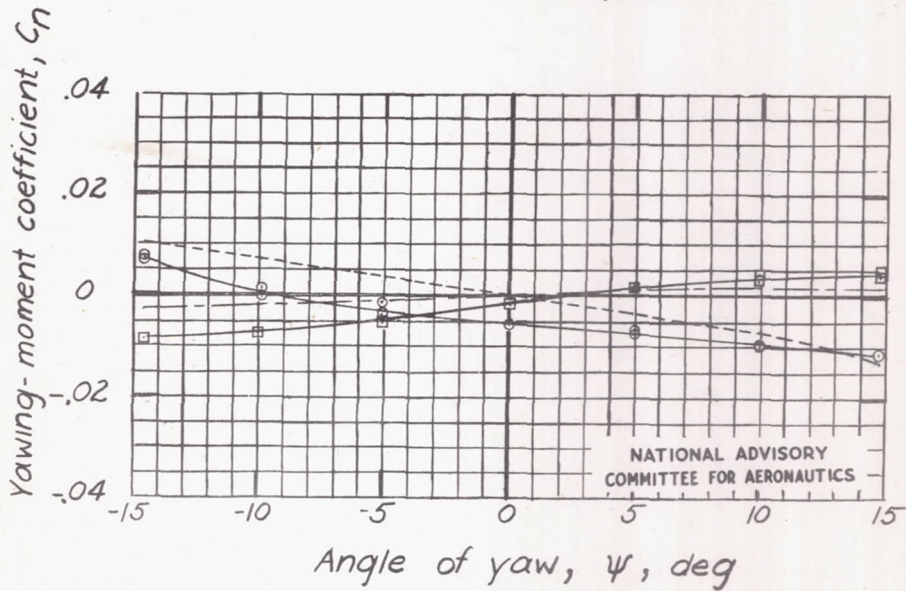
Angle of yaw, ψ , deg

(a) Climbing attitude; $\alpha, 10^\circ$; $\delta_f, 0^\circ$.

Figure 8.- Directional-stability characteristics of XF6F-4 airplane; rudder locked at 0° when on airplane.

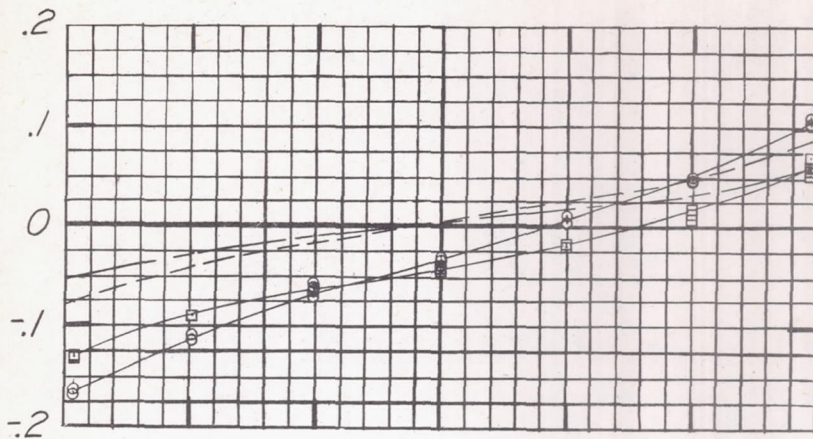


	Vertical tail	Power	Lift coefficient, C_L
—○—	On	Rated ($T_C=0.11$)	0.43
—□—	Off	Rated ($T_C=0.11$)	.43
- -○- -	On	Propeller off	.40
- -□- -	Off	Propeller off	.40



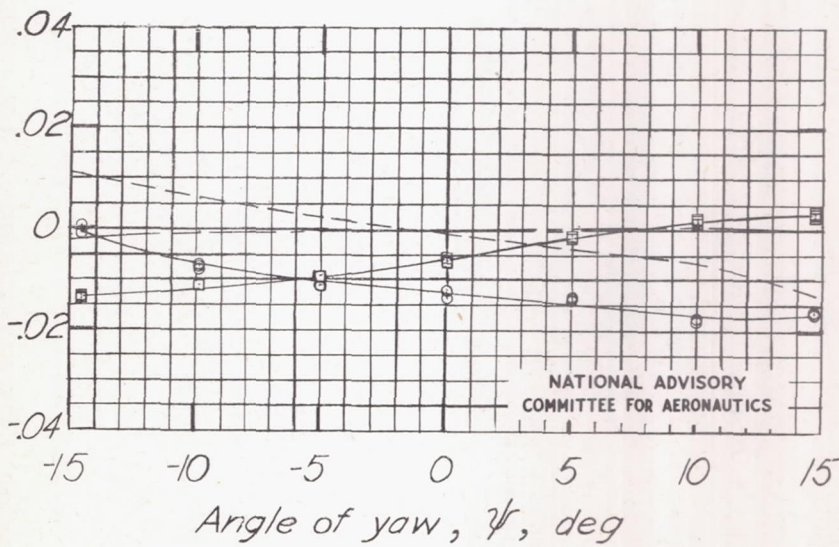
(b) Climbing attitude; $\alpha, 3.4^\circ$; $\delta_f, 0^\circ$.
Figure 8.- Continued.

Lateral-force coefficient, C_y



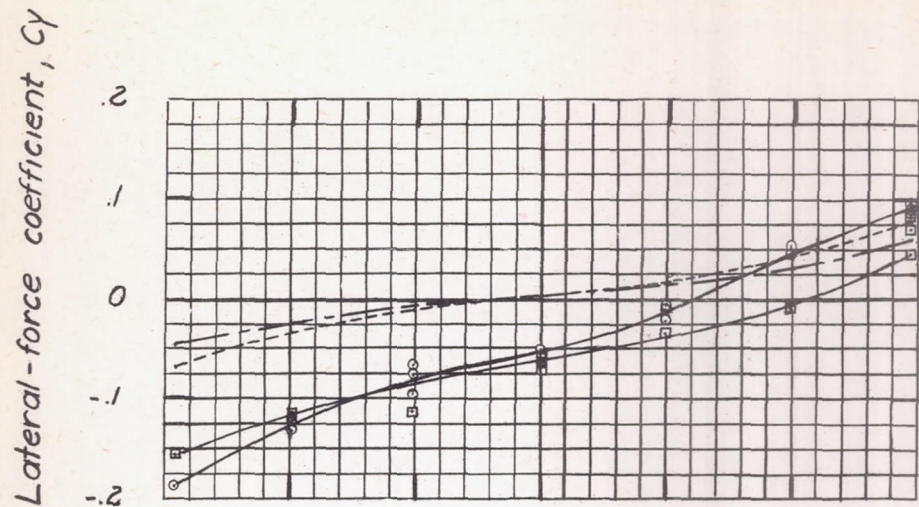
Yawing-moment coefficient, C_n

Vertical tail	Power	Lift coefficient, C_L
○	On Rated ($T_c=0.30$)	0.96
□	Off Rated ($T_c=0.30$)	.96
—	On Propeller off	.80
- - -	Off Propeller off	.80

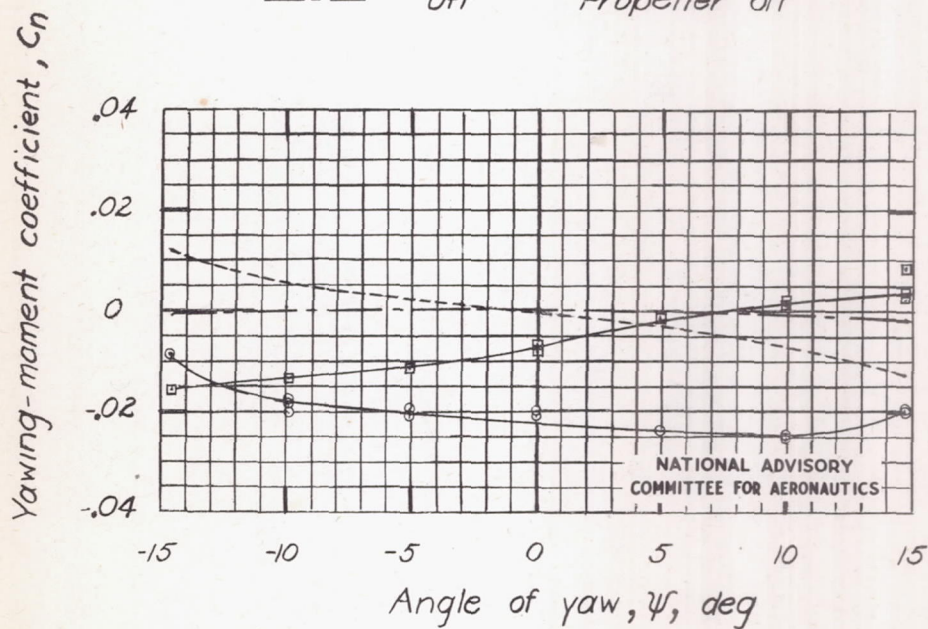


NATIONAL ADVISORY
COMMITTEE FOR AERONAUTICS

(c) Climbing attitude; $\alpha, 8.9$; $\delta_f, 0^\circ$.
Figure 8.- Continued.

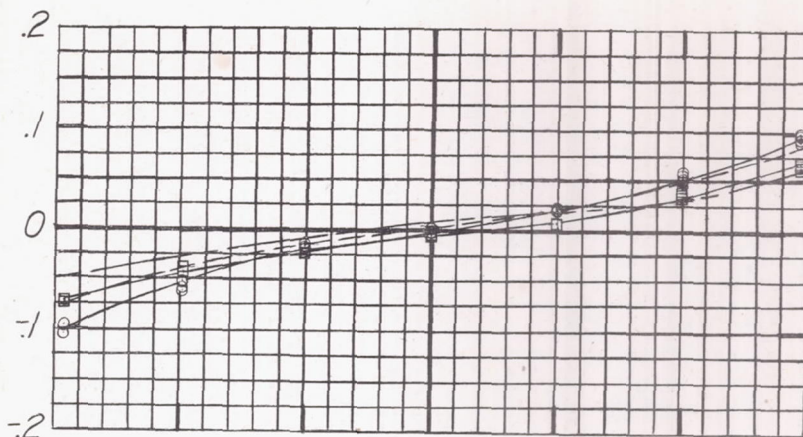


	<u>Vertical tail</u>	<u>Power</u>	<u>Lift coefficient, C_L</u>
○	On	Rated ($T_C = 0.51$)	1.39
□	Off	Rated ($T_C = 0.51$)	1.39
- - -	On	Propeller off	1.04
- · - ·	Off	Propeller off	1.04



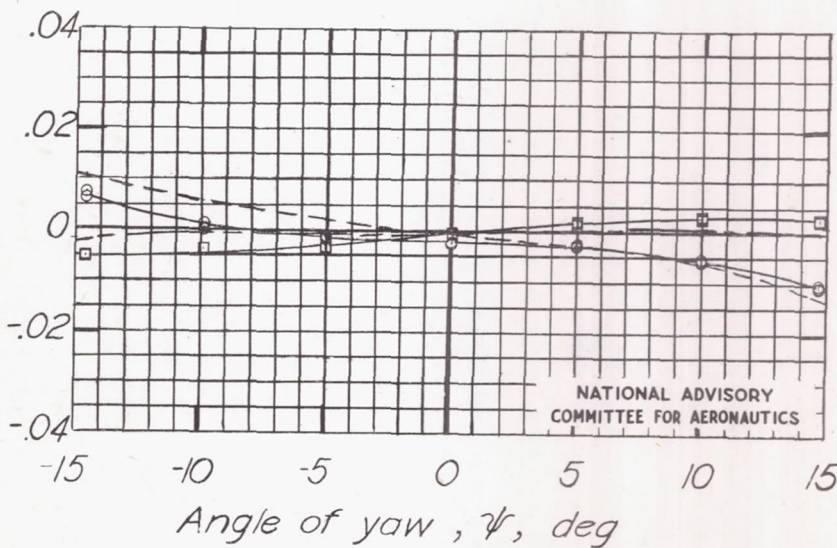
(d) Climbing attitude; $\alpha, 12.3^\circ$; $\delta_f, 0^\circ$.
Figure 8.-Continued.

Lateral-force coefficient, C_y



Vertical tail	Power	Lift coefficient, C_L
—○—	$T_c=0.01$	0.83
—□—	$T_c=0.01$.83
---	Propeller off	.83
- - -	Propeller off	.83

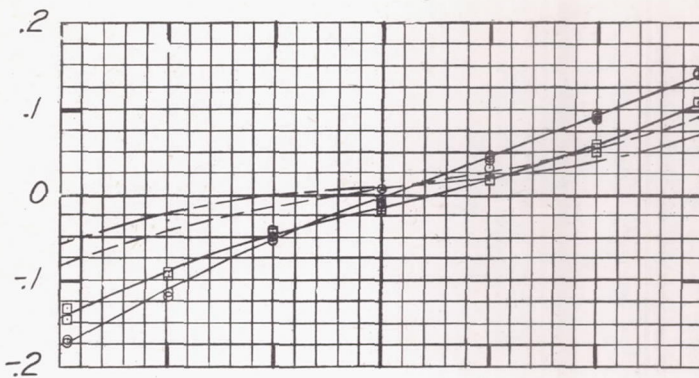
Yawing-moment coefficient, C_n



NATIONAL ADVISORY
COMMITTEE FOR AERONAUTICS

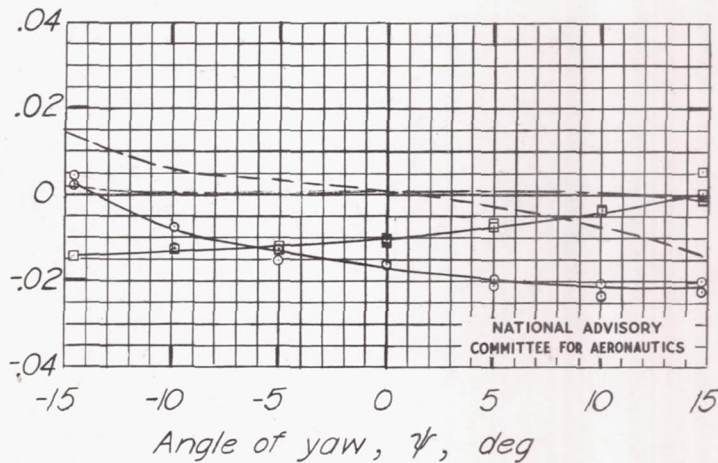
(e) Gliding attitude; $\alpha, 9.2^\circ$; $\delta_f, 0^\circ$.
Figure 8.- Continued.

Lateral-force coefficient, C_y



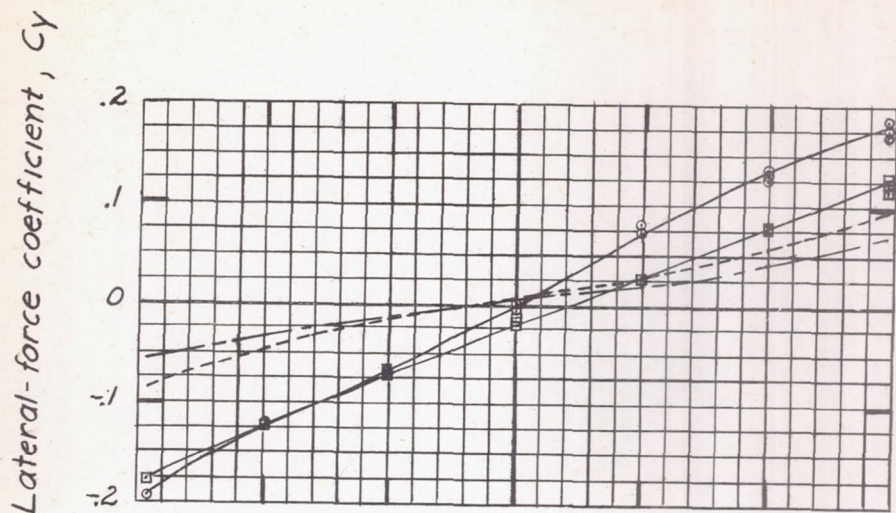
Vertical tail	Power	Lift coefficient, C_L
○	On 0.65 Rated ($T=0.33$)	1.37
□	Off 0.65 Rated ($T=0.33$)	1.37
---	On Propeller off	1.11
- · -	Off Propeller off	1.11

Yawing-moment coefficient, C_n

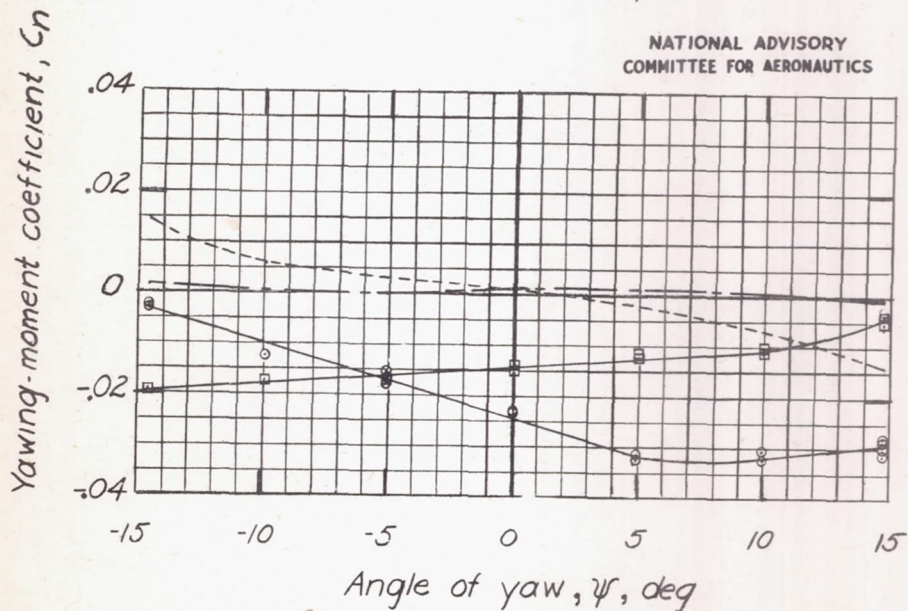


NATIONAL ADVISORY
COMMITTEE FOR AERONAUTICS

(f) Landing-approach attitude; $\alpha, 5.8^\circ$; $\delta_f, 50^\circ$.
Figure 8.- Continued.

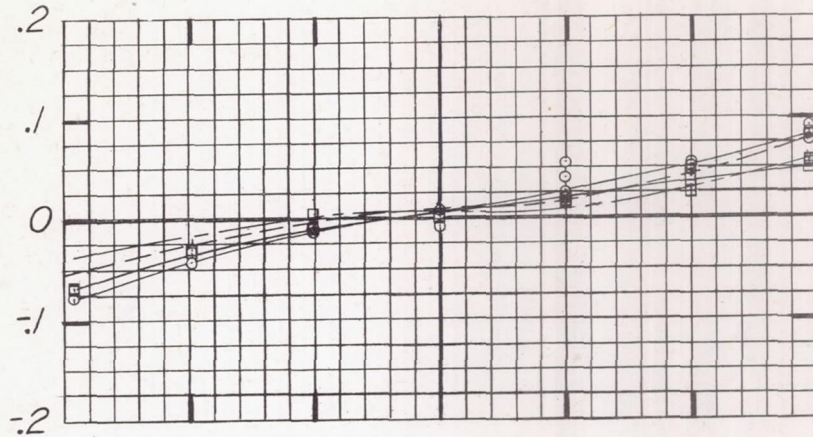


	<u>Vertical tail</u>	<u>Power</u>	<u>Lift coefficient, C_L</u>
—○—	On	Rated ($T_c = 0.5$)	1.39
—□—	Off	Rated ($T_c = 0.5$)	1.39
- -○- -	On	Propeller off	1.04
- -□- -	Off	Propeller off	1.04



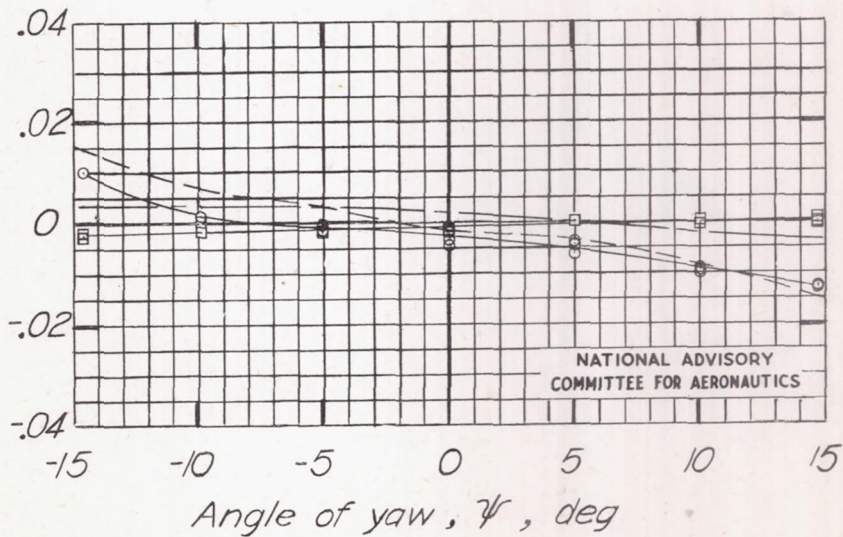
(g) Wave-off attitude; $\alpha, 4.9^\circ$; $\delta_f, 50^\circ$.
Figure 8.- Continued.

Lateral-force coefficient, C_y



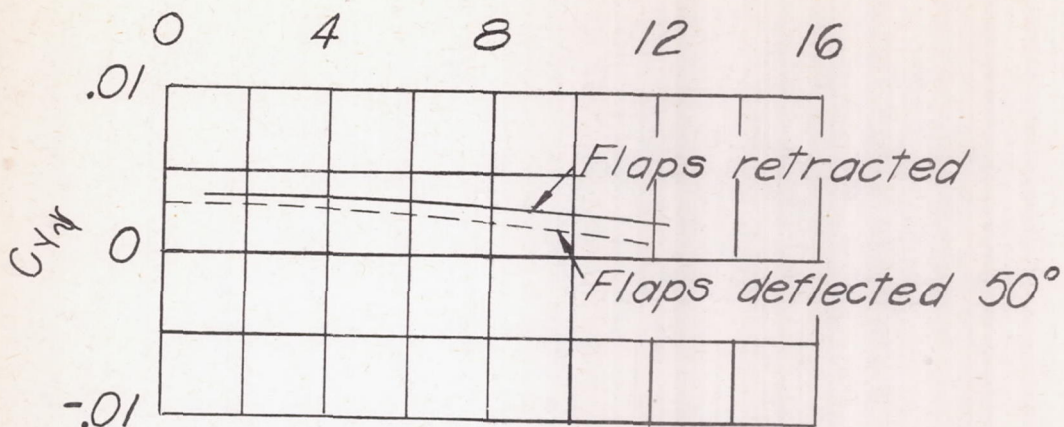
Vertical tail	Power	Lift coefficient, C_L
○	On $T_c = 0.01$	1.58
□	Off $T_c = 0.01$	1.58
---	On Propeller off	1.56
- · -	Off Propeller off	1.56

Yawing-moment coefficient, C_n



NATIONAL ADVISORY
COMMITTEE FOR AERONAUTICS

(h) Landing attitude ; $\alpha, 11.8^\circ$; $\delta_f, 50^\circ$.
Figure 8.- Concluded.



NATIONAL ADVISORY
COMMITTEE FOR AERONAUTICS

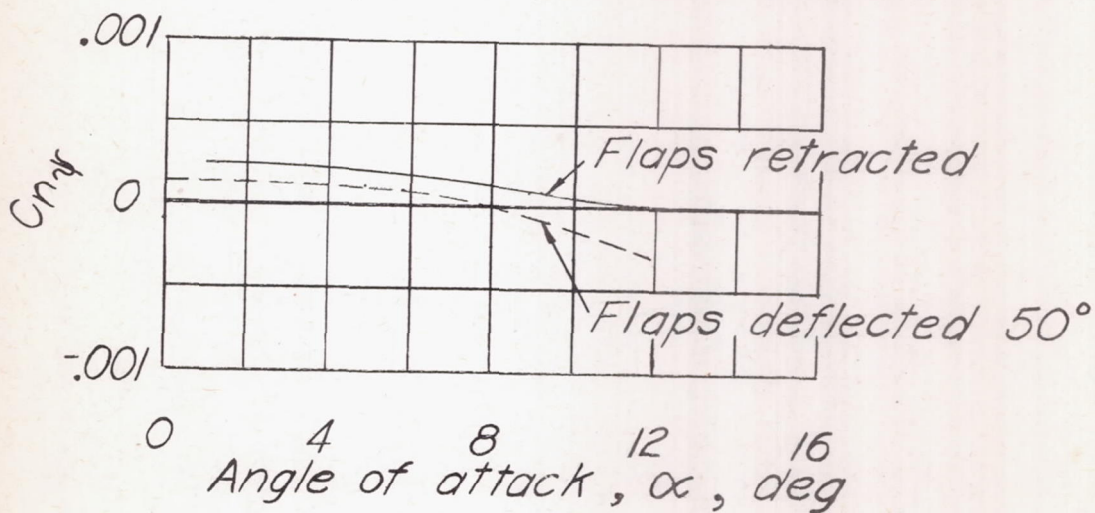


Figure 9.- Contribution of wing-fuselage combination to $C_{N\psi}$ and $C_{Y\psi}$. Vertical tail and propeller removed.

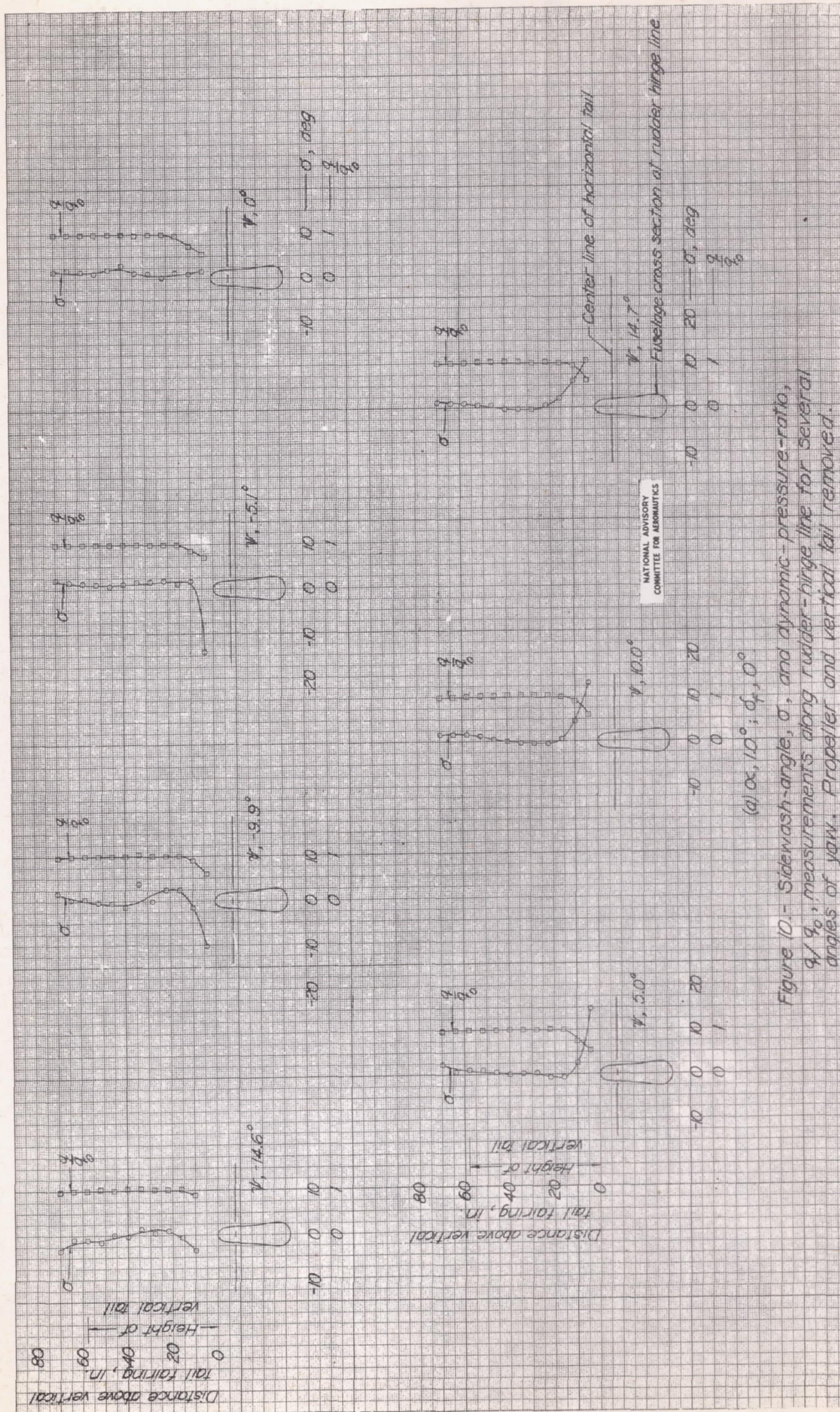
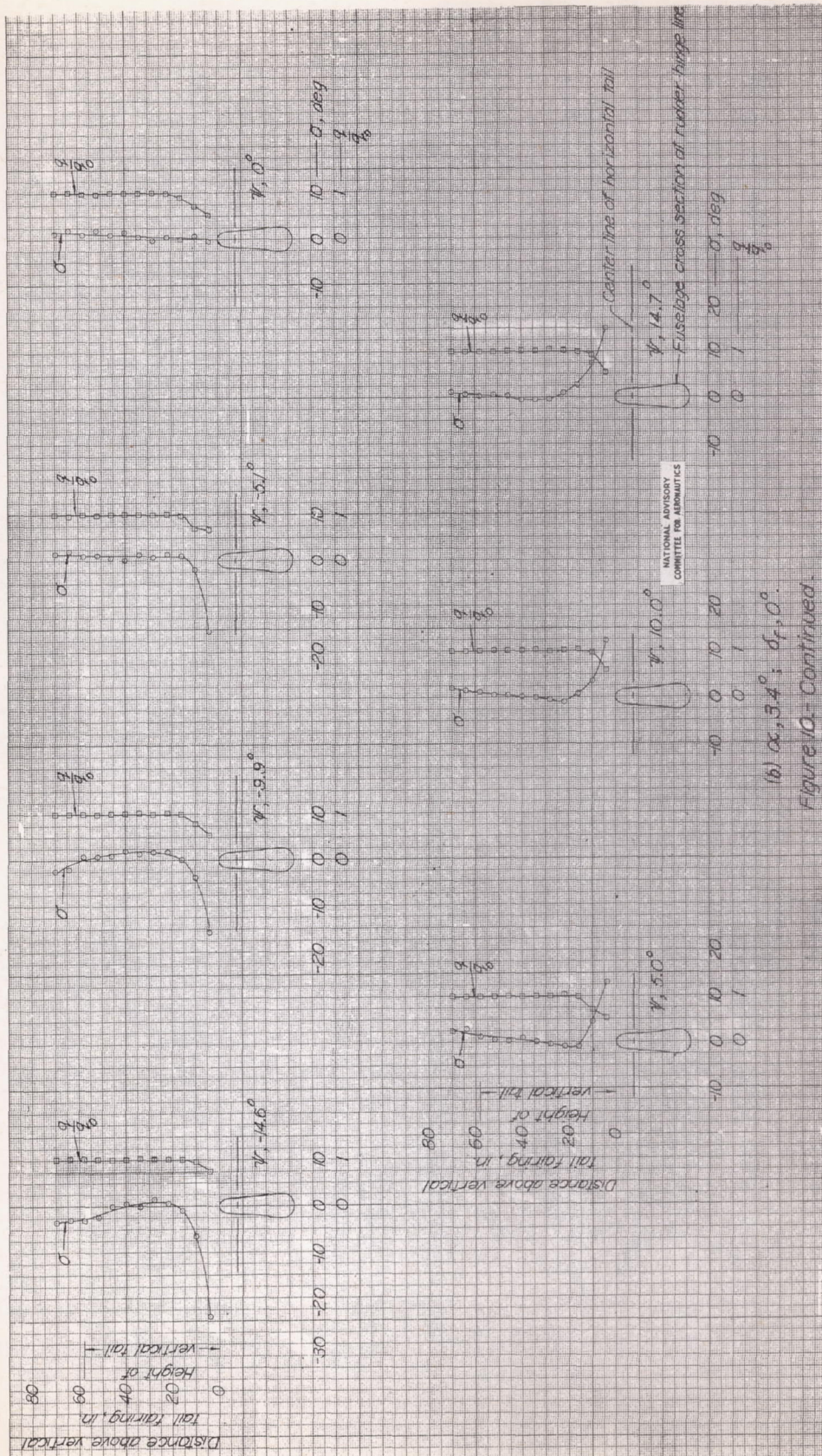
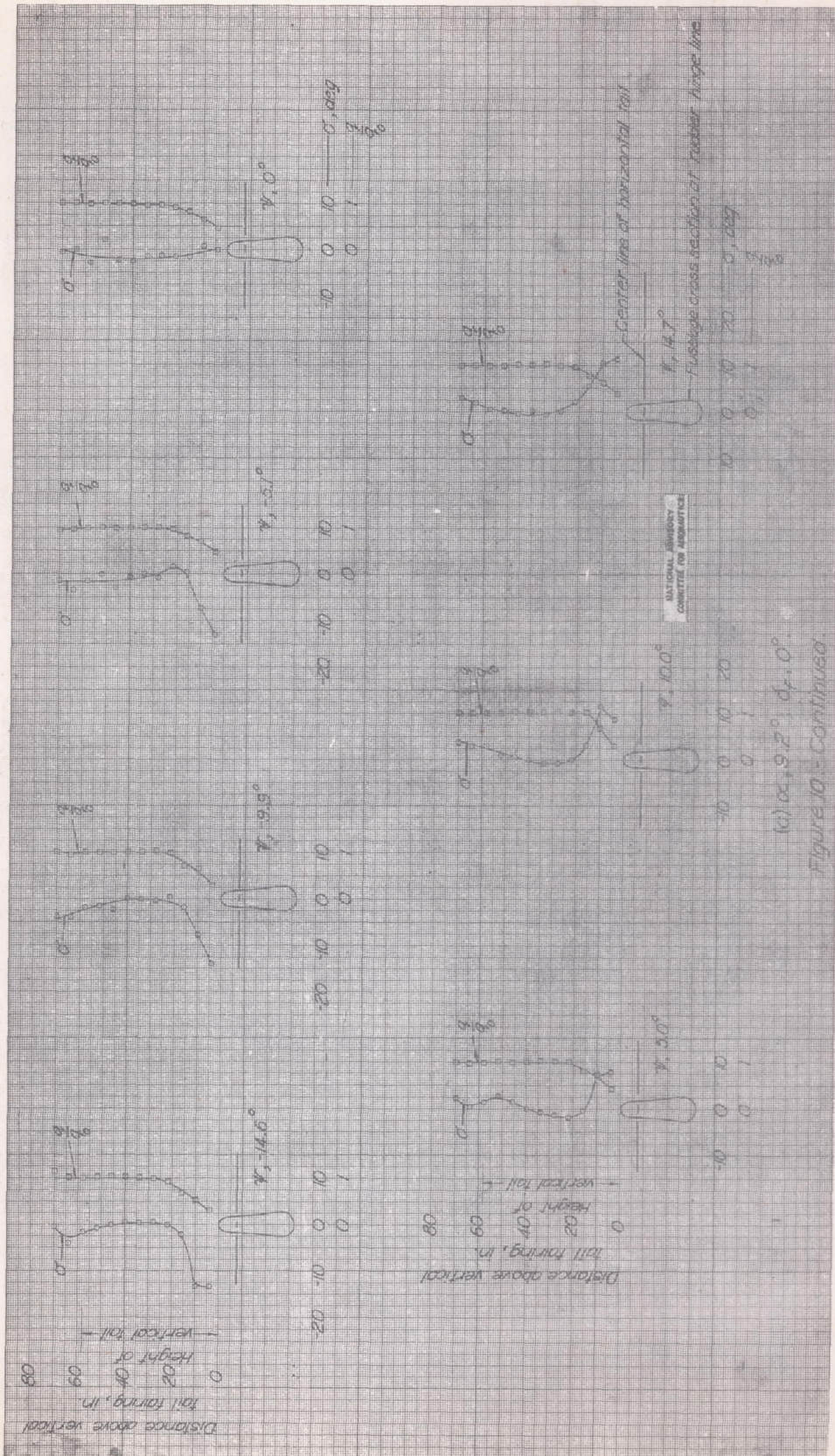
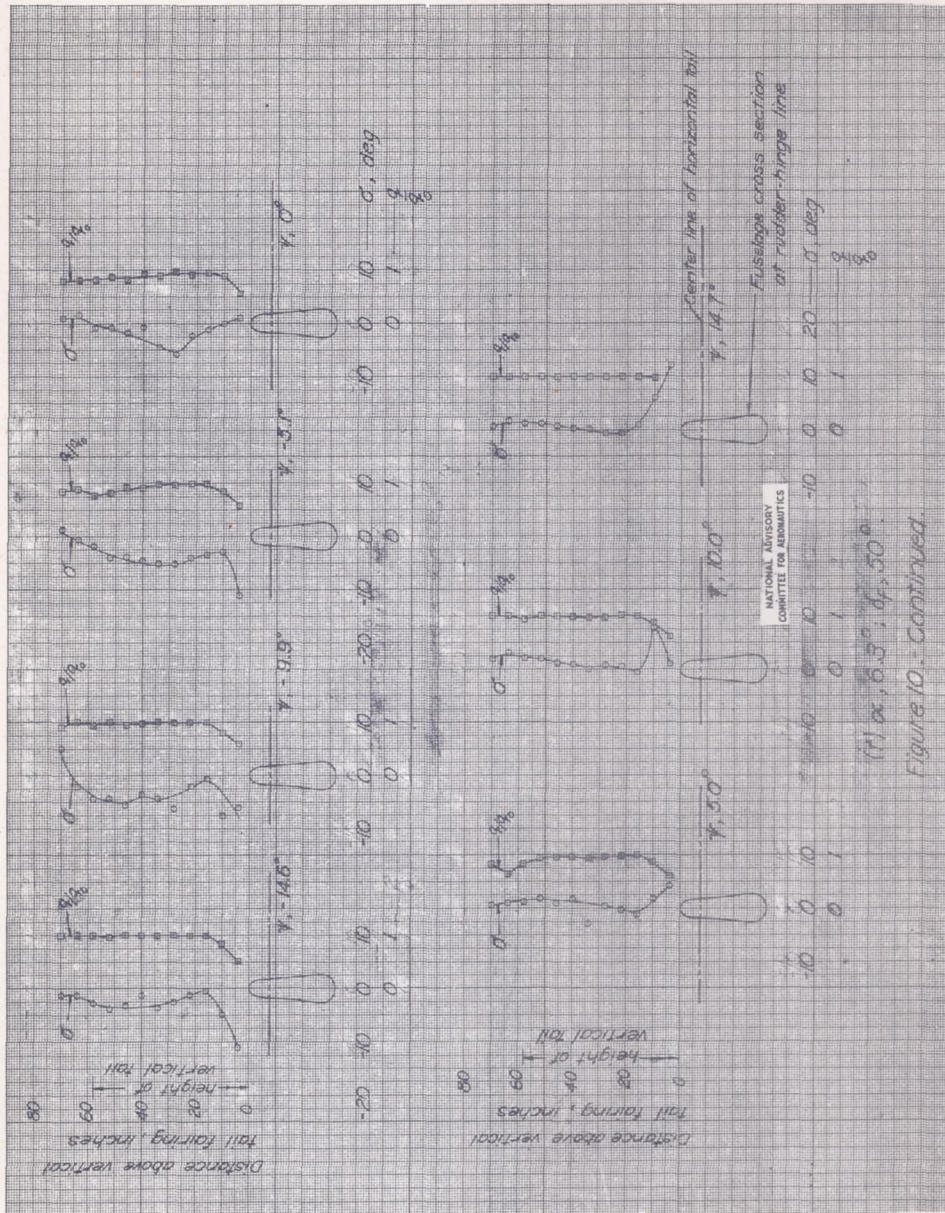
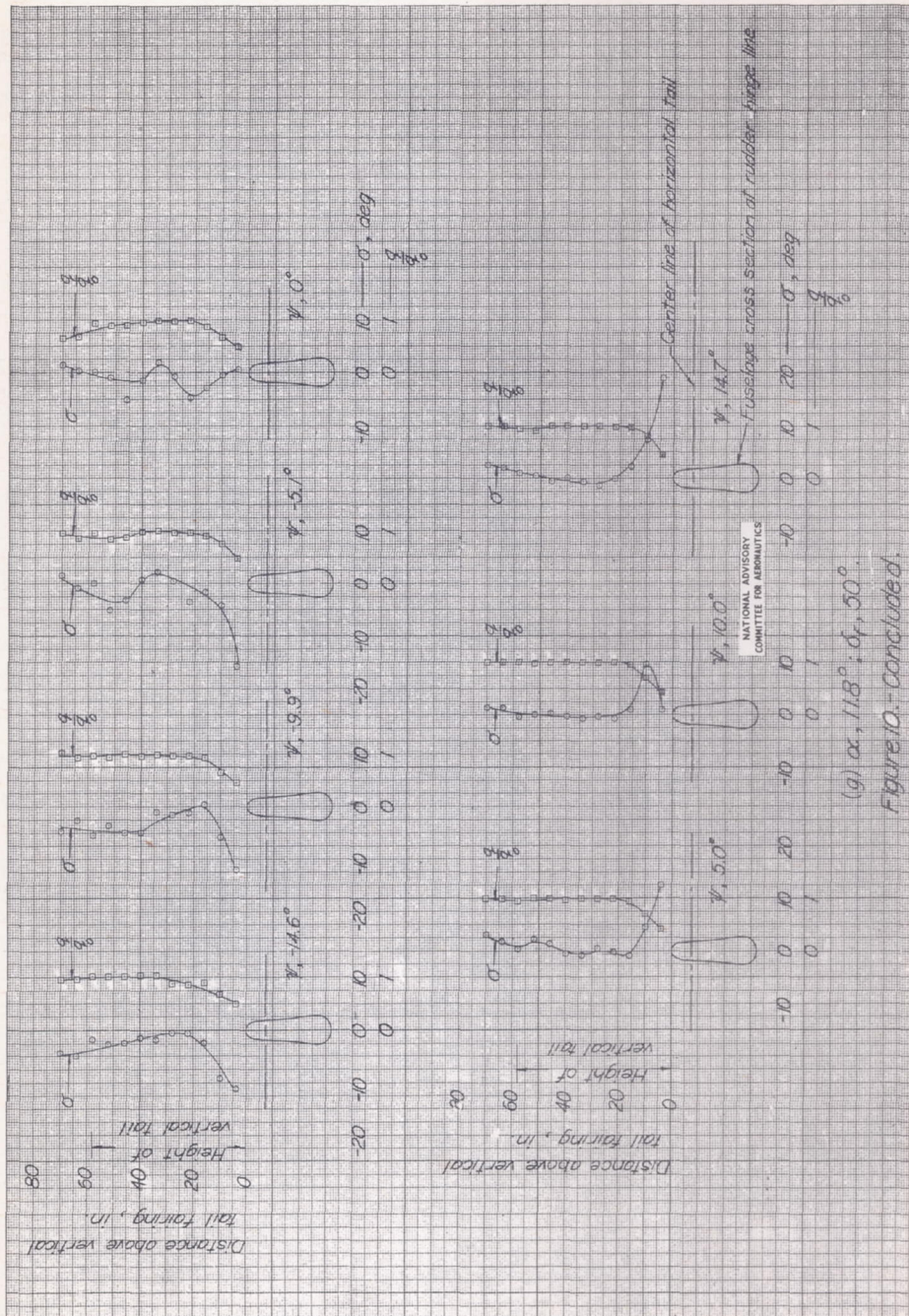


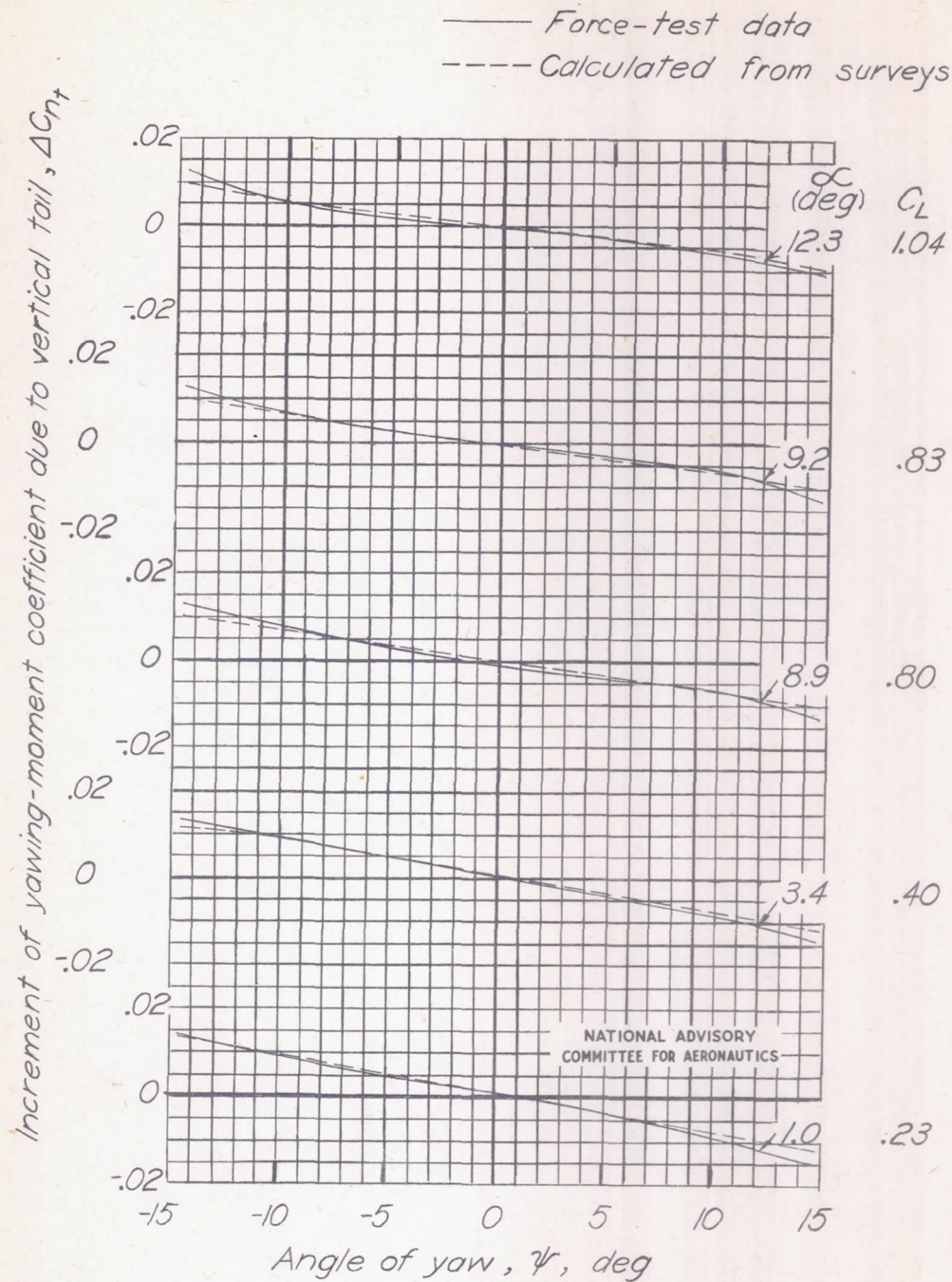
Figure 10.- Sidewash-angle, σ , and dynamic-pressure-ratio, ψ , measurements along rudder-hinge line for several angles of yaw. Propeller and vertical tail removed.





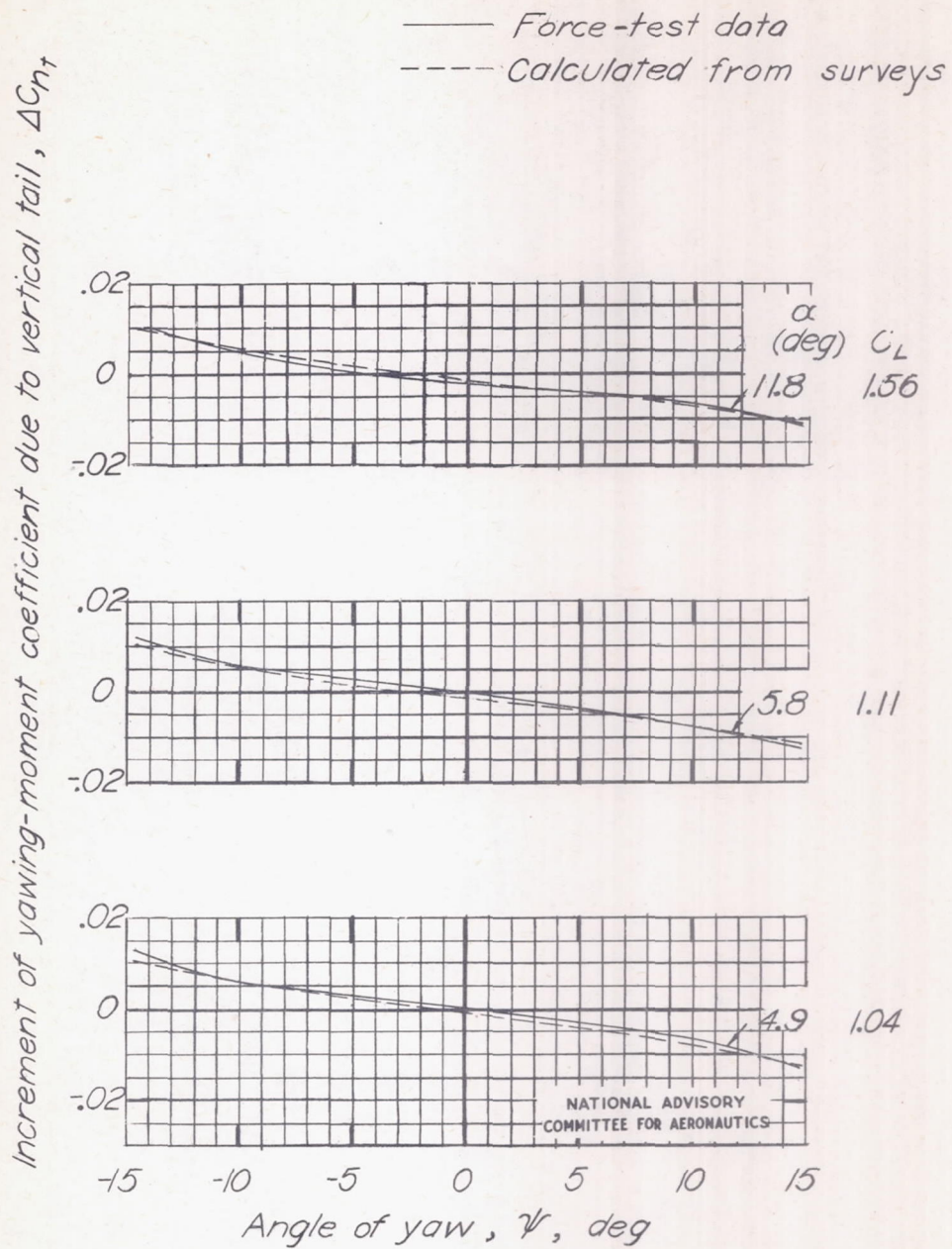






(a) $\delta_f, 0^\circ$.

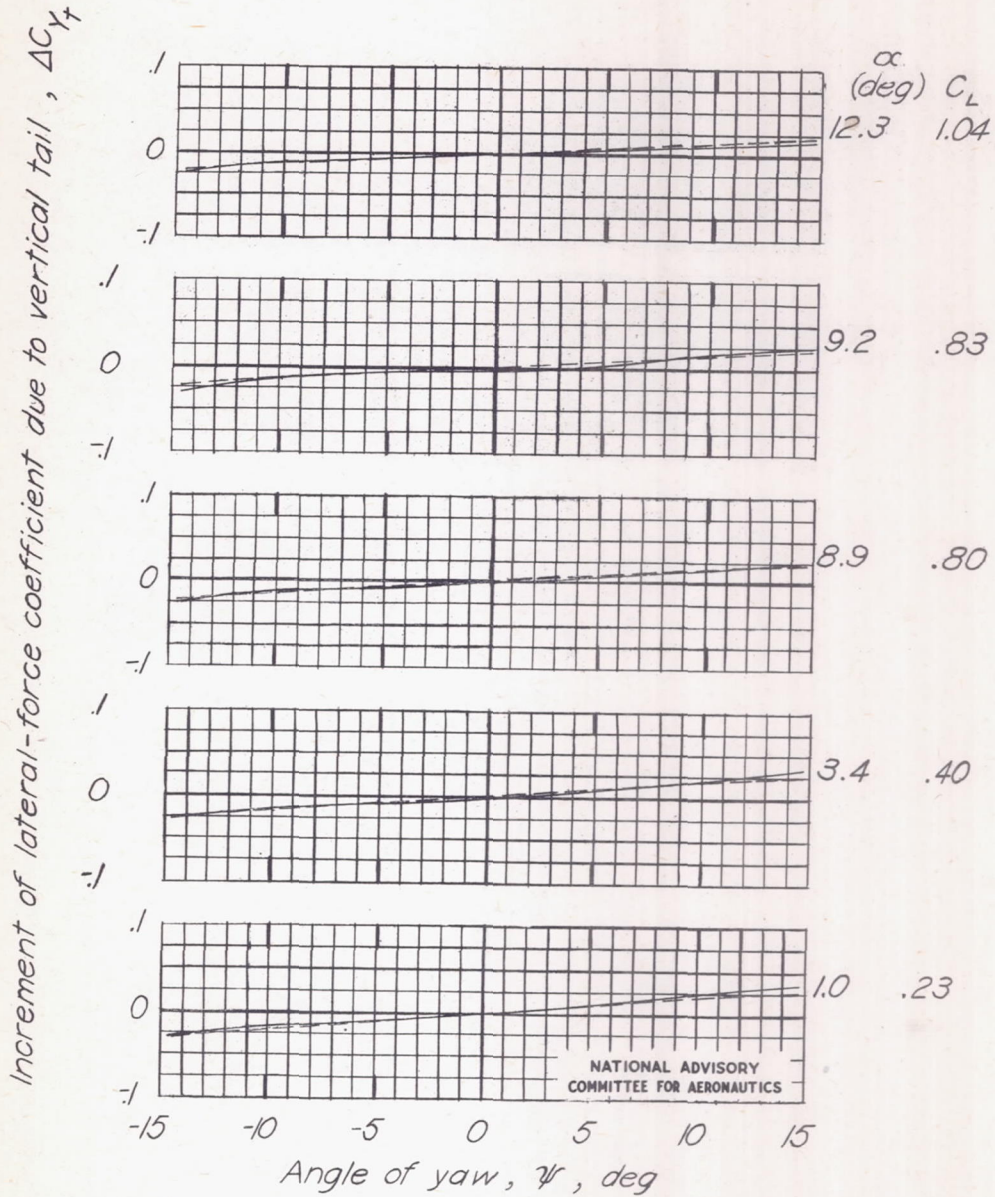
Figure 11.- Comparison of increment of C_n due to vertical tail as determined from the force-test data and from the air-flow surveys. Propeller removed.



(b) $\delta_f, 50^\circ$.

Figure 11.- Concluded.

— Force-test data
 - - - Calculated from surveys

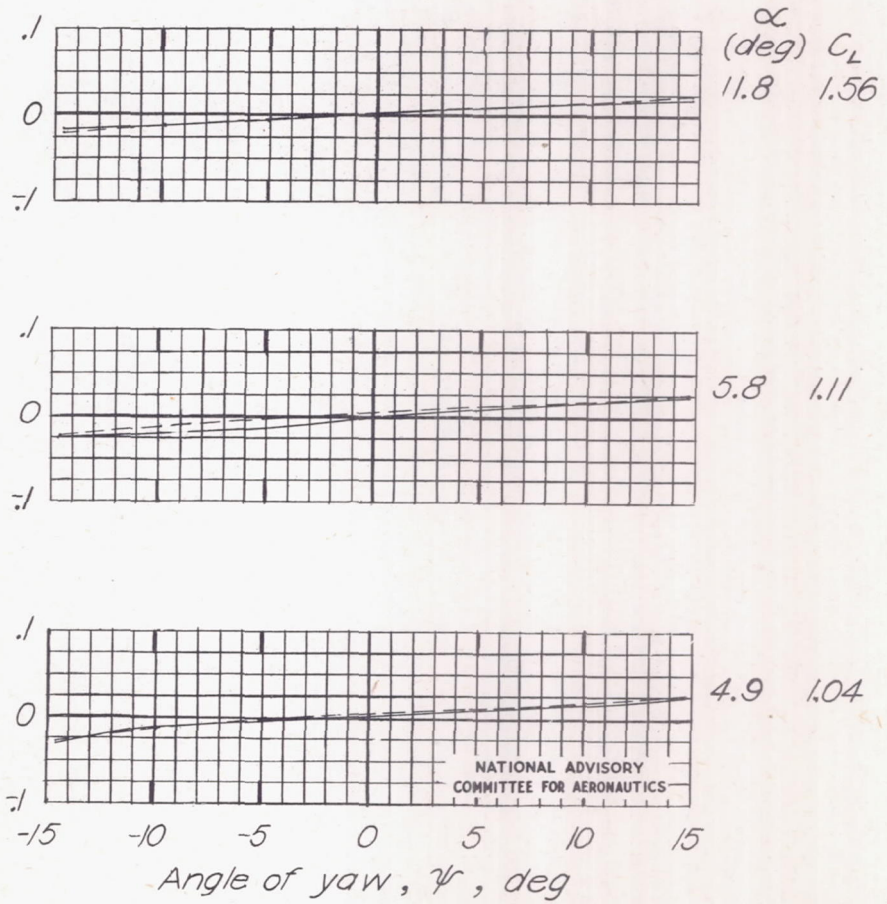


(a) $\delta_f, 0^\circ$.

Figure 12.- Comparison of increment of C_Y due to vertical tail as determined from the force-test data and from the air-flow surveys. Propeller removed.

Increment of lateral-force coefficient due to vertical tail, ΔC_{Y_f}

— Force-test data
 ---- Calculated from surveys



(b) $\delta_f, 50^\circ$.

Figure 12.- Concluded.

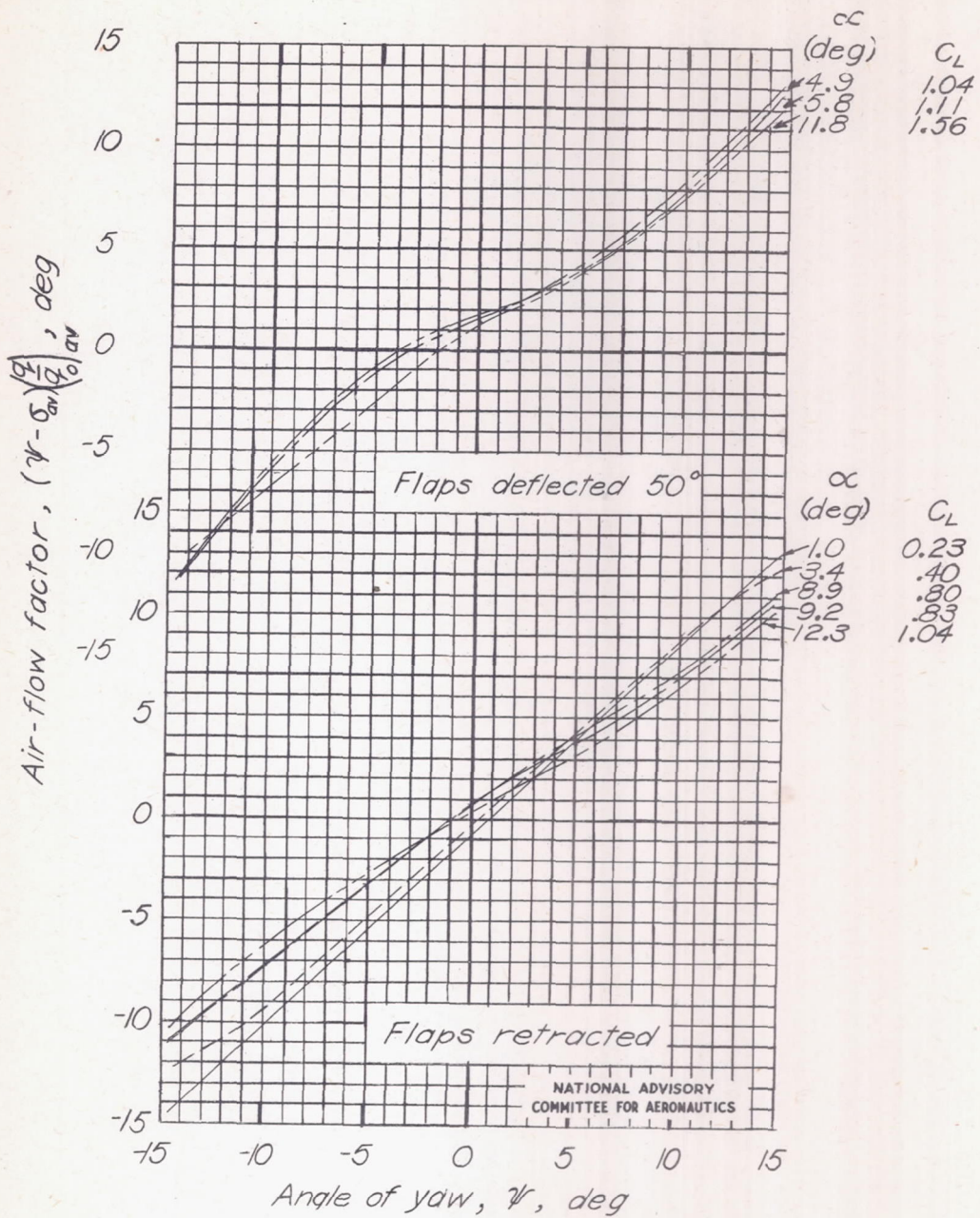
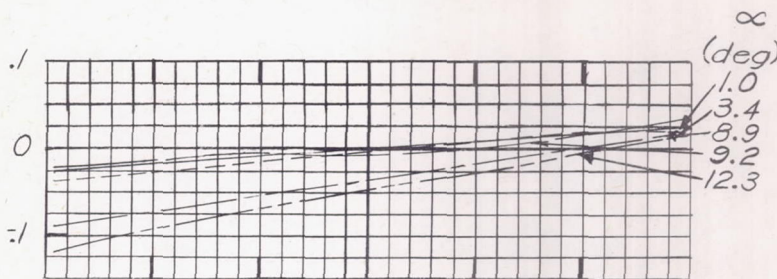


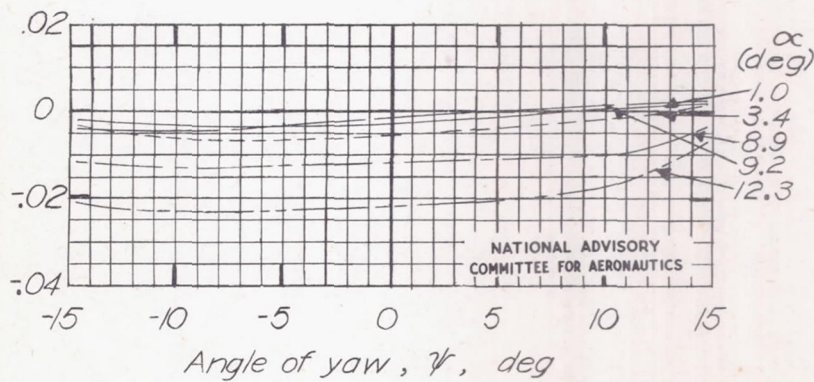
Figure 13.- Variation of air-flow factor with angle of yaw. Propeller removed.

Increment of lateral-force coefficient due to propeller operation, ΔC_{Yp}



Increment of yawing-moment coefficient due to propeller operation, ΔC_{np}

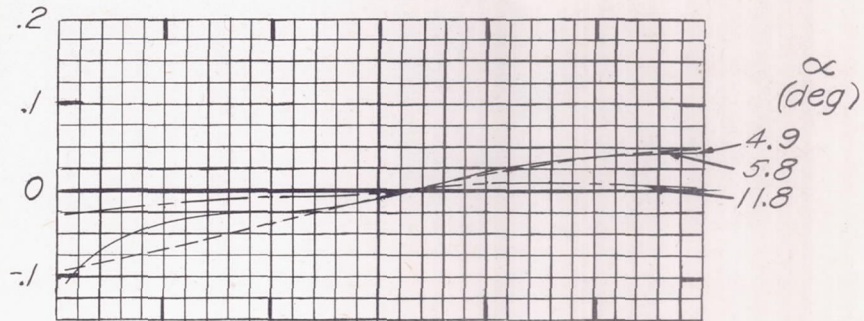
α , deg	Power	Lift coefficient, C_L
1.0	Rated ($T_c=0.05$)	0.24
3.4	Rated ($T_c=0.11$)	.43
8.9	Rated ($T_c=0.30$)	.96
9.2	$T_c=0.01$.83
12.3	Rated ($T_c=0.51$)	1.39



(a) $\delta_f, 0^\circ$.

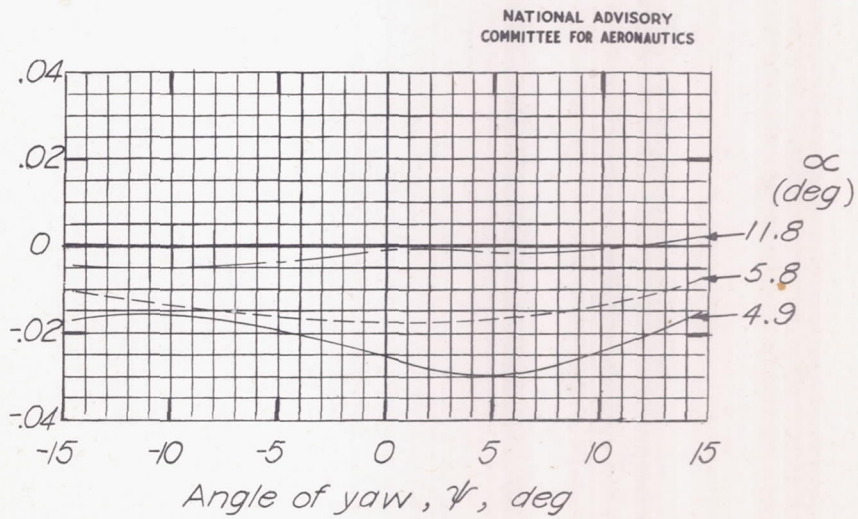
Figure 14.- Effects of propeller operation on the directional-stability characteristics of the XF6F-4 airplane.

Increment of lateral-force coefficient due to propeller operation, ΔC_{Yp}



α , deg	Power	Lift coefficient, C_L
4.9	Rated ($T_c=0.51$)	1.39
5.8	0.65 Rated ($T_c=0.33$)	1.37
11.8	$T_c=0.01$	1.58

Increment of yawing-moment coefficient due to propeller operation, ΔC_{np}



(b) $\delta_f, 50^\circ$.

Figure 14.- Concluded.

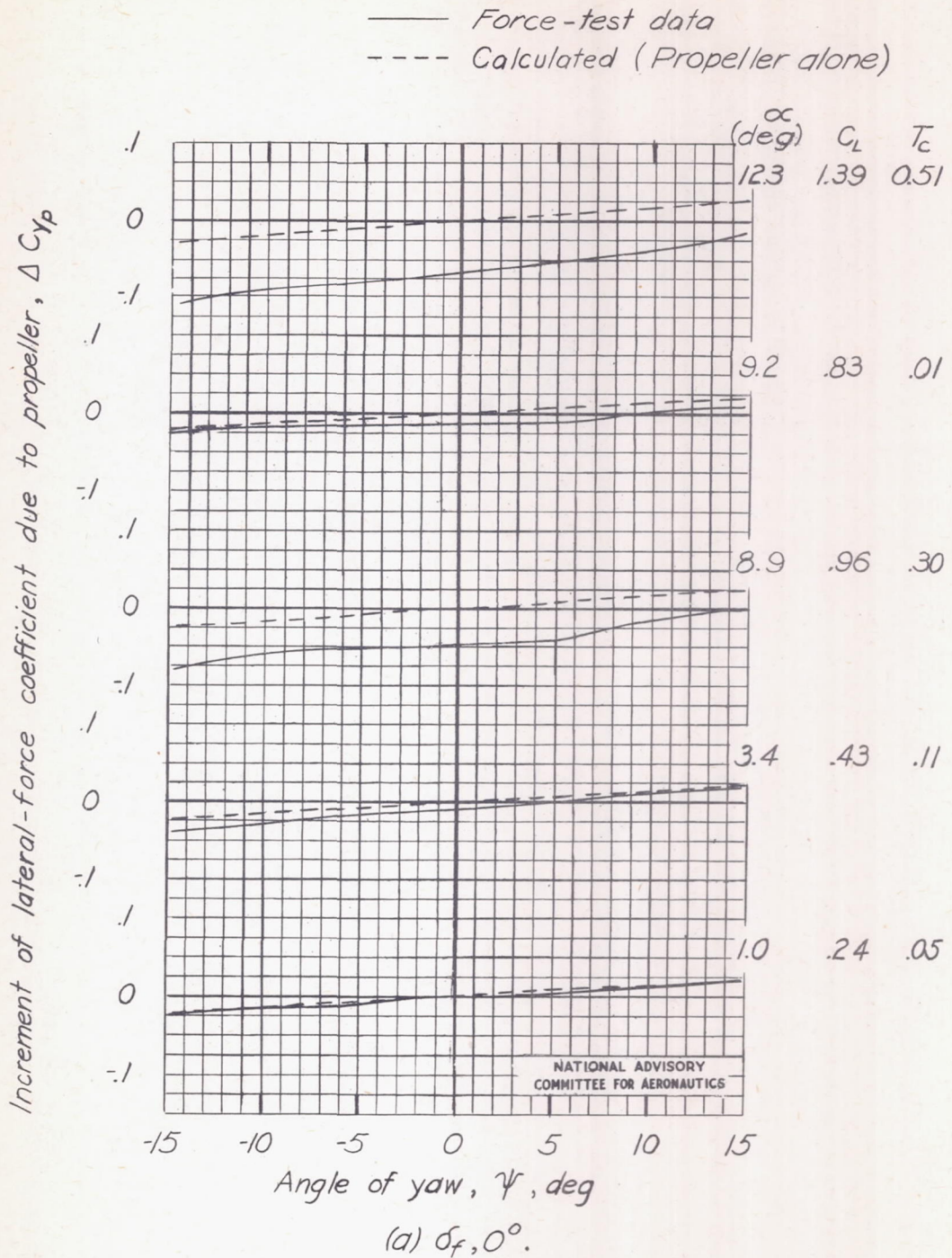
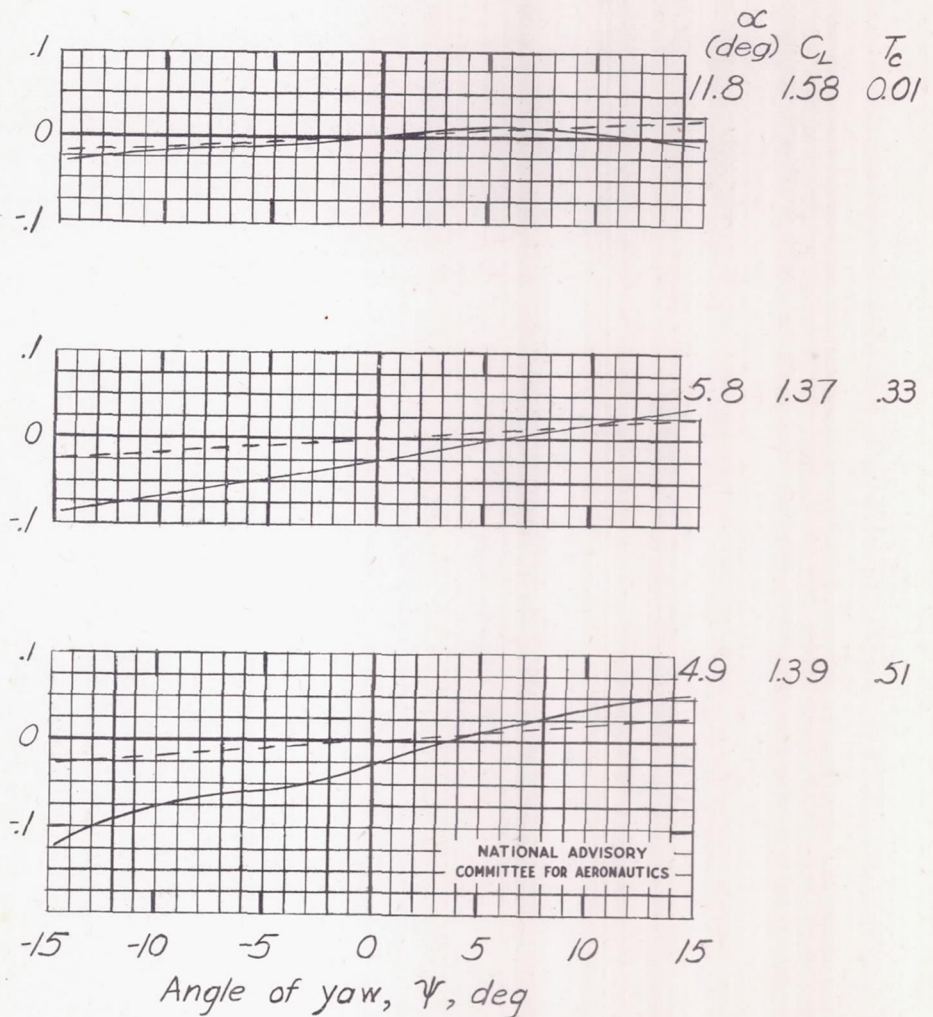


Figure 15.- Experimental and calculated effects of propeller operation on the variation of C_Y with Ψ for the airplane with vertical tail removed.

Increment of lateral-force coefficient due to propeller, ΔC_{Yp}

— Force-test data
 - - - Calculated (Propeller alone)



(b) $\delta_f, 50^\circ$.

Figure 15.- Concluded.

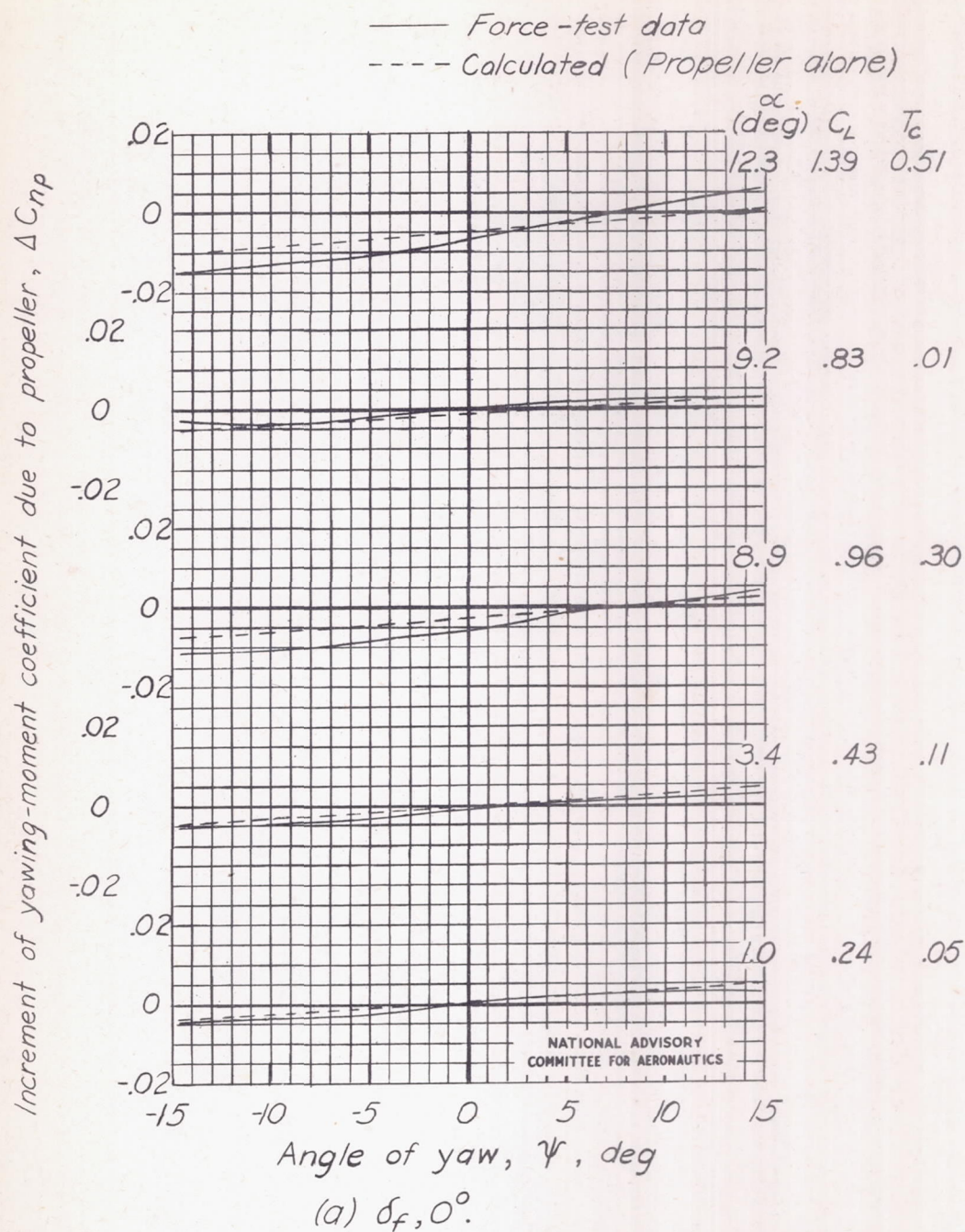
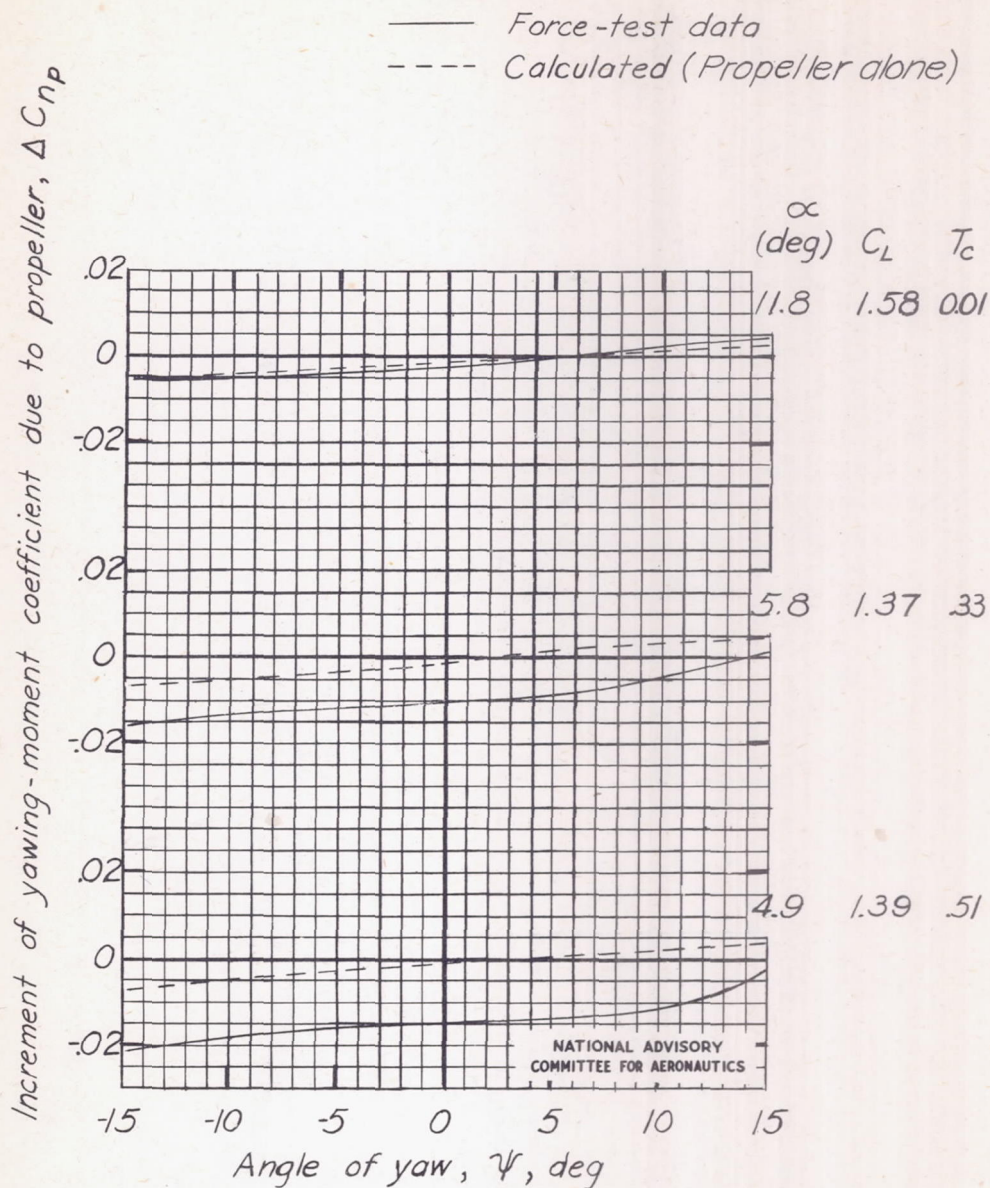


Figure 16.- Experimental and calculated effects of propeller operation on the variation of C_n with Ψ for the airplane with vertical tail removed.



(b) $\delta_f, 50^\circ$.

Figure 16.- Concluded.

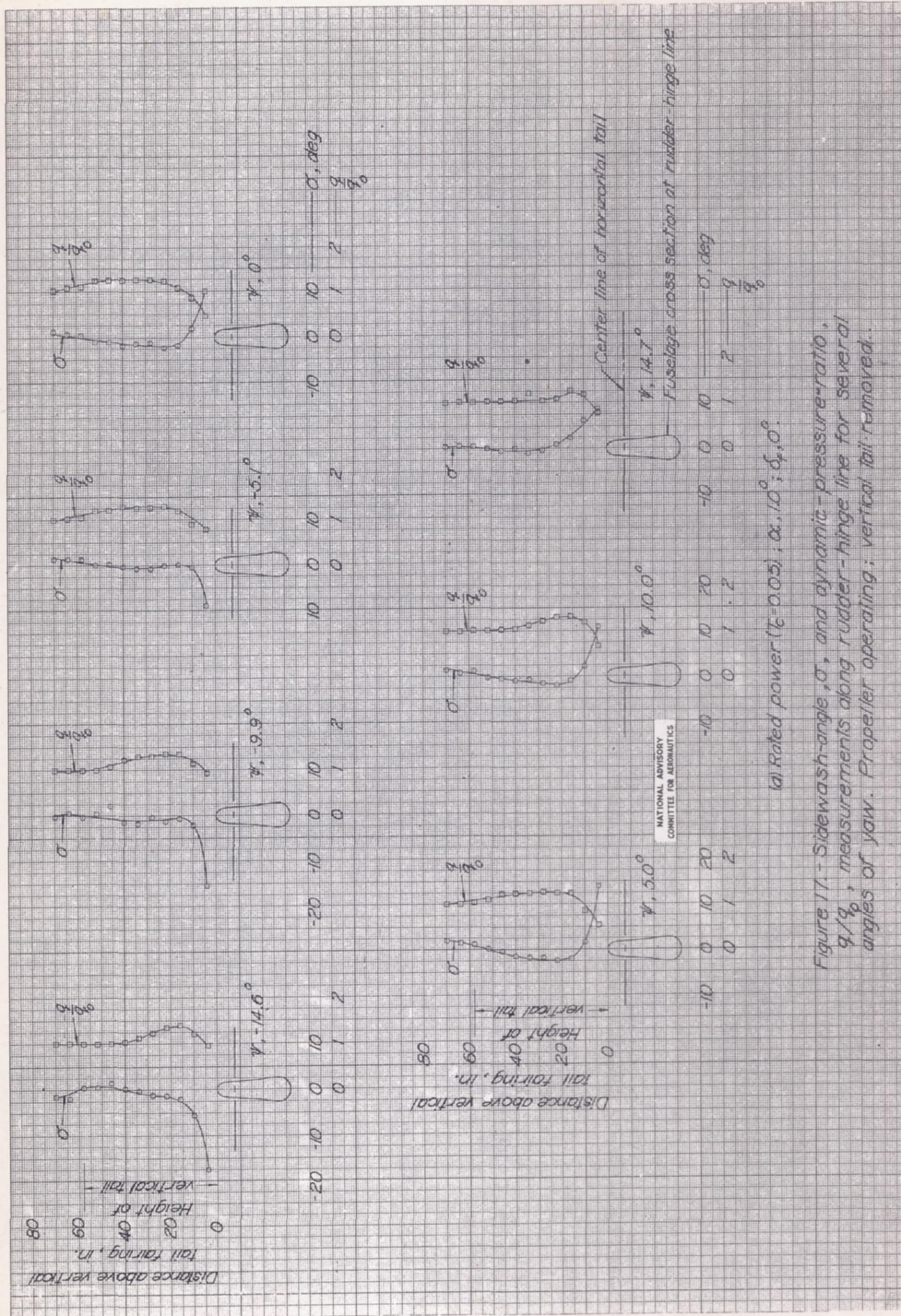
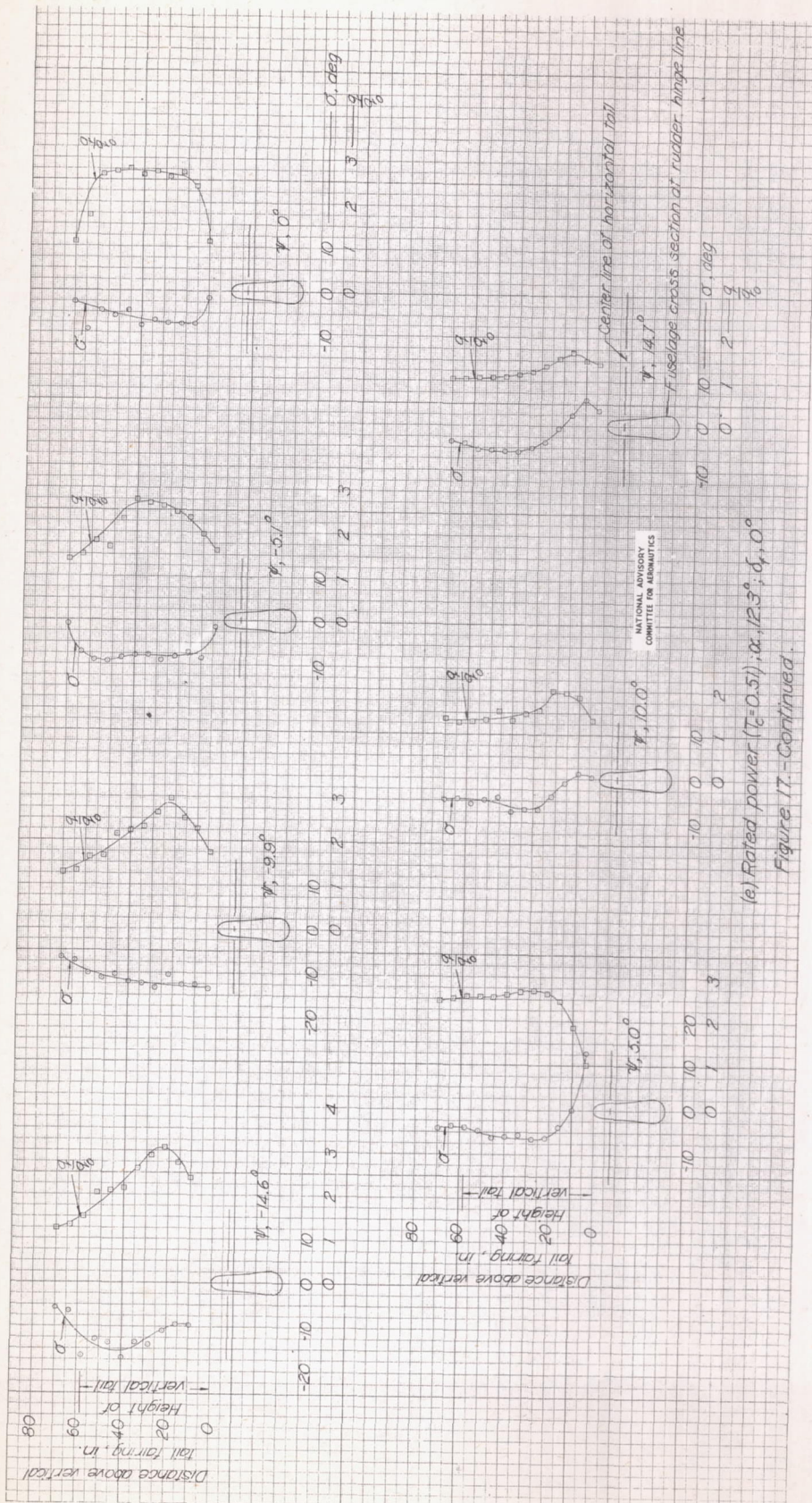
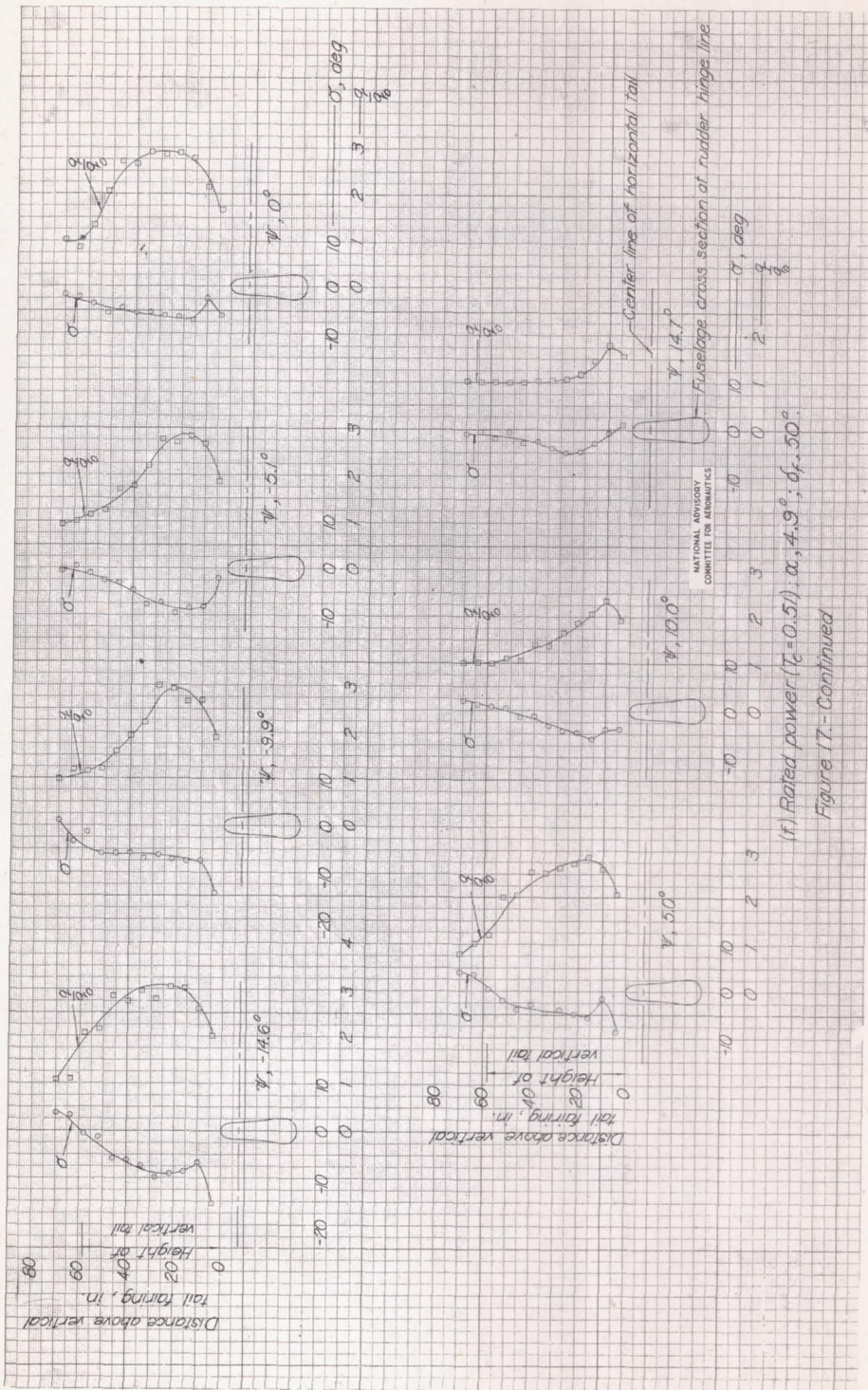
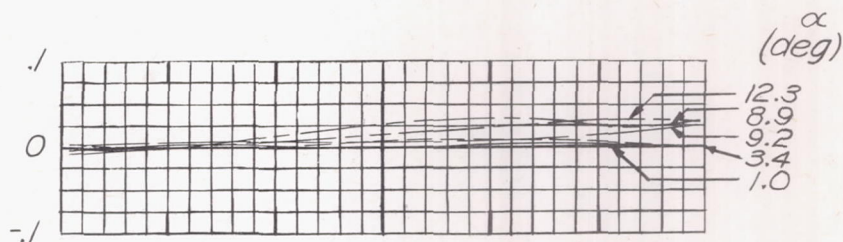


Figure 17 - Sidewash-angle, ψ , and dynamic pressure ratio, σ , measurements along rudder-hinge line for several angles of yaw. Propeller operating; vertical tail removed.



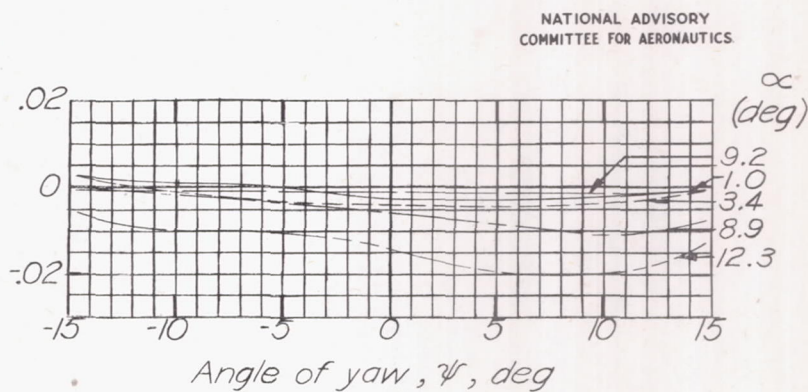


Increment of tail lateral-force coefficient due to propeller slipstream, $\Delta C_{Y_{ts}}$



α, deg	Power	Lift coefficient, C_L
1.0	Rated ($T_c=0.05$)	0.24
3.4	Rated ($T_c=0.11$)	.43
8.9	Rated ($T_c=0.30$)	.96
9.2	$T_c=0.01$.83
12.3	Rated ($T_c=0.51$)	1.39

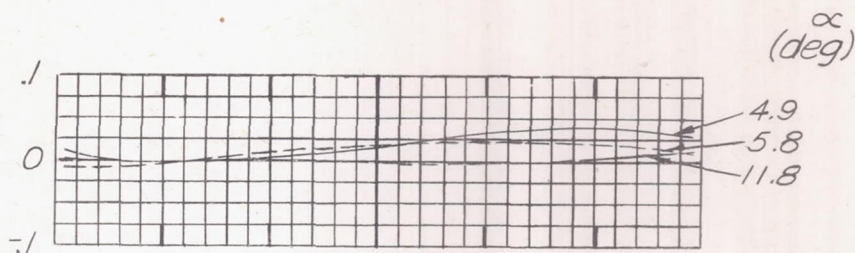
Increment of tail yawing-moment coefficient due to propeller slipstream, $\Delta C_{n_{ts}}$



(a) $\delta_f, 0^\circ$

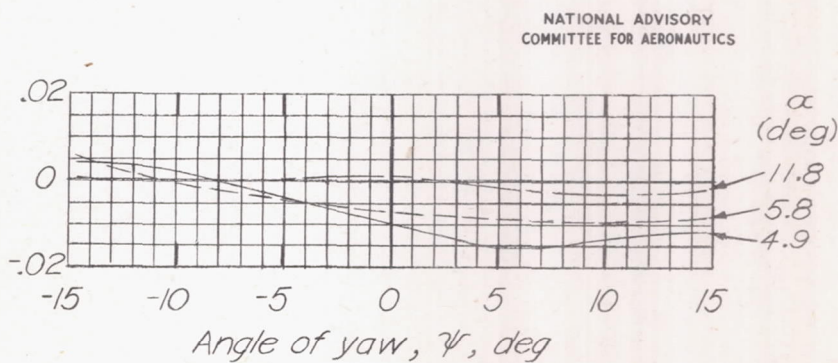
Figure 18.- Effect of the propeller slipstream on the contribution of the vertical tail to the airplane directional stability characteristics.

Increment of tail lateral-force coefficient due to propeller slipstream, $\Delta C_{Y_{ts}}$



α , deg	Power	Lift coefficient, C_L
4.9	Rated ($T_C=0.51$)	1.39
5.8	0.65 Rated ($T_C=0.33$)	1.37
11.8	$T_C=0.01$	1.58

Increment of tail yawing-moment coefficient due to propeller slipstream, $\Delta C_{n_{ts}}$



(b) $\delta_f, 50^\circ$.

Figure 18. - Concluded.

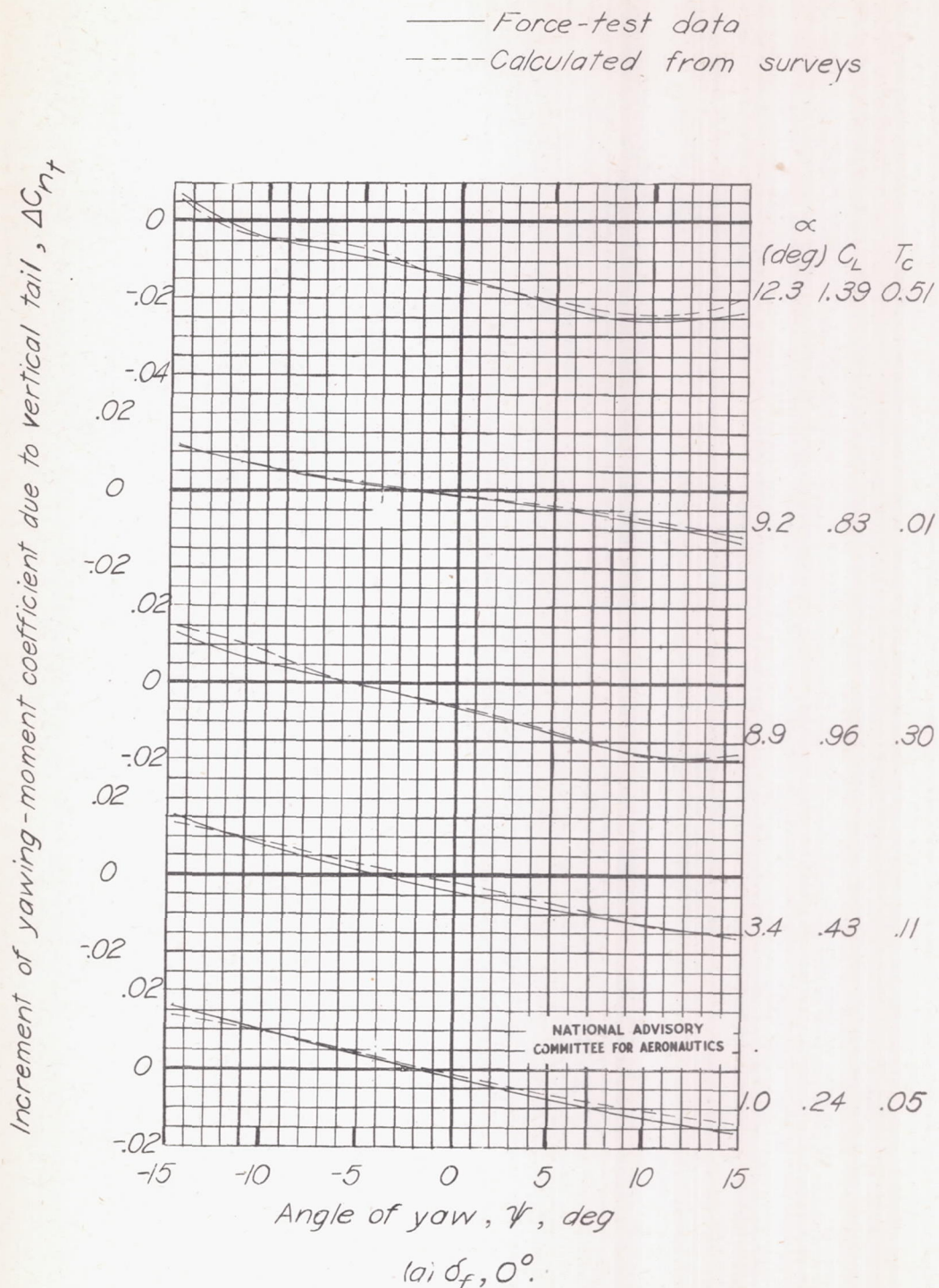
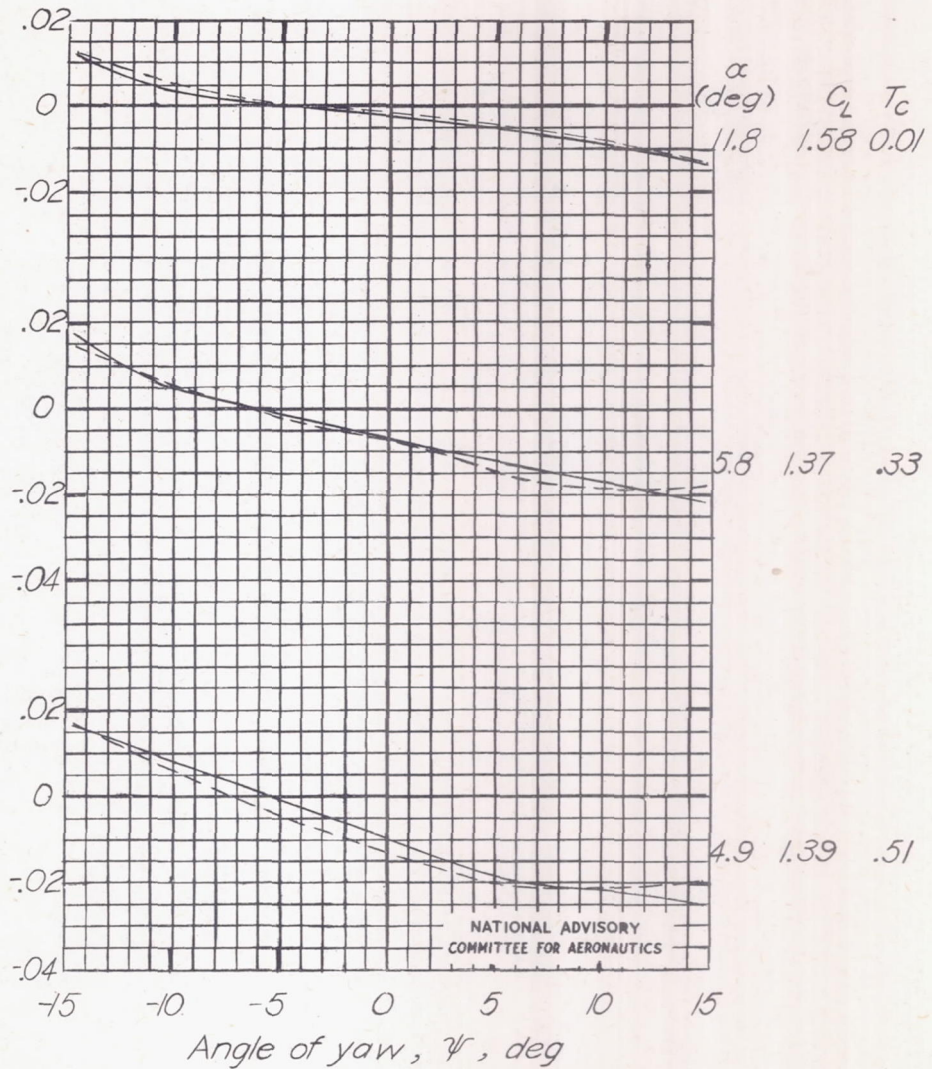


Figure 19.- Comparison of increment of C_n due to vertical tail as determined from the force-test data and from the air-flow surveys. Propeller operating.

— Force-test data
 --- Calculated from surveys

Increment of yawing-moment coefficient due to vertical tail, $\Delta C_{n\dot{\gamma}}$



NATIONAL ADVISORY
 COMMITTEE FOR AERONAUTICS

(b) $\delta_f, 50^\circ$.

Figure 19.- Concluded.

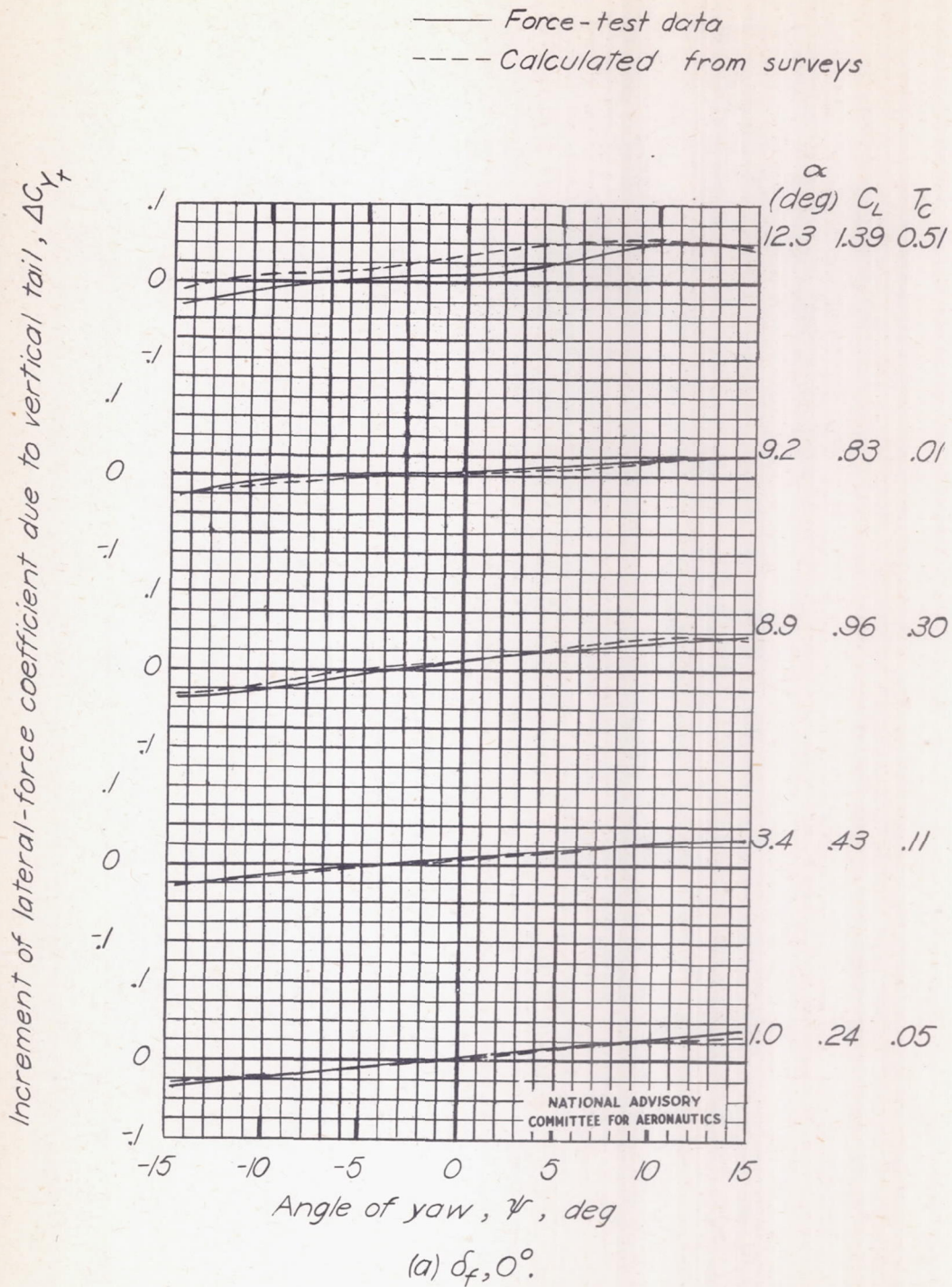
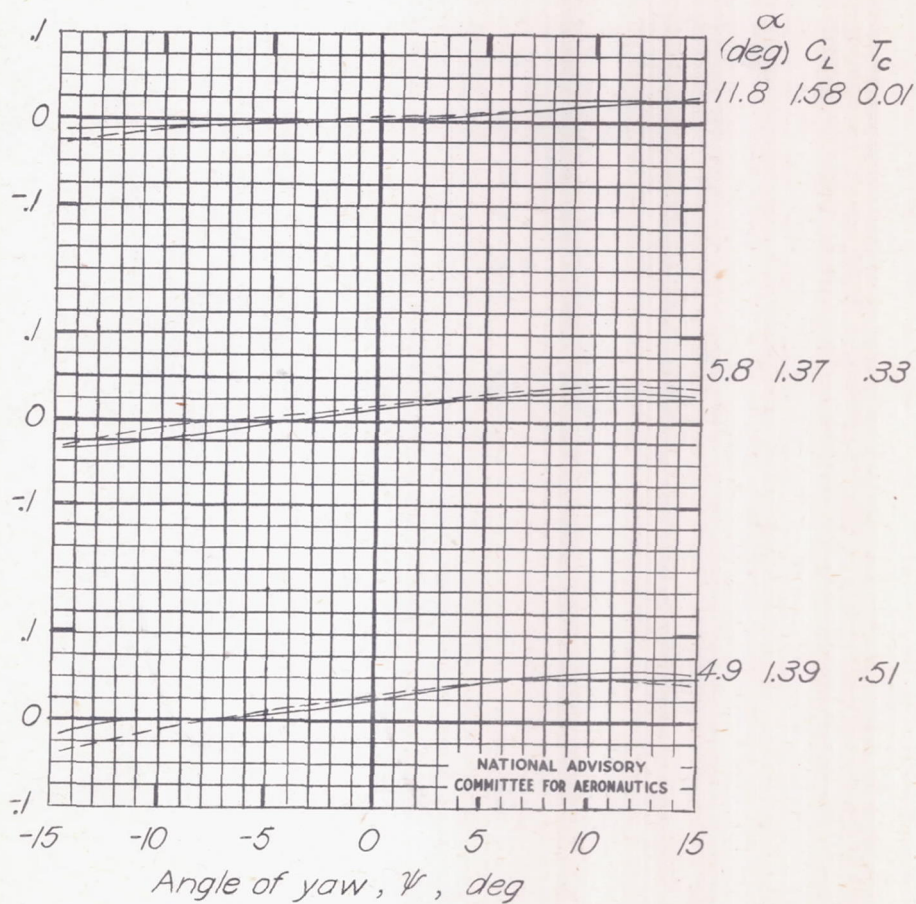


Figure 20.- Comparison of increment of C_Y due to vertical tail as determined from the force-test data and from the air-flow surveys. Propeller operating.

— Force-test data
 - - - Calculated from surveys

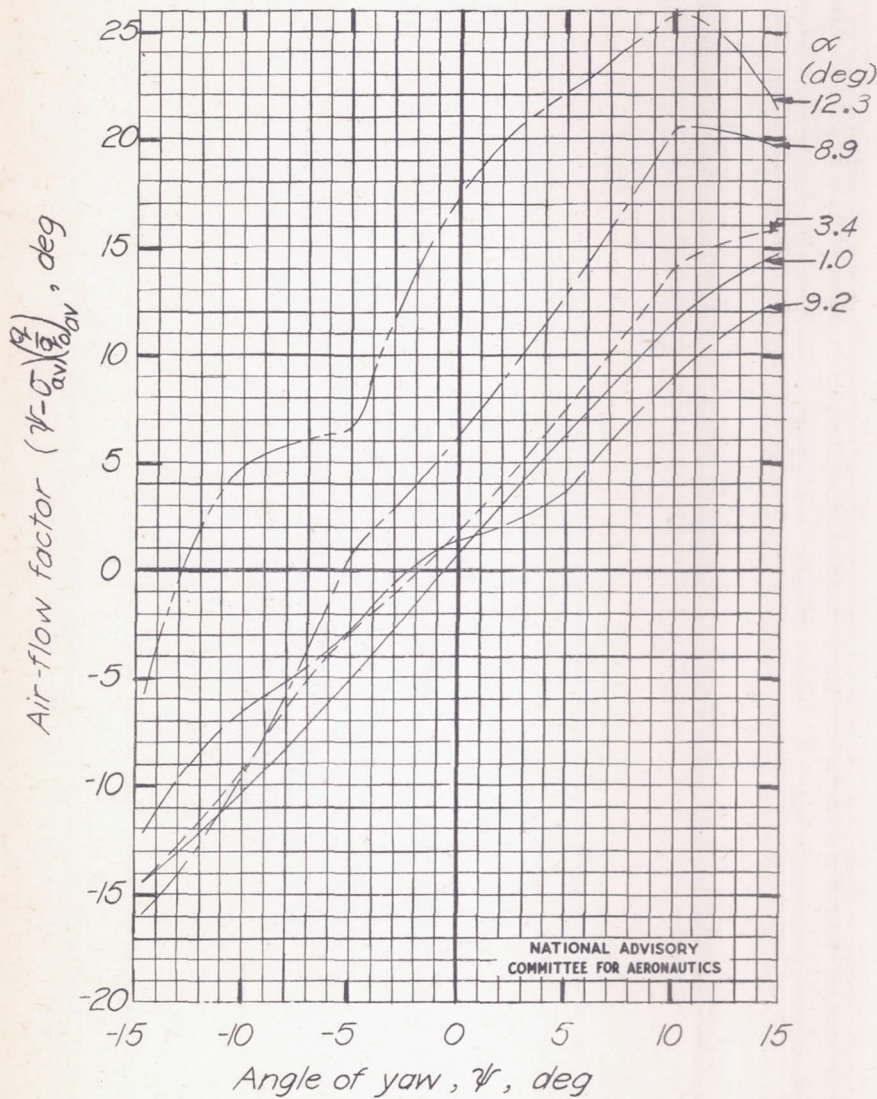
Increment of lateral-force coefficient due to vertical tail, ΔC_{Y_f}



(b) $\delta_f, 50^\circ$

Figure 20.-Concluded.

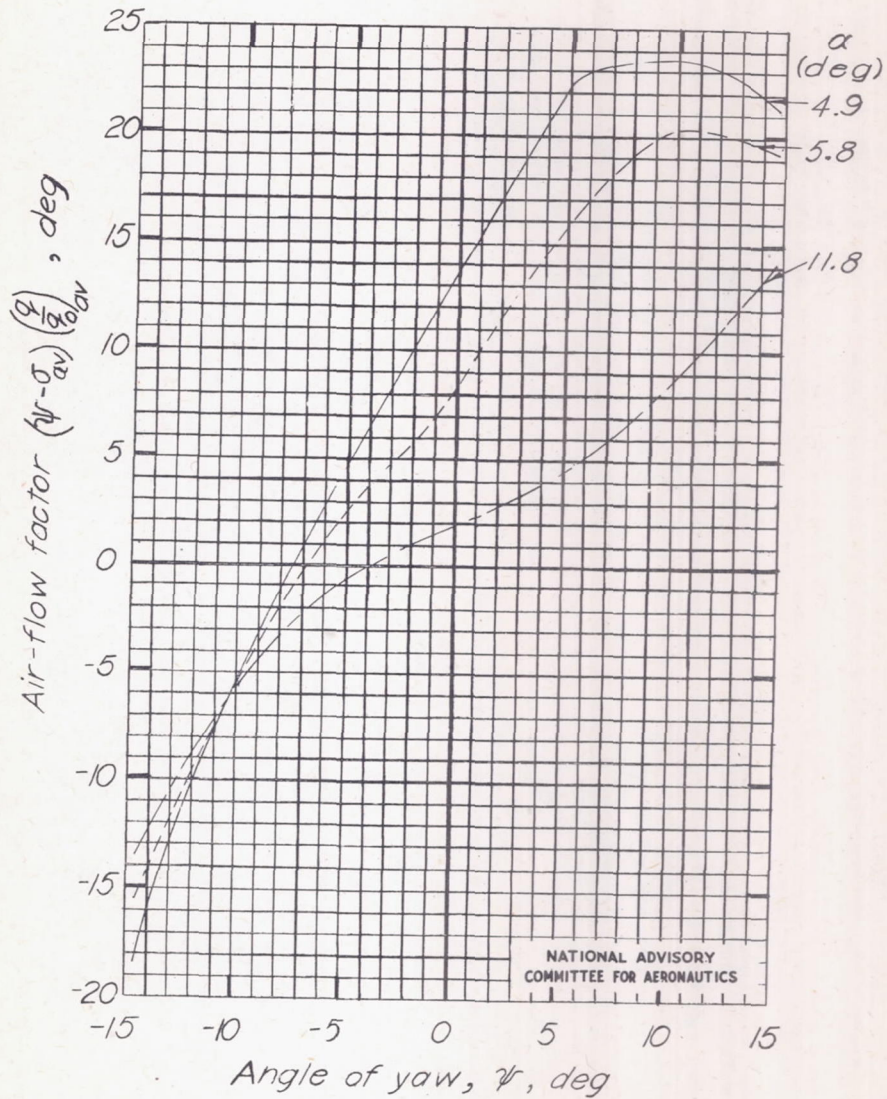
α , deg	Power	Lift coefficient, C_L
1.0	Rated ($T_c=0.05$)	0.24
3.4	Rated ($T_c=0.11$)	.43
8.9	Rated ($T_c=0.30$)	.96
9.2	$T_c=0.01$.83
12.3	Rated ($T_c=0.51$)	1.39



(a) $\delta_f, 0^\circ$.

Figure 21.- Variation of air-flow factor with angle of yaw. Propeller operating.

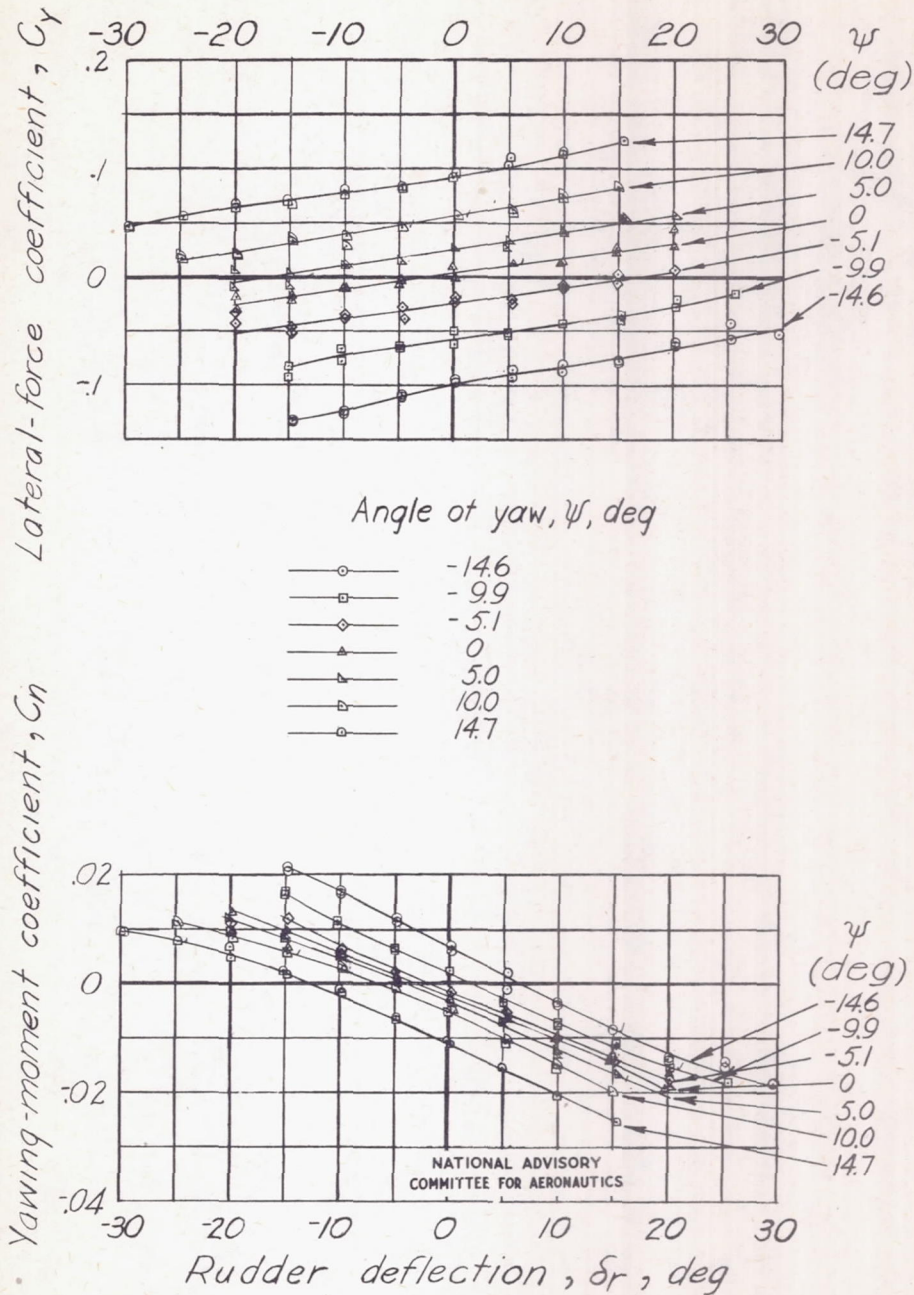
α , deg	Power	Lift coefficient, C_L
— 4.9	Rated ($T_c=0.51$)	1.39
- - - 5.8	0.65 Rated ($T_c=0.33$)	1.37
- · - · 11.8	$T_c = 0.01$	1.58



NATIONAL ADVISORY
COMMITTEE FOR AERONAUTICS

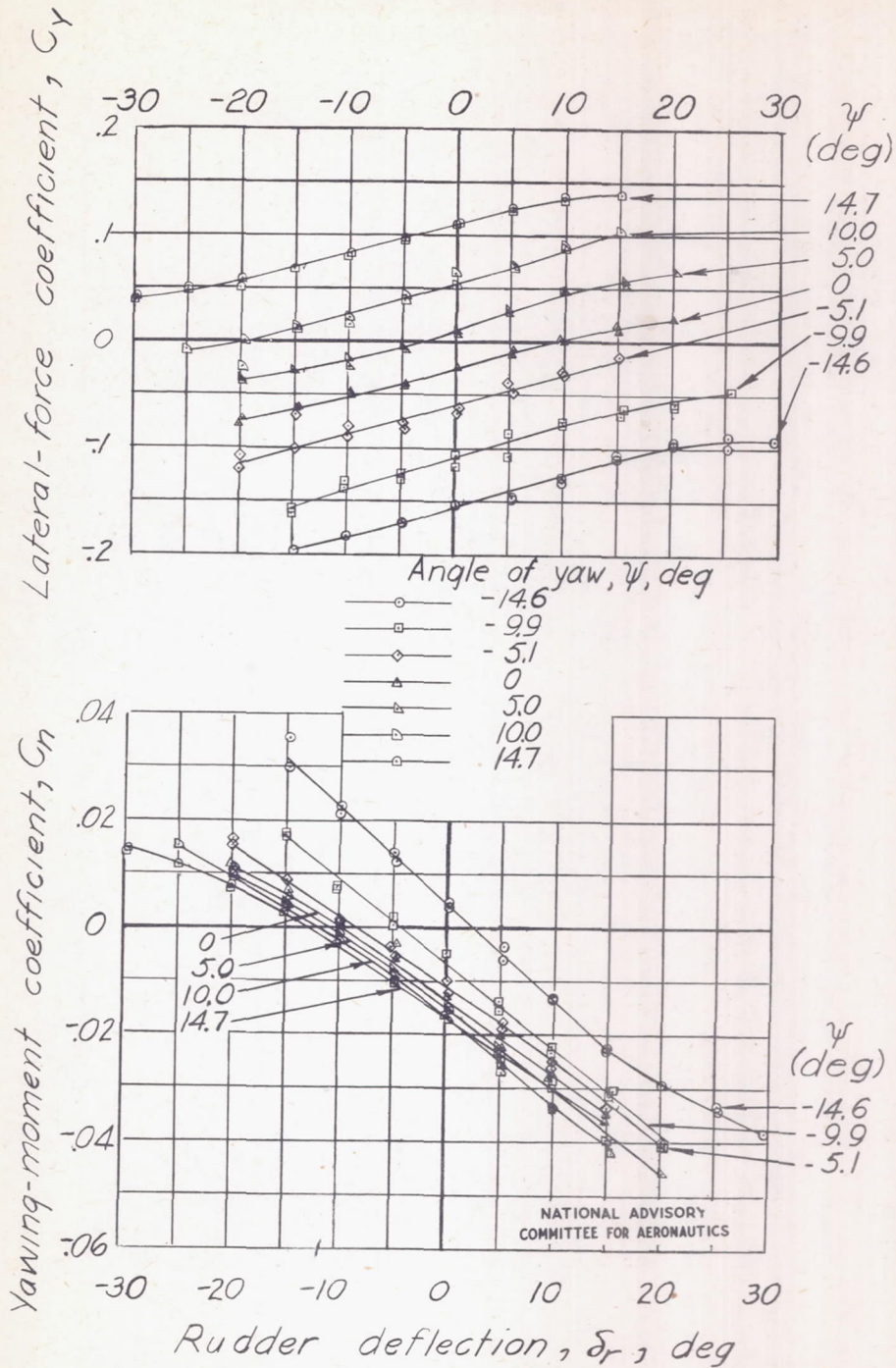
(b) $\delta_f, 50^\circ$.

Figure 21.- Concluded.



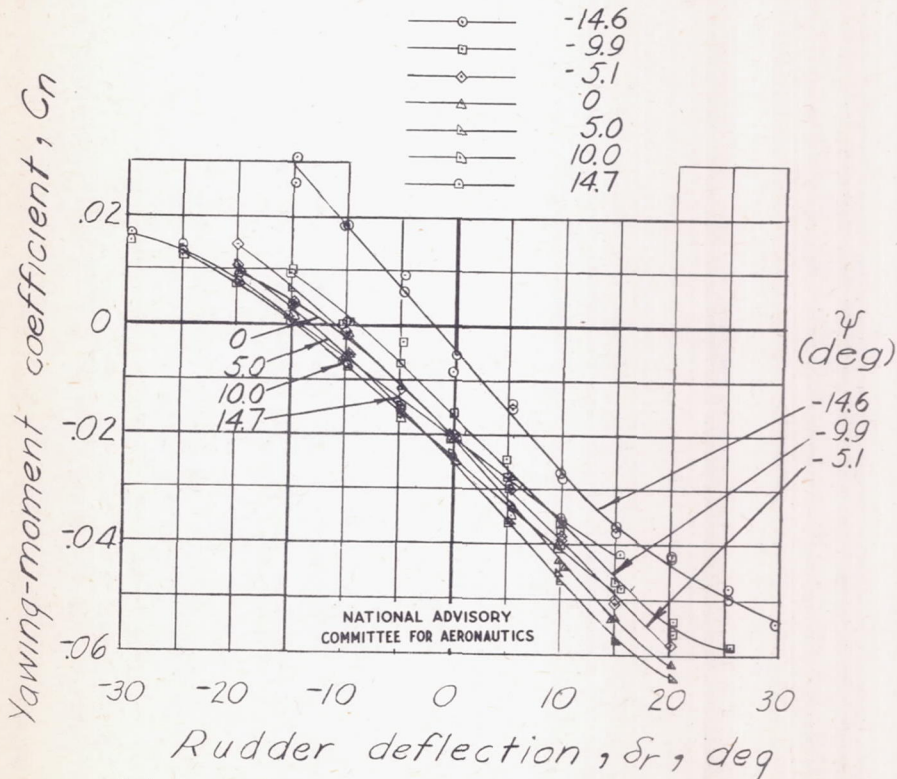
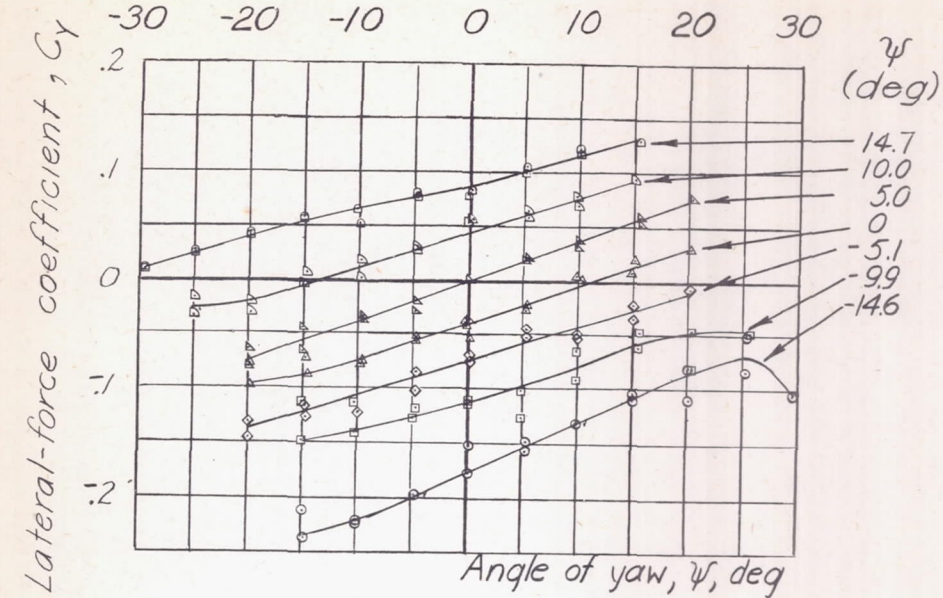
(a) Gliding condition; $T_C, 0.01$; $\alpha, 9.2^\circ$;
 $C_L, 0.83$; $\delta_F, 0^\circ$.

Figure 22. - Variation of C_n and C_y with δ_r for several angles of yaw. Propeller operating.



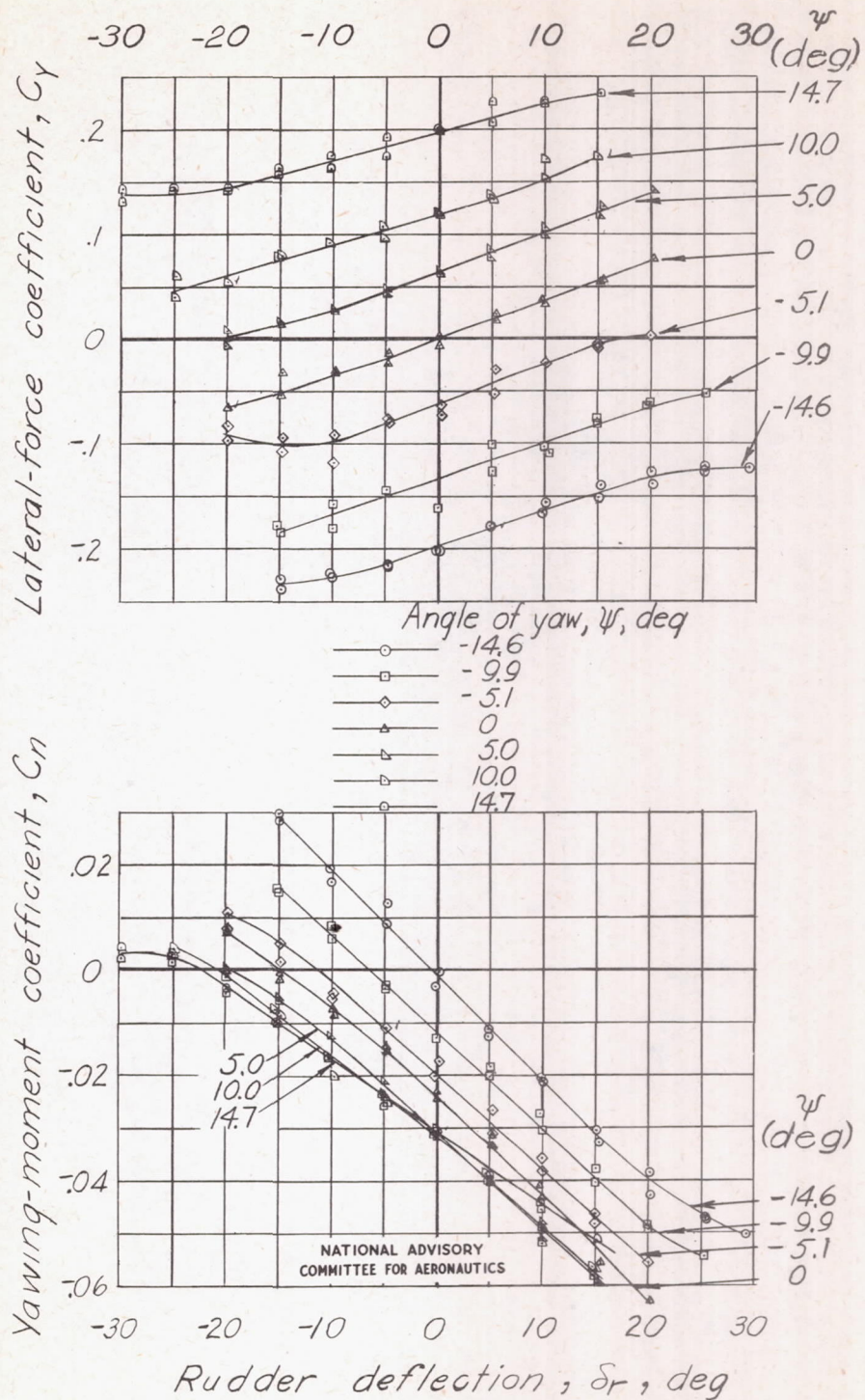
(b) Climbing condition; rated power ($T_C=0.30$); $\alpha, 8.9^\circ$;
 $C_L, 0.96$; $\delta_f, 0^\circ$.

Figure 22.- Continued.



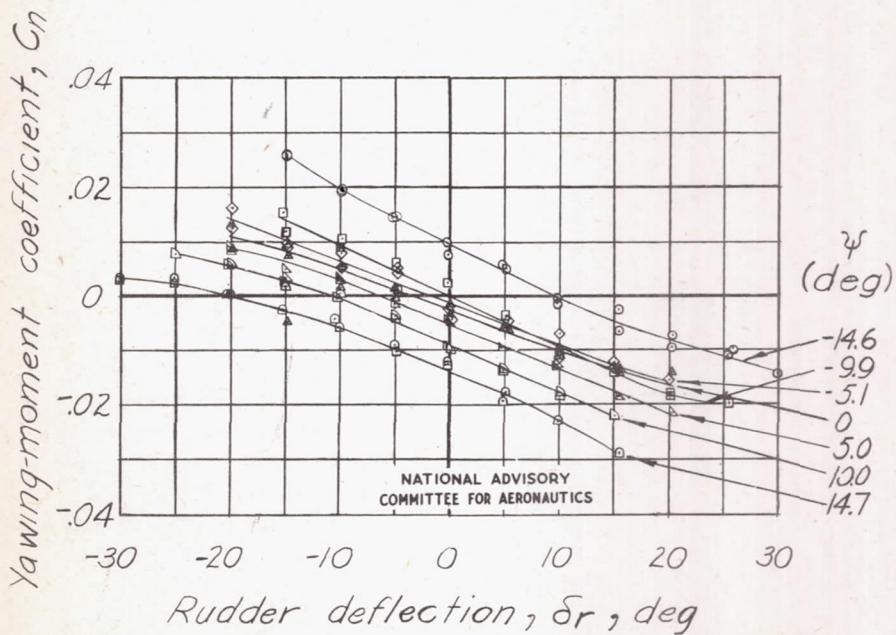
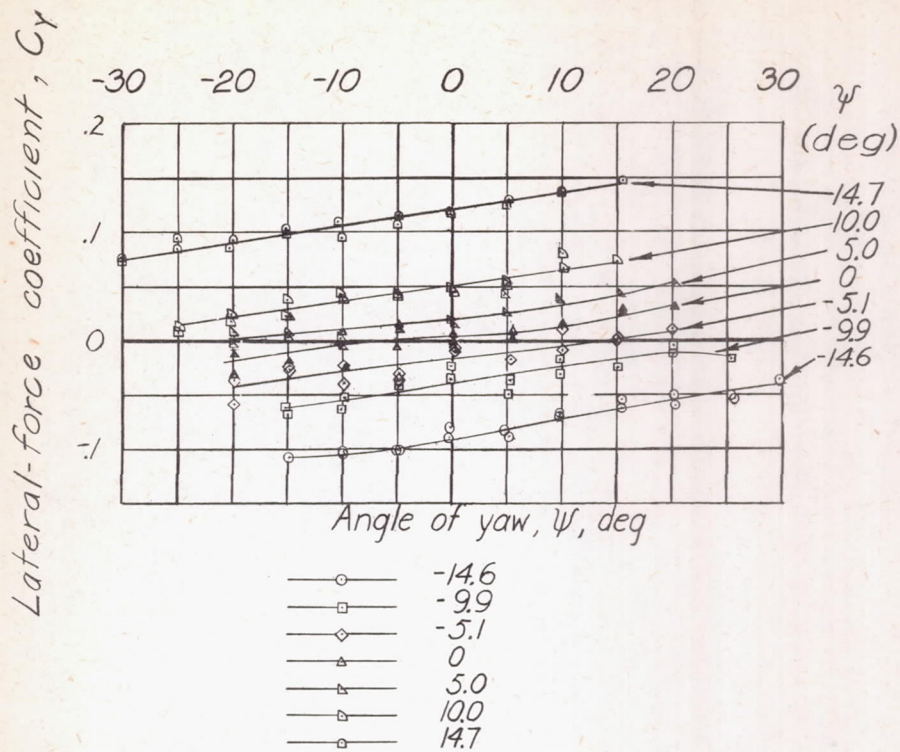
(c) Climbing condition; rated power ($T_C=0.51$);
 $\alpha, 12.3^\circ$; $C_L, 1.39$; $\delta_f, 0^\circ$.

Figure 22.- Continued.



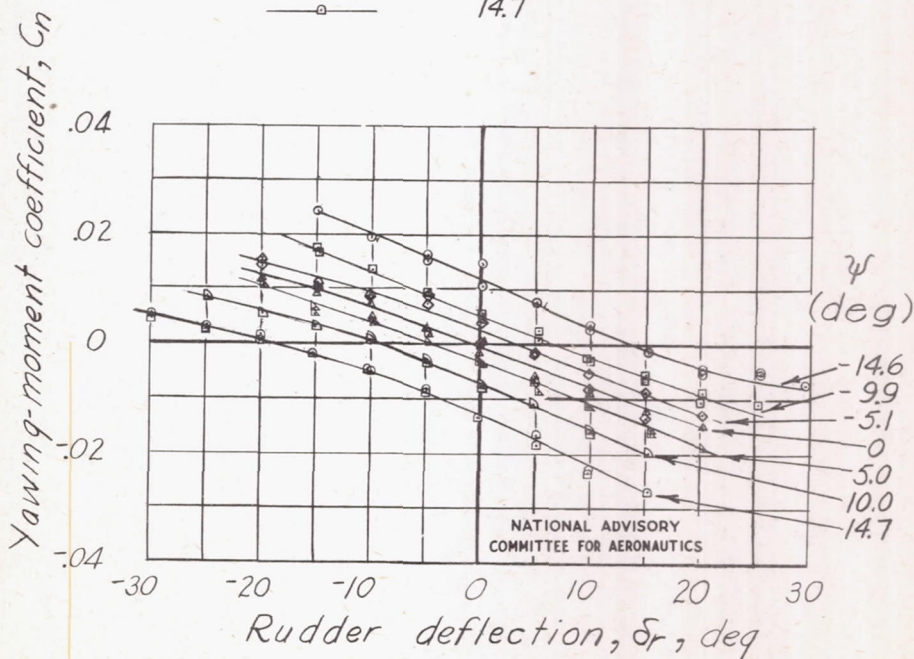
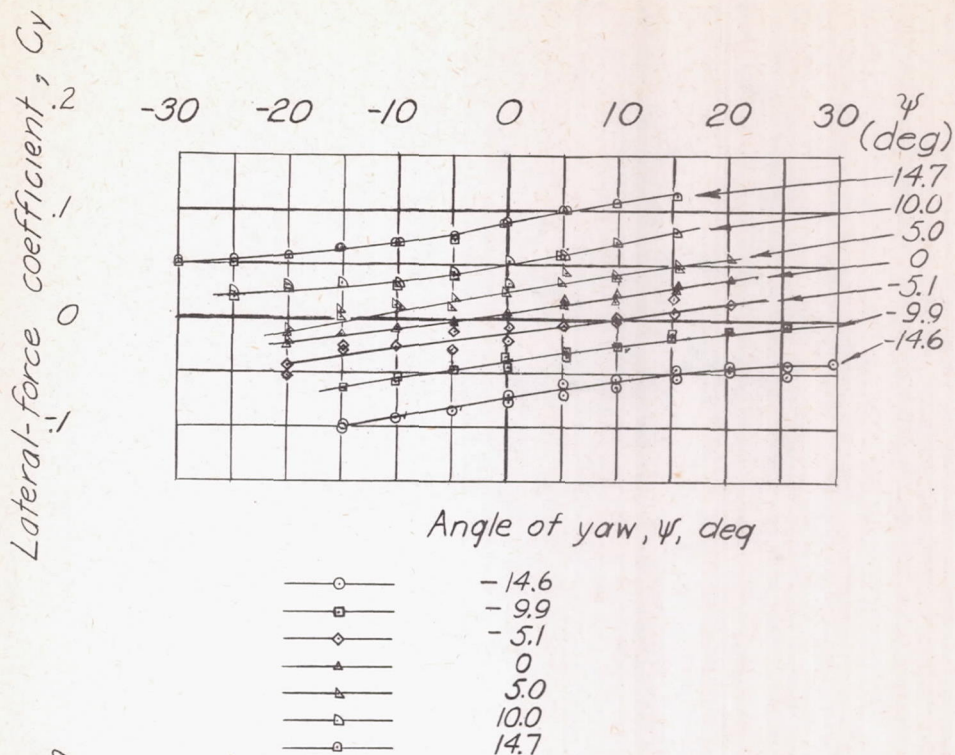
(d) Wave-off condition; rated power ($T_C=0.51$);
 $\alpha, 4.9^\circ$; $C_L, 1.39$; $\delta_f, 50^\circ$.

Figure 22.- Continued.



(e) Landing condition; $T_C, 0.01$; $\alpha, 11.8^\circ$; $C_L, 1.58$; $\delta_f, 50^\circ$.

Figure 22.-Concluded.



(a) $\alpha, 9.2^\circ$; $C_L, 0.83$; $\delta_f, 0^\circ$.

Figure 23. - Variation of C_n and C_y with δ_r for several angles of yaw. Propeller removed.

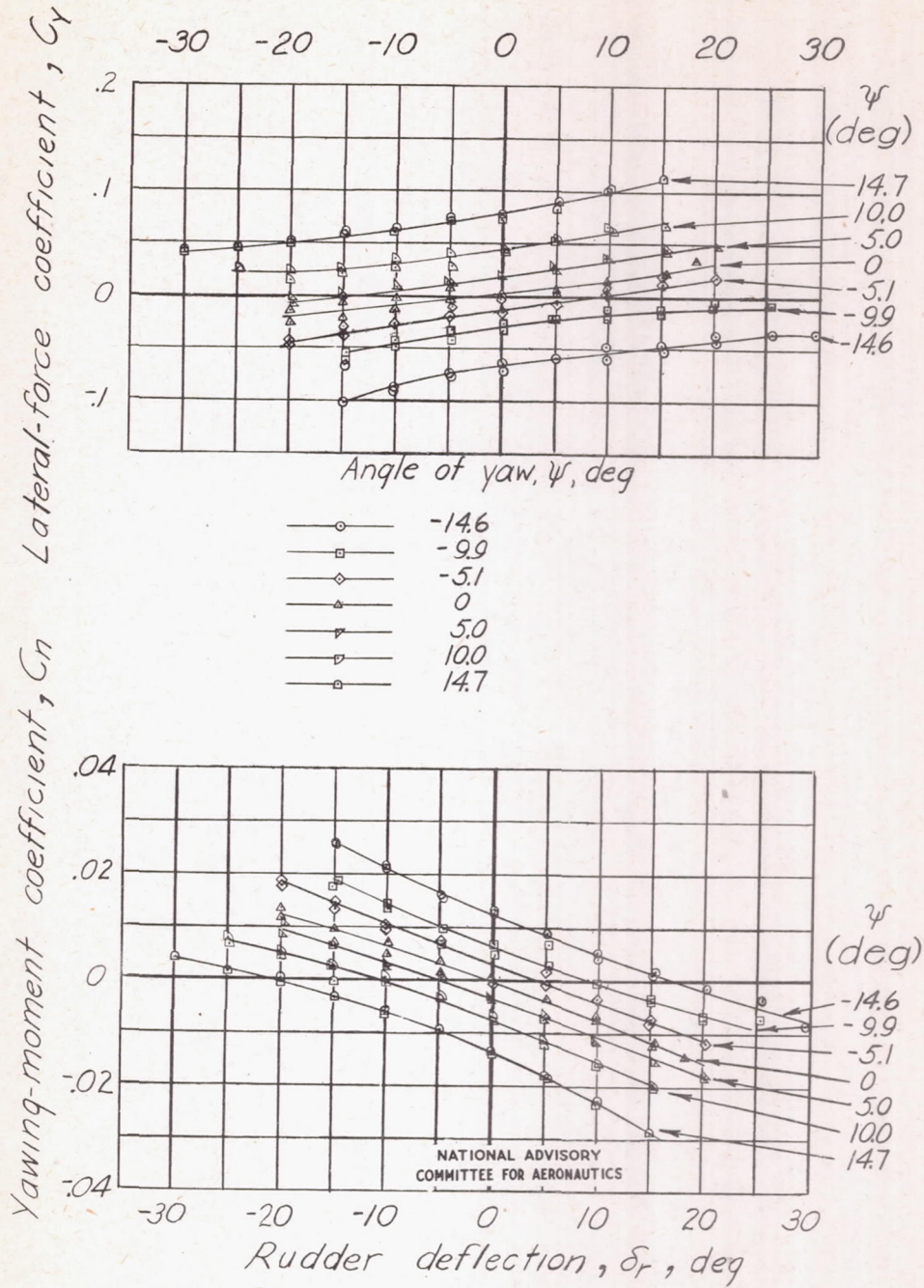


Figure 23.-Continued.

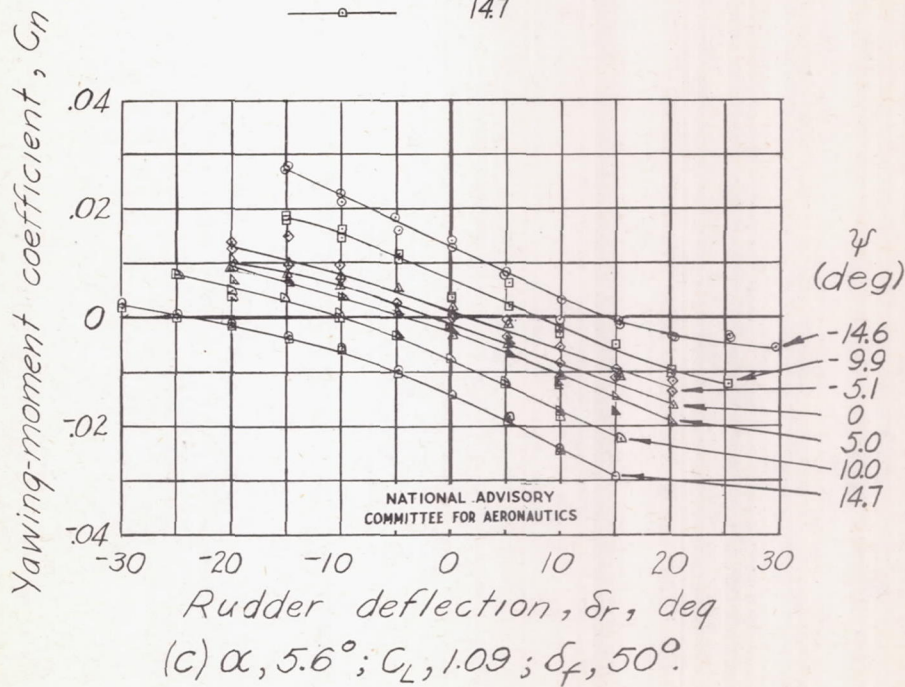
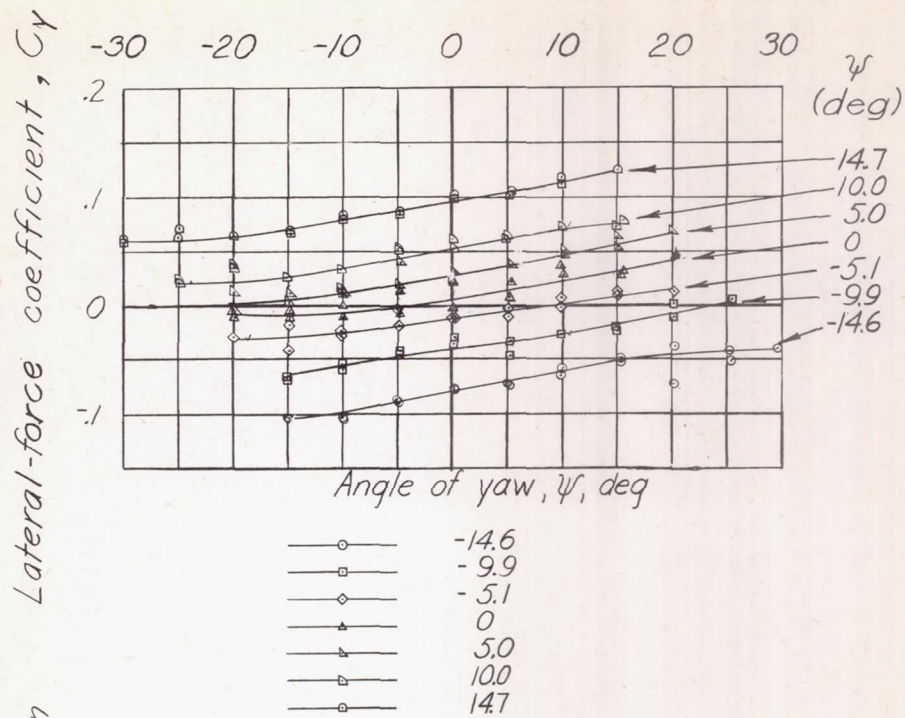


Figure 23.-Continued.

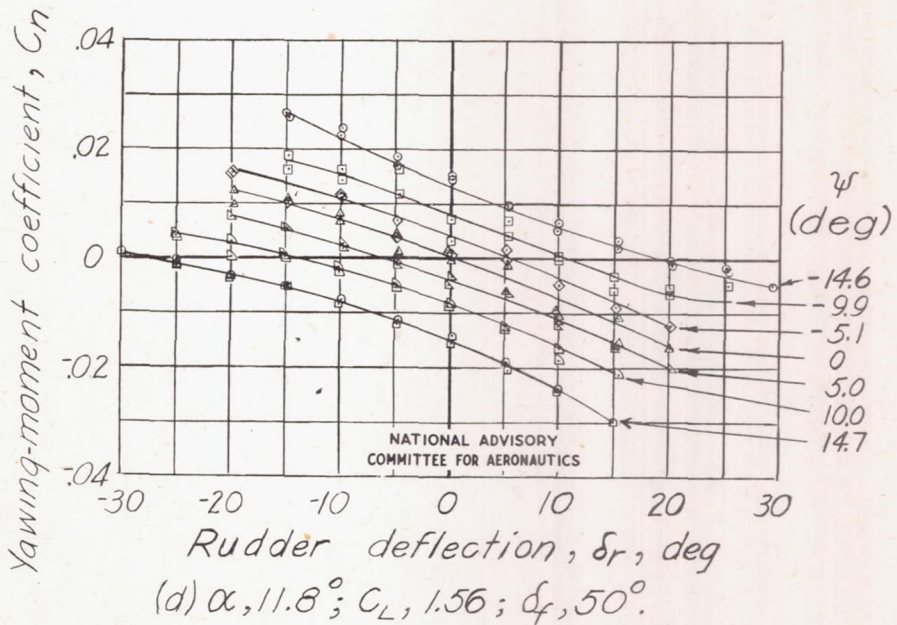
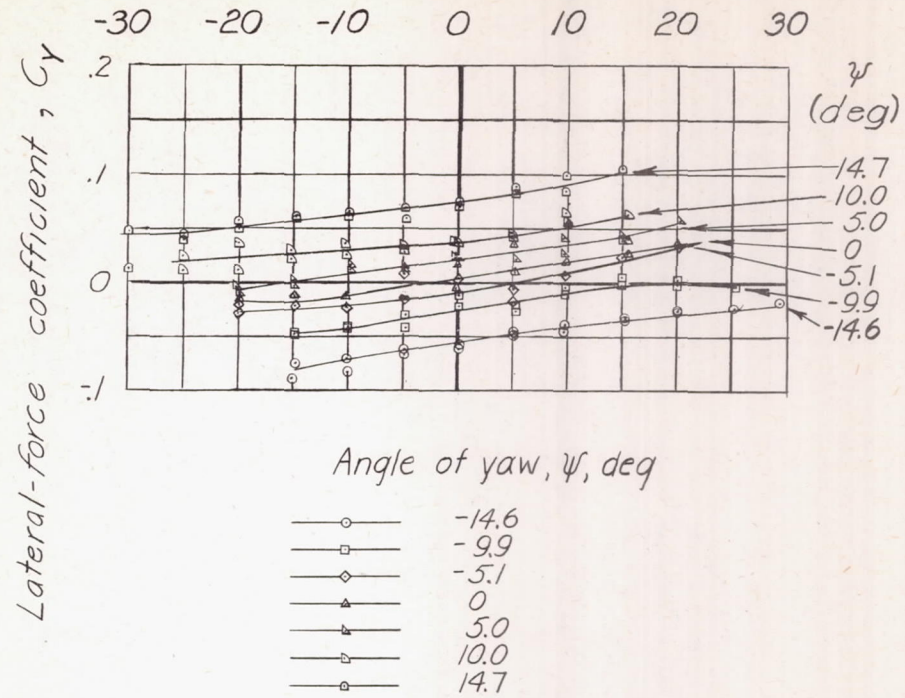
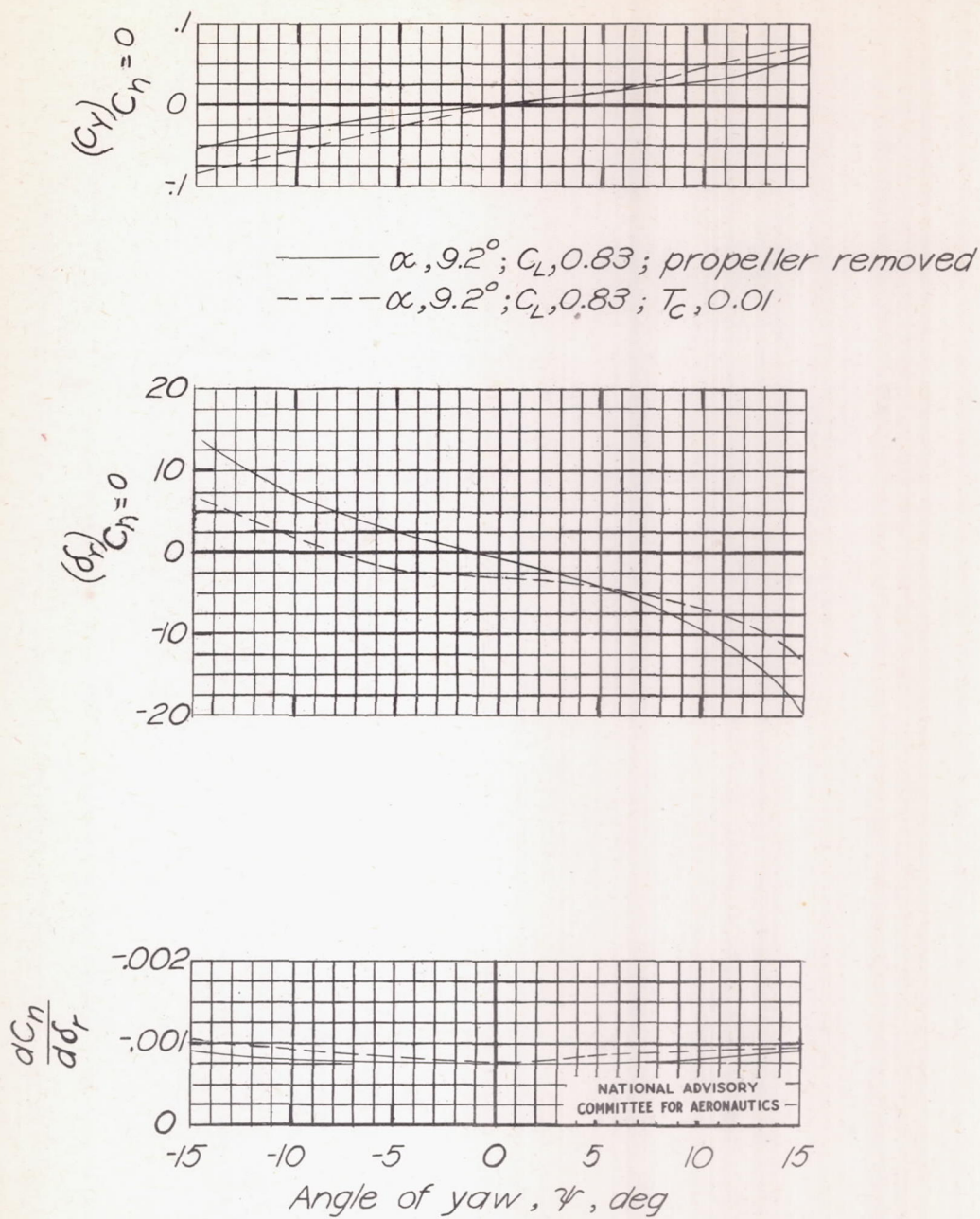
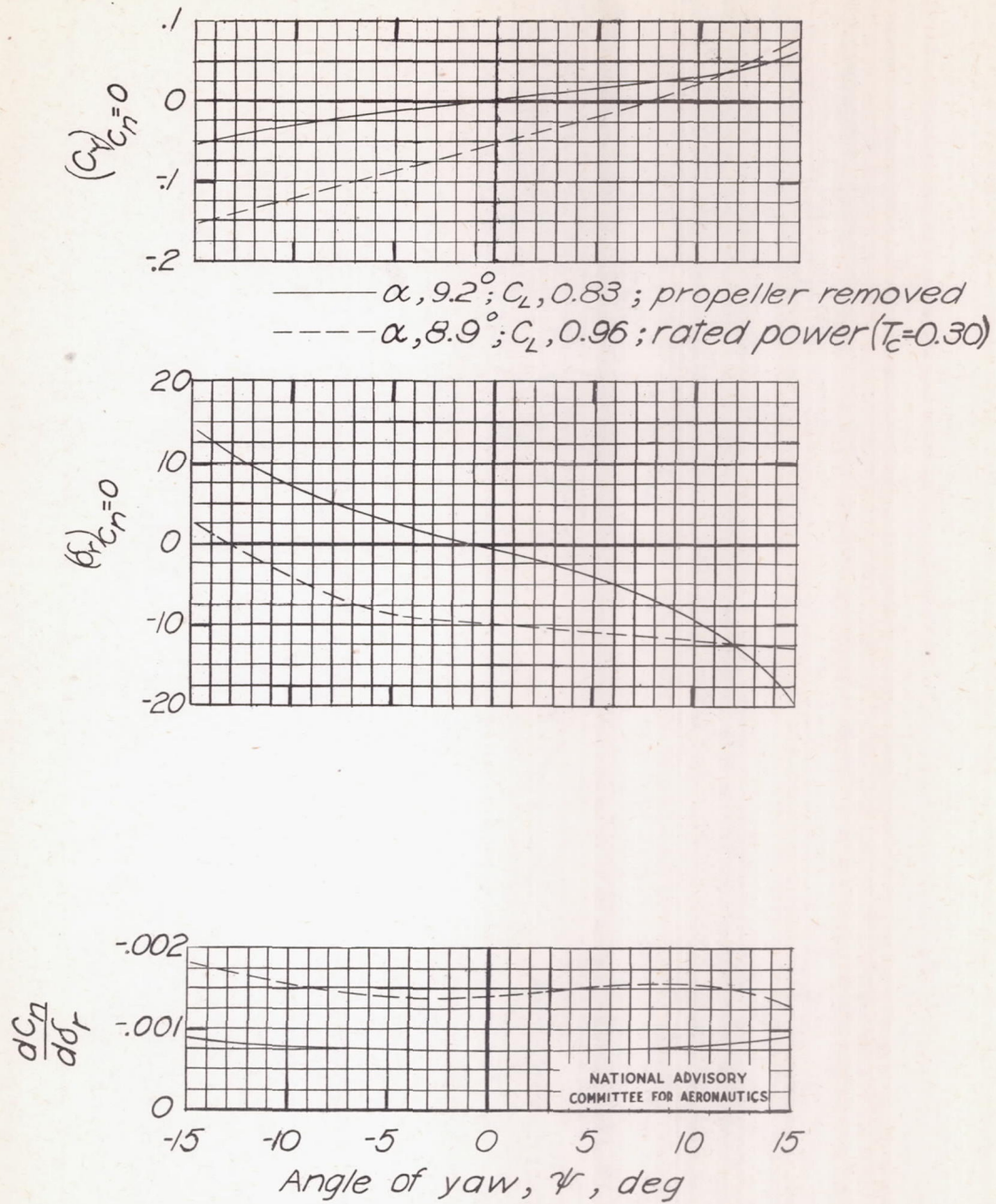


Figure 23.- Concluded.



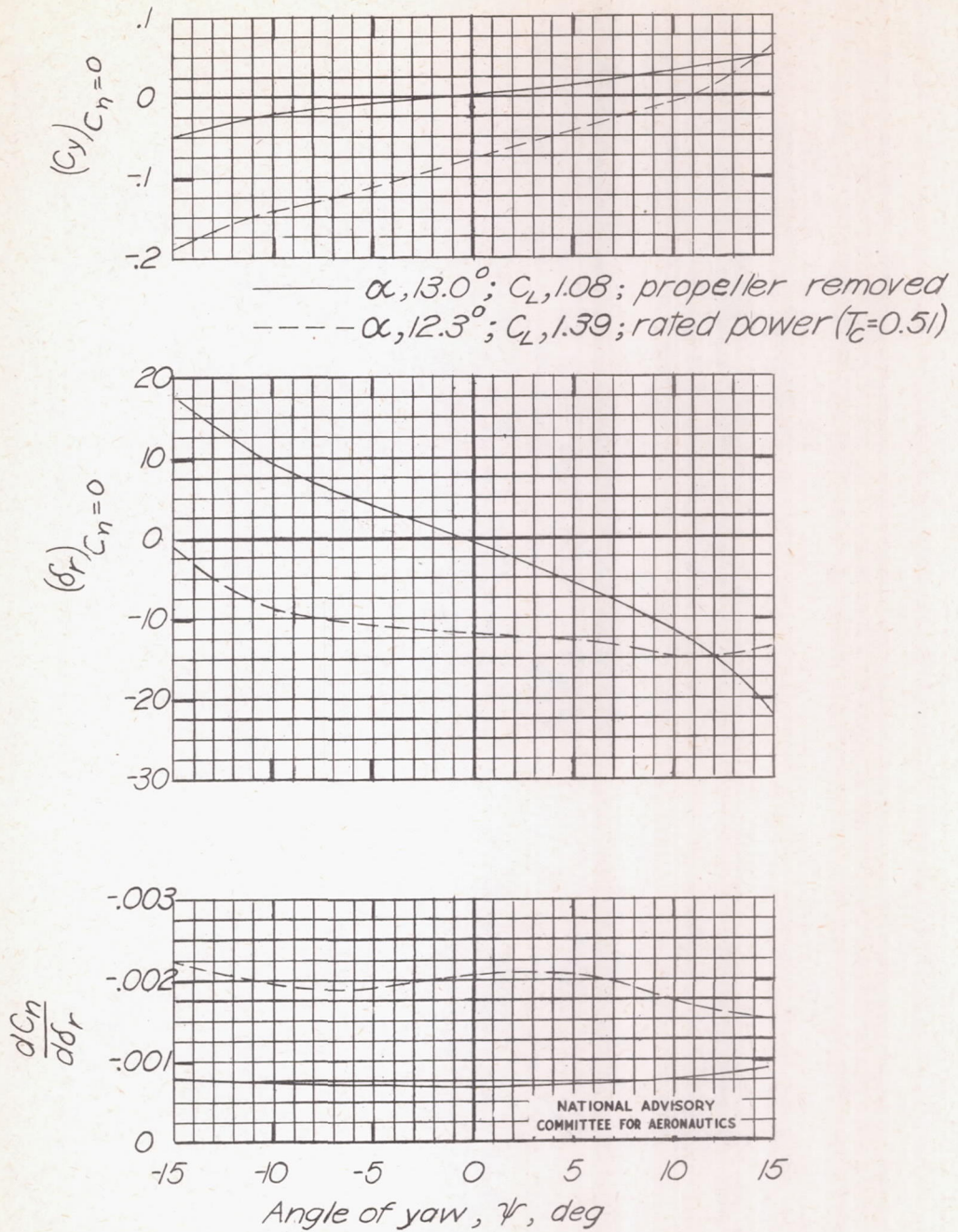
(a) Gliding condition; $\delta_f, 0^\circ$

Figure 24.- Directional trim characteristics of the XF6F-4 airplane.



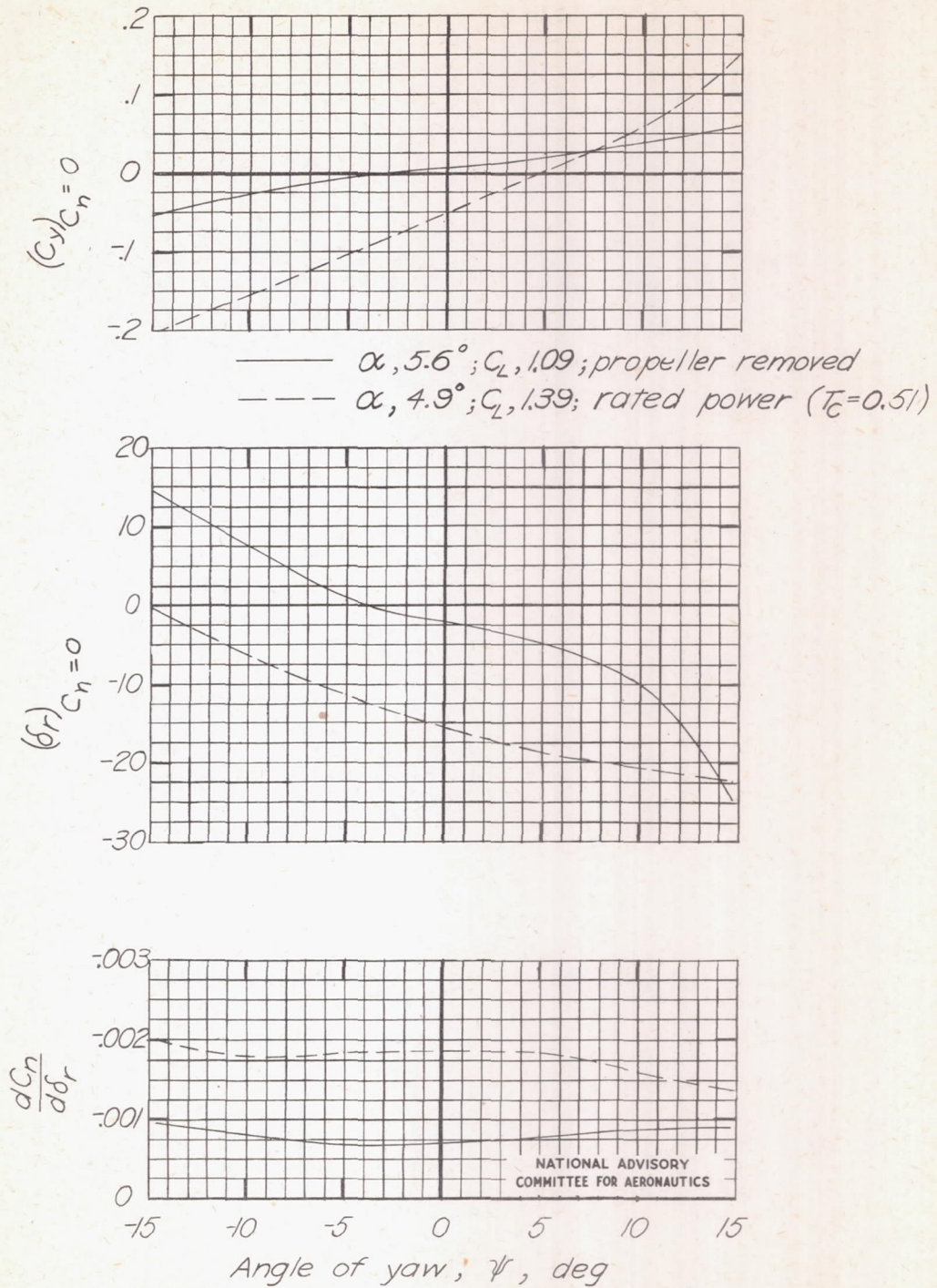
(b) Climbing condition ; $\delta_f, 0^\circ$.

Figure 24.- Continued.



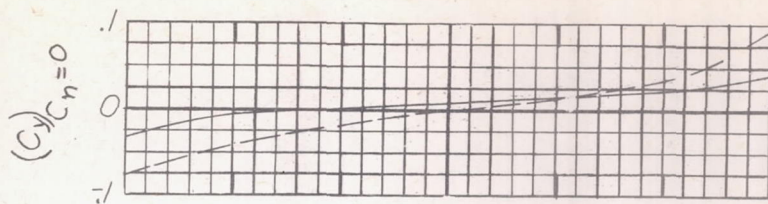
(c) Climbing condition; $\delta_f, 0^\circ$.

Figure 24.-Continued.

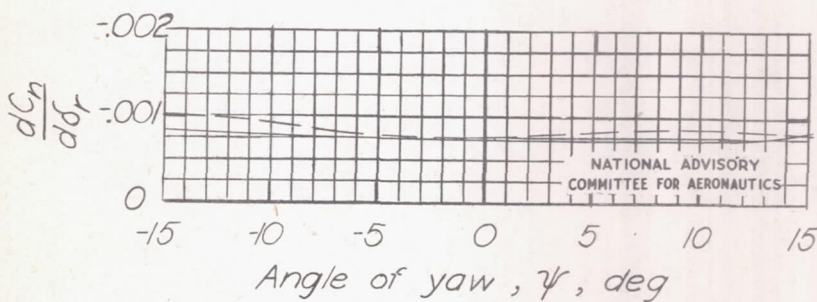
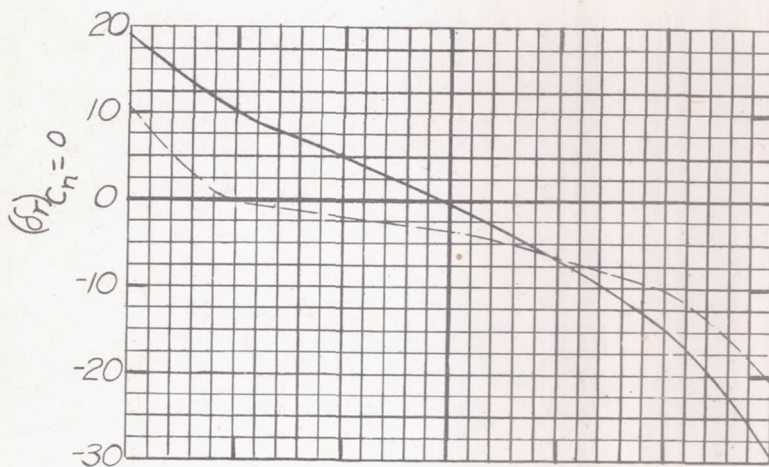


(d) Wave-off condition; $\delta_f, 50^\circ$.

Figure 24.- Continued.



— $\alpha, 11.8^\circ; C_L, 1.56; \text{propeller removed}$
 - - - $\alpha, 11.8^\circ; C_L, 1.58; T_C, 0.01$



(e) Landing condition ; $\delta_f, 50^\circ$

Figure 24.-Concluded.